


1-1-2015

Development Of Scaffold Architectures And Heterotypic Cell Systems For Hepatocyte Transplantation

Dalia Alzebdeh
Wayne State University,

Follow this and additional works at: http://digitalcommons.wayne.edu/oa_dissertations

 Part of the [Biomedical Engineering and Bioengineering Commons](#), and the [Materials Science and Engineering Commons](#)

Recommended Citation

Alzebdeh, Dalia, "Development Of Scaffold Architectures And Heterotypic Cell Systems For Hepatocyte Transplantation" (2015). *Wayne State University Dissertations*. Paper 1283.

This Open Access Dissertation is brought to you for free and open access by DigitalCommons@WayneState. It has been accepted for inclusion in Wayne State University Dissertations by an authorized administrator of DigitalCommons@WayneState.

**DEVELOPMENT OF SCAFFOLD ARCHITECTURES AND HETEROTYPIC CELL
SYSTEMS FOR HEPATOCYTE TRANSPLANTATION**

by

DALIA ABDELRAHIM ALZEBDEH

DISSERTATION

Submitted to the Graduate School

of Wayne State University,

Detroit, Michigan

in partial fulfillment of the requirements

for the degree of

DOCTOR OF PHILOSOPHY

2015

MAJOR: BIOMEDICAL ENGINEERING

Approved by:

Advisor

Date

© COPYRIGHT BY
DALIA ABDELRAHIM ALZEBDEH
2015
All Rights Reserved

DEDICATION

To Mom and Dad with Love.....

ACKNOWLEDGMENTS

First, I would like to acknowledge the financial and emotional support that my family has provided me all along my PhD journey, specifically my father Abdulrahim and my big brother Rami. The support and encouragement that my mom Manar and my sisters Enas and Wea'am gave me were priceless. And without the mental and physical strength that Allah has rewarded me with, all of that would have not been achieved (thank you Allah).

I acknowledge the supervision and mentorship my advisor Dr. Howard Matthew who is really good at them. My acknowledgment also to my committee members Dr. Thomas Kocarek and Dr. Harini Sundararaghavan for their invaluable feedback, especially Dr. Kocarek and his group (Ms. Mary Gargano) for his generous supply of the hepatocytes. Very special thank you to Dr. Michele Grimm for her continuous support in the past four years in so many ways, I really can't thank you enough Dr.Grimm.

I would like also to thank the biomedical engineering department at Wayne State University for the funding opportunities they provided for me in the past four years, especially Dr. Michele Grimm and Dr. Juri Gelovani.

Finally, many thanks to my kids Leen and Ali for their unconditional love. Although I have not been around for them for many years, I hope I have set a role model that with some patience and sacrifice you can achieve your dreams no matter what life throws at you.

TABLE OF CONTENTS

Dedication	iii
Acknowledgements.....	iv
Table of Contents	v
List of Figures	xi
List of Tables	v
CHAPTER ONE: Background and Relevance	1
1.1 The Liver: Anatomy and Physiology Overview	1
1.2 Orthotopic Liver Transplantation and Other Solutions	3
CHAPTER TWO: Current Treatments and Research in Hepatic Tissue Engineering	6
2.1 Main Challenges in the Hepatic Tissue Engineering Field	6
2.2 The Extracellular Matrix (ECM) Materials	6
2.2.1 Chitosan	8
2.2.2 Glycosaminoglycans (GAGs)	10
2.3 The Need to Re-create and Maintain the Polarized Plasma Membrane of Hepatocytes	12
2.4 Co-Culture Systems and the Need for Three Dimensional Models	14
2.5 Co-Culturing with Mesenchymal Stem Cells	19
2.6 Porous Constructs and Dynamic Perfusion Systems	21
2.7 Commercially Available Liver Models for Drug Screening	22
2.8 Recent Hepatocyte Transplantation Research: Scaffold-less Approach	24
CHAPTER THREE: Hypotheses and Specific Aims	26

CHAPTER FOUR: The Effects of Scaffold Designs on Hepatocyte Distribution and Viability in Three Dimensional, Chitosan/Heparin Scaffolds	29
4.1 Introduction.....	29
4.2 Experimental Work.....	30
4.2.1 Materials	30
4.2.2 Collagen (Type I) Extraction from Rat Tail Tendons	30
4.2.3 Hepatocyte Isolation and Culture in Collagen Gel Sandwich Configuration ..	31
4.2.4 Hepatocyte Membrane Polarization Assessment via Immunofluorescence	32
4.2.5 Hepatocyte Metabolic Functions Assays (Albumin Synthesis and Urea Secretion).....	33
4.2.6 Bulb-Shape Scaffold Fabrication, Cell Seeding and Cell Distribution Evaluation	33
4.2.7 Surface Freezing and Central Freezing Scaffolds Fabrication, Cell Seeding and Cell Distribution Evaluation	35
4.2.8 Volumetric Flow Rate Calculations	37
4.3 Results	40
4.3.1 Hepatocyte Morphology and Metabolic Functions in the Collagen Gel Sandwich Configuration (Static Cultures; The Control for all Experiments)	40
4.3.2 Bulb-Shape Chitosan Scaffold Microstructure and Seeding Efficiency	43

4.3.3 Comparison between Two Scaffold Designs: Surface Freezing or Central Freezing	45
4.3.4 Metabolic Functions for Hepatocytes in the Surface Freezing Scaffold	47
4.4 Discussion	48
4.5 Conclusions and Future Work	49
CHAPTER FIVE: The Effects of Cell Seeding Architecture on Hepatocyte Distribution and Viability in Three Dimensional, High-Porous Chitosan/Heparin Scaffolds .	50
5.1 Introduction.....	50
5.2 Experimental Work.....	51
5.2.1 Materials	51
5.2.2 Seeding with Single Cell Suspension	51
5.2.3 Seeding with Pre-Formed Aggregates	52
5.2.4 Aggregation Efficiency Analysis and Aggregates Viability	52
5.2.5 Histology Processing and Hematoxylin & Eosin Staining	53
5.2.6 Lactate Dehydrogenase Activity Assay	53
5.2.7 AlamarBlue Viability Assay	54
5.3 Results	54
5.3.1 Aggregation Efficiency and Aggregates Viability	54
5.3.2 Hepatocyte Metabolic Functions and Viability at Different Seeding/Culturing Flow Rates and Temperatures	55
5.4 Discussion	67
5.5 Conclusions and Future Work	69

CHAPTER SIX: The Effects of Co-Culturing Hepatocytes with Bone Marrow Mesenchymal

Stem Cells	70
6.1 Introduction.....	70
6.2 Experimental Work.....	71
6.2.1 Materials	71
6.2.2 Bone Marrow Mesenchymal Stem Cells Isolation and Culture.....	71
6.2.3 Chitosan-Heparin Disc Scaffolds Fabrication and SEM Imaging	72
6.2.4 Cell Labeling with Fluorescent Dyes	73
6.2.5 Cell Seeding and Culture into Three Different Architectures	74
6.2.6 AlamarBlue® Viability Test in the Chitosan-Heparin Disc Scaffolds.....	74
6.2.7 Spheroids Sizes Measurement and Statistical Analysis for Spheroids Formed in Disc Scaffolds	75
6.2.8 Monotypic and Heterotypic Perfusion Cultures in Chitosan-Heparin Scaffolds	75
6.2.9 Hepatocyte Metabolic Functions Assays (Albumin Synthesis and Urea Secretion)	76
6.3 Results	76
6.3.1 Pores Dimensions and Architecture as Shown by Scanning Electron Microscopy (SEM).....	76
6.3.2 Cell Morphology in the Disc Scaffolds	77
6.3.3 Spheroids' Sizes at 50,000 cells/cm ² and 100,000 cells/cm ² Seeding Densities	83
6.3.4 AlamarBlue® Viability Assay	85

6.3.5 Hepatocyte Metabolic Functions and Viability	85
6.3.6 Mathematical Model for Urea Production Rate.....	88
6.3.7 Metabolic Performance of Heterotypic Cultures in the Perfusion System .	94
6.3.8 Cell Morphology and Neo-Tissue Formation in Perfused Scaffolds Heterotypic Cultures	96
6.4 Discussion	99
6.5 Conclusions and Future Work	102
CHAPTER SEVEN: The Effects of Encapsulating Hepatocytes With or Without Bone Marrow Mesenchymal Stem Cells within Chitosan-GAG Fibers on Hepatocytes Viability	
7.1 Introduction.....	104
7.2 Experimental Work.....	105
7.2.1 Materials	105
7.2.2 GAG-Chitosan Polyelectrolyte Complexes Formation into Fibers	106
7.2.3 Culturing Hepatocytes in Chitosan-GAG-Collagen Fibers	107
7.2.4 Cell Distribution in a Bundle of Chitosan-Hyaluronic acid- Heparin- Double Strength Collagen Fibers	108
7.3 Results	110
7.3.1 Membrane Thickness for Different Formulas of GAG-Chitosan Polyelectrolyte Complexes Fibers	110
7.3.2 Encapsulated Hepatocytes (with and without MSCs) Morphology.....	113
7.3.3 Metabolic Performance of Encapsulated Hepatocytes with/without MSCs	

7.3.4 Cell Distribution in Fiber Bundle Scaffold	115
7.4 Discussion	116
7.5 Conclusions and Future Work	118
REFERENCES	119
ABSTRACT.....	135
AUTOBIOGRAPHICAL STATEMENT.....	137

LIST OF FIGURES

Figure 1: Functional unit of the liver.	2
Figure 2: Human liver sinusoid.....	3
Figure 3: Chitosan molecular structure	8
Figure 4: Covalent immobilization of GAGs to chitosan.....	12
Figure 5: Epithelial cell membrane polarity.	13
Figure 6: Liver sinusoid.....	14
Figure 7: Different ECM components present in the space of Disse.....	16
Figure 8: Mechanisms of interaction between mesenchymal stem cells and hepatocytes	20
Figure 9: Liver models.....	24
Figure 10: Scaffold fabrication.	34
Figure 11: Perfusion Bioreactor System.....	35
Figure 12: Schematic diagram illustrating the fabrication method for the two scaffold's designs.....	36
Figure 13: Bioreactor setup for seeding hepatocytes into the scaffolds..	37
Figure 14: Pores architectures and dimensions.....	38
Figure 15: Phase contrast images for hepatocyte in collagen gel sandwich configuration culture.....	40
Figure 16: Green CMFDA CellTracker™ labeling.....	41
Figure 17: Gap junction Connexin32 labeling.....	41
Figure 18: Tight junction ZO-1 labeling.....	42
Figure 19: Metabolic assays of hepatocytes in collagen gel configuration.	42
Figure 20: Scanning electron microscopy images for the bulb-shape scaffold..	43
Figure 21: H&E histology images of seeded scaffold..	44
Figure 22: SEM images of two designs.	45

Figure 23: H&E staining images of cross sectional areas for seeded scaffolds.....	46
Figure 24: Metabolic functions for scaffold cultured hepatocyte in the surface frozen scaffold	47
Figure 25: Aggregation efficiency and viability.	55
Figure 26: Metabolic performance and viability of perfused, scaffold-seeded hepatocytes	57
Figure 27: H&E histology images of cross sectional areas for seeded scaffolds.	57
Figure 28: Metabolic performance of perfused, scaffold-seeded hepatocytes	59
Figure 29: H&E histology images of cross sectional areas for seeded scaffolds	60
Figure 30: SEM photos of cross sectional areas for seeded scaffolds with	61
Figure 31: Metabolic performance of perfused, scaffold-seeded hepatocytes	63
Figure 32: AlamarBlue® cell health indicator assay.	64
Figure 33: H&E histology images of seeded scaffolds.....	65
Figure 34: H&E histology images of a longitudinal section of scaffold seeded with pre-formed spheroids.	65
Figure 35: SEM photos of a longitudinal section at the center port of scaffold seeded with pre-formed spheroids.....	67
Figure 36: Fabrication of chitosan disc scaffolds.	73
Figure 37: SEM images of chitosan disc scaffolds.	77
Figure 38: Cell morphology in the disc scaffold system.	78
Figure 39: Phase contrast images and digital color fluorescent images of hepatocyte/BM- MSC co-cultures in disc scaffolds.....	80
Figure 40: Fluorescent intensities quantification for all seeding architectures.....	81
Figure 41: Mean grey value Intensities for anti-Connexin 32 and anti-ZO-1.	82
Figure 42: Spheroids mean diameters for seeding density of 50,000 cells/ cm ² and 100,000 cells/ cm ²	84
Figure 43: AlamarBlue® reduction rate for the two seeding densities.....	86

Figure 44: Metabolic functions of hepatocytes/BM-MSCs cultured disc scaffolds.....	88
Figure 45: Schematic diagrams represent two scenarios: high and low metabolic functions and the two zones in a given aggregate.	89
Figure 46: Total urea production rate for condition #1 (predicted vs. measured).....	94
Figure 47: Metabolic performance of perfused, scaffold-seeded with monotypic and heterotypic cells suspension	95
Figure 49: H&E histology images of cross sectional areas for MSCs-hepatocytes perfused scaffolds	98
Figure 50: Masson Trichrome staining images of cross sectional areas for MSCs-hepatocytes perfused scaffolds.....	99
Figure 51: Wall shear stress magnitudes	101
Figure 52: Hepatocytes encapsulated in fibers.	108
Figure 53: Fiber bundle fabrication method.....	109
Figure 54: SEM photos of the fiber's membrane.....	111
Figure 55: Phase contrast images and SEM images of encapsulated hepatocytes	112
Figure 56: Phase contrast images illustrating the membranes formed in each of the listed formulations.....	113
Figure 57: Phase contrast images of encapsulated hepatocytes.....	114
Figure 58: Digital images of encapsulated hepatocytes.....	114
Figure 59: Metabolic performance of monotypic and heterotypic cells suspension in fibers.....	115
Figure 60: Digital image of fixed hepatocytes in fiber bundle scaffold.	116
Figure 61: Cell distribution and fibers architecture in a wrapped bundle.....	116

LIST OF TABLES

Table 1: Clinical Trials for Temporary Extracorporeal Liver Devices.....	5
Table 2: The potential of each cell type in the normal liver to secrete certain types of ECM components.....	17
Table 3: Summary of observations for setup #1	55
Table 4: Summary of observations for setup #2	58
Table 5: Summary of observations for setup #3	62
Table 6: Seeding architectures.....	74
Table 7: Summary of observations for fibers made from different GAG formulations.	110

CHAPTER ONE

BACKGROUND AND RELEVANCE

1.1 The Liver: Anatomy and Physiology Overview

The liver is the largest internal organ that weighs around 1.2-1.6 kg. It performs over than 500 metabolic functions that can be classified in three main categories: (1) secretion; e.g. proteins like albumin, urea and bile, (2) storage; glycogen and fat, and (3) detoxification utilizing the broad range of cytochrome P450 enzymes that hepatocytes have.

The liver consists of smaller hexagonal-shaped functional units named hepatic lobules. Each lobule has a central vein which is the terminal of the hepatic venules, and at the corners the portal triads which consist of a venule (branch of portal vein), an arteriole (branch of hepatic artery), and a bile duct (Fig. 1). The liver is consider a very dense organ with hepatocytes predominate in both number and volume [1]. The total number of hepatocytes in a rat weighing 400g is estimated to be 18.5×10^8 ; which is equivalent to 1.4×10^5 per unit volume (mm^3)[2].

The functional unit of the liver is called acinus (plural acini) (Fig. 1); it consists of ellipsoidal mass of hepatocytes aligned around the hepatic arterioles and portal venules just as they anastomose into sinusoids. Each acinus can be divided into three zones based on its proximity to the arterial blood supply; where zone one represents the hepatocytes that are closest to the arterioles and hence best oxygenated, while zone three refers to the hepatocytes that are farthest from the arterioles and have the poorest supply of oxygen. Therefore, hepatocytes in zone one are the first ones to be exposed to blood coming from GI system. In addition, and based on the blood supply for each zone, each zone has its unique enzymatic system for detoxification

purposes. The oxygen concentrations in the sinusoid are in the range from 25 mmHg (perivenous) to 70mmHg (periportal) [3].

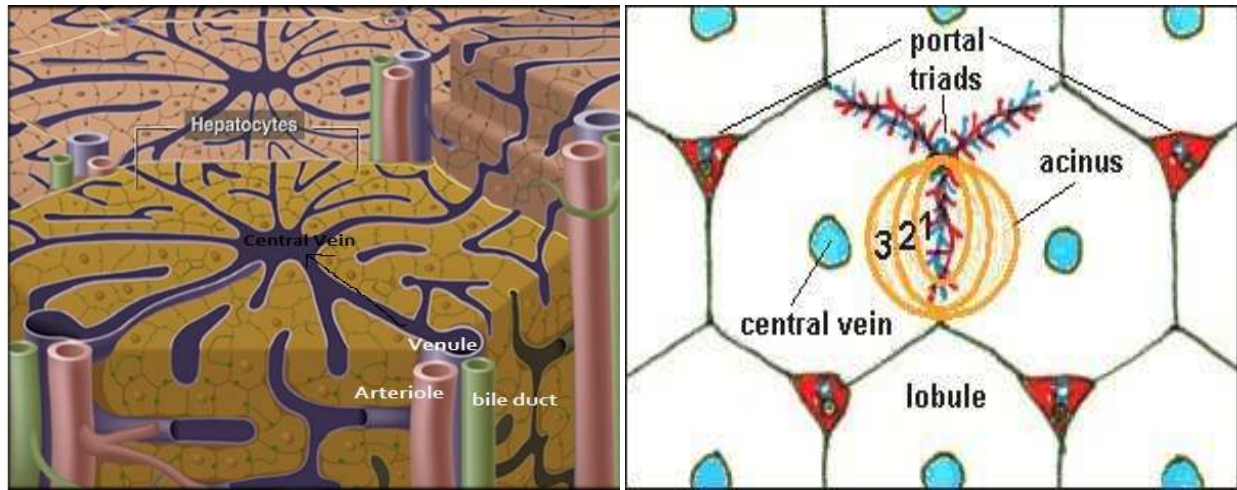


Figure 1: Functional unit of the liver. Hepatic lobules as hexagonal-shaped functional units (left) [4] . Hepatic acini overlaid onto lobules in the diagram (right) [5].

The lobules mainly consist of one-cell-thick chords of hepatocytes forming canals that are called “sinusoids” (Fig. 2A). Sinusoids are lined, along with the hepatocytes, with endothelial cells, stellate cells and Kupffer cells. The blood flows in the sinusoids where plasma and proteins can migrate through endothelial cells via a unique feature called fenestrations (100-150 nm) into the *Space of Disse*. At this space, direct contact with the hepatocytes occurs and uptake of nutrients and oxygen by the hepatocytes takes place. The uniqueness of hepatic environment comes from the space of Disse as it lacks any continuous barriers and it is rich with different types of basement membrane proteins (Fig. 2B).

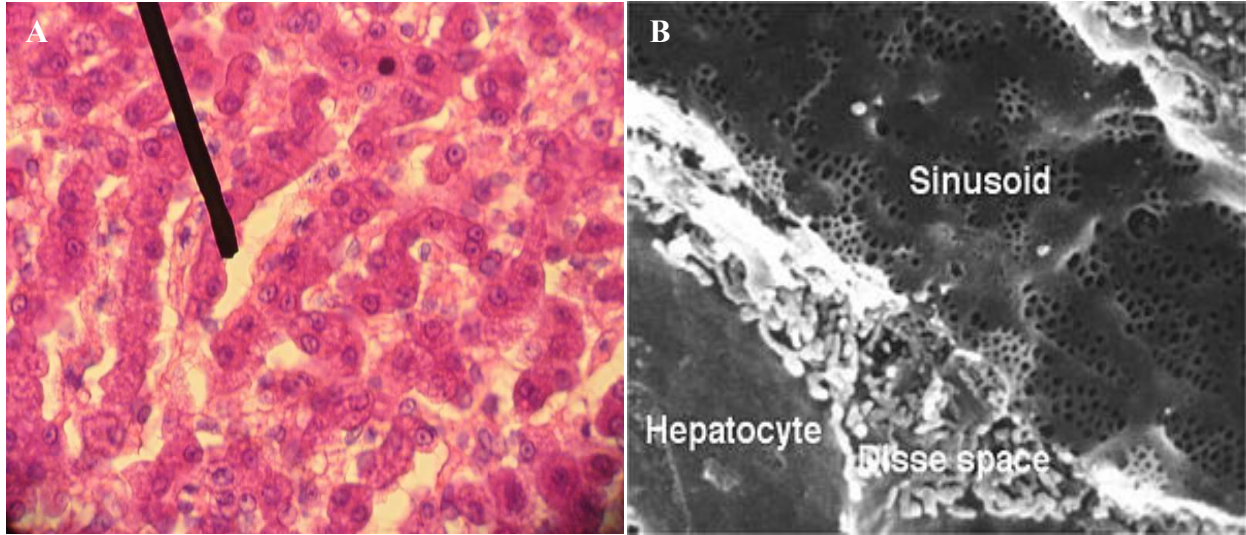


Figure 2: Human liver sinusoid. (A) Digital image (H&E staining) showing the hepatocytes organized in one-cell-thick chords [6]. (B) Rat liver sinusoid SEM image (width of sinusoid is 5 μm) showing the fenestrated endothelial cells (100 nm in diameter), the microvilli of hepatocytes and the space of Disse [7].

1.2 Orthotopic Liver Transplantation and Other Solutions

Liver diseases can be resulted from hepatotoxicity; for example hepatotoxicity caused by drug-induced liver injury (DILI). The manifests come in various forms: (1) functions dysregulation, (2) injury to hepatic parenchyma, (3) cell replacement/necrosis, or (4) cancer. Some examples of such injuries are: steatosis, fibrosis and cirrhosis and the result could lead to “end-stage liver diseases” and the need for liver transplant.

According to the Organ Procurement and Transplantation Network (OPTN) - U.S. Department of Health and Human Services, there are 15,428 candidates on the waiting list for a liver transplantation as of January 4th, 2015[8]. The majority of eligible patients die while on the waiting list because of the severe donor shortage. The estimated cost for such procedure is \$577,100 according to the United Network for Organ Sharing (UNOS), adding to that almost \$21,900 for annual follow-up and medications [9].

Orthotopic Liver Transplantation (OLT) is still the only treatment for end-stage liver diseases. Despite its therapeutic potential, the procedure is limited by: donor organ shortage, the need for a life-long immunosuppressive therapy and very high cost (~\$500,000). Temporary liver support systems are meant to replace a greater spectrum of liver functions over a short period of time (days to weeks) and may also serve as a bridge to OLT by allowing more time to find a better match between donor and recipient or stabilize the patient prior to surgery. Various non-biological approaches, such as hemodialysis, hemoperfusion, plasmapheresis and plasma exchange, have had a limited success because of the insufficient replacement of the synthetic and metabolic functions of the liver. Extracorporeal biological treatments, i.e. life support systems that are analogous in concept to kidney dialysis machines, specifically designed for liver failure patients, have shown some beneficial results but are difficult to implement in a clinical setting. An example of extracorporeal system is the bioartificial liver system (BAL), in which hepatoma cell lines or isolated hepatocytes are incorporated into a bioreactor and induced to perform the hepatic functions by processing the blood or plasma of liver failure patients [10, 11]. Although these systems are more complicated than the filtration and dialysis systems, they can offer the biochemical and specific functions which are not offered by the no-cells systems. Table 1 summarizes some clinical trials for temporary extracorporeal liver support systems [10].

Hepatocyte transplantation offers the possibility of increasing the survival rate as it can be used as a therapeutic tool. This is dependent upon the ability to re-assemble isolated hepatocytes into a functional organ by allowing the use of organs which would be considered too traumatized for whole liver transplants. However, such organs may be an adequate source of healthy hepatocytes. Hepatocyte transplantation also has great potential for providing cures for a variety of liver-based, metabolic diseases, e.g., treatment for glycogen storage disease

type 1a [12], familial hypercholesterolemia [13] and Congenital hyperbilirubinemia (Crigler–Najjar syndrome) [14].

Device	Configuration	Cell Mass and Source	Perfusate and Treatment Protocol	Trial Phase
Whole Liver Perfusion				
Whole pig, baboon or human liver			Whole blood, 5 hours median perfusion time, most patients received 1 or 2 perfusions	I/II
Dialysis and Filtration Systems				
MARS (Teraklin AG, Rostock, Germany)	Albumin-loaded hemofilter, 60-kD cut-off	None	Whole blood, 12–132 hours	I/II
Liver Dialysis Unit (HemoCleanse Technologies, West Lafayette, IN)	Hemodiabsorption across 5-kD cut-off cellulosic membranes	None	Whole blood, 6 hours/day; up to 5 days	FDA Approved
Prometheus (Fresenius Medical Care AG, Bad Hornburg, Germany)	Hemofilter, 250-kD cutoff, connected to two adsorber cartridges, in series with conventional dialyzer	None	Whole blood, up to 12 hours divided into 2 treatments over 2 days	I
Bioartificial Livers				
HepatAssist (Circe Biomedical, Lexington, MA)	Hollow-fiber, polysulphone, 0.15–0.20 µm pore size	50 g cryopreserved primary porcine hepatocytes on microcarrier beads	Plasma, 6 hours/session; up to 14 sessions	II/III
BLSS (Excorp Medical, Oakdale, MN)	Hollow-fiber, cellulose acetate, 100-kD cutoff	70–100 g primary porcine hepatocytes	Whole blood, 12 hours/session; up to 2 sessions	I/II
ELAD (Vital Therapies, La Jolla, CA)	Hollow-fiber, cellulose acetate, 120-kD cutoff	100 g human hepatoblastous CJA cells per cartridge, up to 4 cartridges/device	Plasma, continuous up to 107 hours	II
AMC-BAL (Hep-Art Medical Devices, B.V., Amsterdam, The Netherlands)	Spirally wound, nonwoven polyester matrix, no membrane	70–150 g primary porcine hepatocytes	Plasma, up to 18 hours/sessions up to 2 sessions	I
Radial-flow bioreactor (Sant'Anna University Hospital, Italy)	Radial-flow bioreactor	230 g primary porcine hepatocytes	Plasma, 6–24 hour treatments, mostly in one session	I/II
LiverX-2000 (Algenix, Inc., Minneapolis, MN)	Cells embedded in collagen matrix within hollow-fibers	40 g primary porcine hepatocytes per cartridge, 2 cartridges/device	Blood	I/II
Hybrid bioartificial liver (Hepatobiliary Institute of Nanjing University, China)	Polysulfone hollow-fiber cartridge with 100-kD cut-off combined with adsorption column	100 g primary porcine hepatocytes	Plasma, one 6-hour treatment, except one patient with 2 - 6 hour treatments	I

Table 1: Clinical Trials for Temporary Extracorporeal Liver Devices. ELAD, Extracorporeal liver assist device; BLSS, bioartificial liver support system; AMC-BAL, Amsterdam bioartificial liver system; MARS, molecular adsorbent recycling system; FDA, Food and Drug Administration.[10]

CHAPTER TWO

CURRENT TREATMENTS AND RESEARCH IN HEPATIC TISSUE ENGINEERING

2.1 Main Challenges in the Hepatic Tissue Engineering Field

Primary hepatocytes lose their functions and their specific phenotype when removed from their environment [15]. They are highly dependent on the cell-cell contact and attachment to the extracellular matrix (ECM)[16]. Therefore, when trying to culture hepatocytes in vitro, one should take in consideration the followings: 1) the material used as extracellular matrix [17] , 2) co-culture with non-parenchymal cells [18], and 3) the use of growth factors [19]. The main obstacles to success are closely tied to the high metabolic rate of hepatocytes and the associated limitations in oxygen and nutrient transport especially during cell attachment and adaptation to a new environment. Recent published data suggest that dynamic perfusion of culture medium through three dimensional scaffolds using bioreactors promote new tissue formation and enhances hepatic functions [10, 11, 20, 21]. Each of these factors will be discussed in the following paragraphs of this chapter.

2.2 The Extracellular Matrix (ECM) Materials

The main function of extracellular matrix is to provide tissues with their specific mechanical and biochemical properties. Different cell types that reside in that ECM space are responsible for its synthesis and maintenance, while ECM, in turn, also has an important impact on cellular functions.

Cell–matrix interactions play a dominant role in cell attachment and migration, as well as regulating and promoting cellular differentiation and gene expression levels. These specific

functions are thought to be mediated by cell specific-receptors and cell binding epitopes on many matrix molecules [22].

Various studies have been done on different materials in order to mimic the extracellular matrix, where cells adhere and proliferate. Some of the materials investigated in this field are: poly-L-lactic acid (PLLA), poly (D, L-lactide-co-glycolide) (PLGA), poly(ethylene glycol) (PEG) and polyethylene terephthalate (PET) [23]. Non- polycarbonate materials also was used, for example, the commercially available self-assembling peptide PuraMatrix[®]. This material is a fully synthetic and resorbable hydrogel composed of repeating amino acid sequences of Arginine-Alanine-Aspartic Acid-Alanine prepared in an aqueous solution. PuraMatrix[®] self-assembles into nanofibers on a scale similar to the extracellular matrix when exposed to physiological levels of salt, forming a flowable hydrogel. When hepatocytes were cultured in PuraMatrix[®] nanoscaffolds, they were able to synthesize albumin and secrete urea for up to 90 days of culture [24]. Regarding hepatocytes cultured in bioreactors, the major obstacle is to keep them attached while perfusing the medium and sustain the shear stress [25].

Primarily, chitosan and collagen have been studied extensively as they are biocompatible and enhance attachment and proliferation for many types of cells like hepatocytes [26-29]. Dunn et al. [28] were able to maintain hepatic specific functions (secretion of albumin, transferrin, fibrinogen, bile acids and urea) for more than 6 weeks in vitro. They cultured primary rat hepatocytes in a sandwich configuration; consisting of two layers of hydrated type I collagen prepared from rat tail tendons. This sandwich configuration successfully maintained the cellular polarity normally found in the liver. In contrast, cells cultured on a single layer of collagen gel failed to maintain hepatic functions.

2.2.1 Chitosan

Chitosan is derived from chitin (naturally found in the arthropod exoskeletons) by deacetylation in different degrees ranging between 50% and 90% (Fig. 3). It is considered biocompatible; as it evokes minimal foreign body reaction, and biodegradable; as implants made of chitosan are hydrolyzed by lysozyme-mediated activity. The degradation rate is inversely proportional to the degree of crystallinity [30]. It has been found that after four hours of incubation time of 50% acetylated chitosan with lysozyme in 0.1 molar phosphate buffer at pH 5.5 and 37°C, the chitosan solution lost 66% of its viscosity which indicated sufficient degradation of it [31, 32]. Due to its (above mentioned) natural properties, chitosan is utilized in research involving implantable applications in many fields such as orthopedic/periodontal, tissue engineering, wound healing and drug/gene delivery [33].

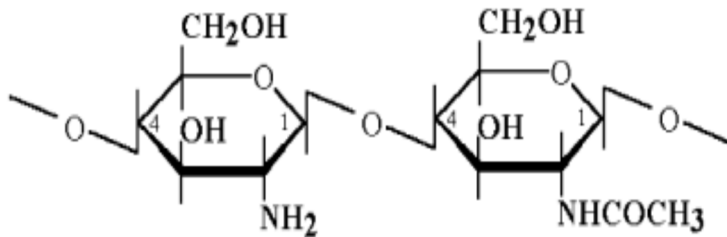


Figure 3: Chitosan molecular structure [30].

Chu et al.[27] extensively studied the effects of chitosan nanofiber scaffolds on hepatocyte cells viability, attachment and hepatic functions. They have showed that chitosan nanofibers promote hepatocytes adhesion, albumin secretion, urea synthesis, cytochrome P4501A1 enzymatic activity and glycogen synthesis compared to control. The cytotoxicity assay for lactate dehydrogenase (LDH) and tumor necrosis factor α (TNF- α inflammatory cytokine)

releases suggested that chitosan nanofibers have no effect compared to the control. On the other hand, Jiankang et al. [34] prepared porous and well-organized (with hepatic chambers and channel network) scaffolds from chitosan that was cross linked with gelatin. The scaffold has pre-defined channels and chambers fabricated by freeze-drying then lyophilization. They seeded these scaffolds with primary hepatocyte by shaking the 24-well plate that has the scaffolds placed in. Their results showed that hepatocytes attached well to the chitosan-gelatin matrix and they secreted albumin and urea during the first week of culture in higher amounts at the well-organized scaffold compared to the porous scaffold.

Chitosan highly- porous scaffolds can be made by controlling the rate of solution freezing, which in turn controls the direction of the thermal gradient. Such scaffolds have large surface-to-volume ratio which enhances hepatocyte attachment and angiogenesis. Chitosan is considered a biologically active material due to the presence of amine group and alcohol group in its chemical structure. This cationic nature allows ionic and covalent interactions with other materials like glycosaminoglycans (GAGs) and Proteoglycans (PGs) [30]. Scientists used this unique property to complex different materials into chitosan scaffolds. T. Bou-Akl [35] in her dissertation, showed that hepatocytes tend to form spheroids (with increase in size over time) when seeded on chitosan membranes. The membranes were modified with GAGs such as: heparin, heparan sulfate, dermatan sulfate and modified dextran. When hepatic functions were evaluated, the highest rates for albumin secretion measured on heparin modified membranes. However, urea secretion results showed lower amounts compared to the collagen gel sandwich configuration (the control). When collagen was added to the modified chitosan membranes, hepatocytes showed higher rates of spread and attachments, but lower albumin synthesis rates. On the other hand, urea secretions increased as the amount of collagen increases, but yet it was

in amounts lower than the control. She concluded that in terms of albumin synthesis, hepatocytes in three dimensional configurations had better functions. While in terms of urea synthesis, hepatocytes in two dimensional cultures performed better. This could be the result of the easier accessibility to oxygen through diffusion from the medium to spread hepatocytes in monolayer cultures. More attempts were made towards enhancing chitosan for better hepatic functions and hepatocytes viability. Li et al. [26] investigated the effects of complexing chitosan scaffolds with sodium alginate and heparin via ionic interactions, on hepatocytes morphology and metabolic activities and they used chitosan membranes as control. Hepatocytes showed more attachment on the modified scaffolds than the control and they were able to maintain their spherical morphology with many microvilli on the cell membranes. Regarding albumin synthesis and urea secretion; the highest rates were within the heparin modified chitosan. *In general, modified chitosan scaffolds maintained better hepatic functions than the unmodified chitosan.* The rationale was that hepatocytes synthesize different types of extracellular proteins which contain GAGs integration sites on them. These sites allow the GAG molecules to bind and form such away between the hepatocytes and the surrounding materials. Similary, with sodium alginate; polyelectrolyte complexes were formed which played a significant role in maintaining hepatocytes attachment and metabolic activities.

2.2.2 Glycosaminoglycans (GAGs)

Proteoglycans (PGs) are localized at the cell surface and in the extracellular matrix. They are believed to have important roles in cell-cell interaction, cell growth and differentiation, localization of bounded proteins to the cell surface and mediate cell functions. The biological interactions mediated by PGs are believed to be due to the presence of the natural

polysaccharides glycosaminoglycan (GAG) chains. Hence, GAGs are considered biocompatible materials. Heparan sulfate (HS) and its highly sulfated form; heparin (HEP), are the most abundant GAGs in the liver and they bind over 100 different proteins, including enzymes, protease inhibitors, lipoproteins, growth factors, chemokines, extracellular matrix proteins, receptor proteins and nuclear proteins [36-38].

GAGs bounded to chitosan scaffolds are expected to facilitate the binding and organization of deposited extracellular matrix components to the implant. Consequently, this process will enhance the integration of implant with existing tissue. As chitosan has the positively charged amino groups; GAGs can be easily immobilized on it either ionically or covalently due to their negative charge. The covalent immobilization of GAGs to chitosan can be achieved by forming an amide bond between the carboxyl group and the amino group using the zero-length cross-linker 1-ethyl-3-[3-dimethylaminopropyl] carbodiimide hydrochloride (EDC); a carboxyl activating agent for amide bonding with primary amines through the reaction illustrated in figure 4 below [39].

Growth factors like fibroblast growth factor (FGF), hepatocyte growth factor (HGF), vascular endothelial growth factor (VEGF) and heparin-binding epidermal growth factor (EGF) are dependent on heparin for biological activity mediated through their high-affinity signal-transducing receptors [36].

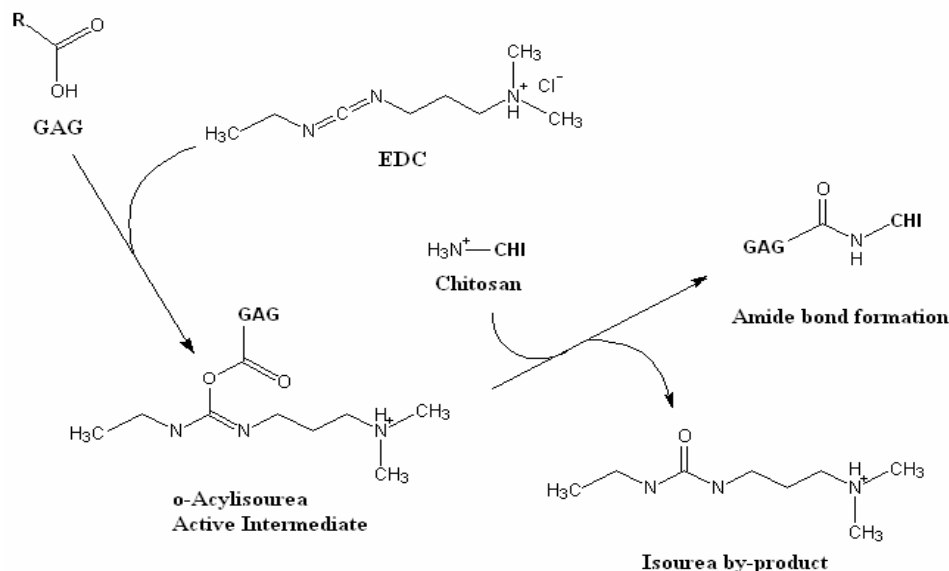


Figure 4: Covalent immobilization of GAGs to chitosan. Schematic representation of the amide bond formation between chitosan (CHI) and GAG [39].

In view of the reported observations, for the present work, heparin has been chosen to modify the chitosan scaffolds. It has been shown that heparin is used as anticoagulant factor as well as a binding site for growth factors. In addition, heparin is able to stimulate some cell types' proliferation like endothelial cells and dermal and epidermal cells as well as being useful for culturing multiple cell types [38, 40, 41]. This choice is supported by our previous studies which showed that chitosan modified with HEP has the best results among other GAGs tested (e.g. dermatan sulfate and hyaluronic acid) in terms of enhancing hepatic functions and hepatocytes viability for the reasons discussed above [35].

2.3 The Need to Re-create and Maintain the Polarized Plasma Membrane of Hepatocytes

Epithelial cells express a special feature of cell membrane polarity which is needed in this type of cells to provide a boundary between different extracellular components. This is achieved by expressing specific lipids and proteins at each segment of the cell membrane; the apical

domain that is in contact with the external environment, and the basal domain which faces the blood circulation. These apical and basal domains are separated by tight junctions that distinguish and maintain their specific lipids and protein composition and prevent any intermixing. Distinctly, hepatocytes express special geometry where their apical domains at the lateral membranes between two neighboring cells and forming the bile canalicular tubules. The basolateral domains face the blood circulation and form the sinusoids (Fig. 5) [42]. Hence, hepatocytes, as epithelial cells, need the basement membrane to be maintained to provide the physical support and the polarity they require. The connective tissues beneath the basement membrane secrete the necessary ECM elements to maintain its integrity.

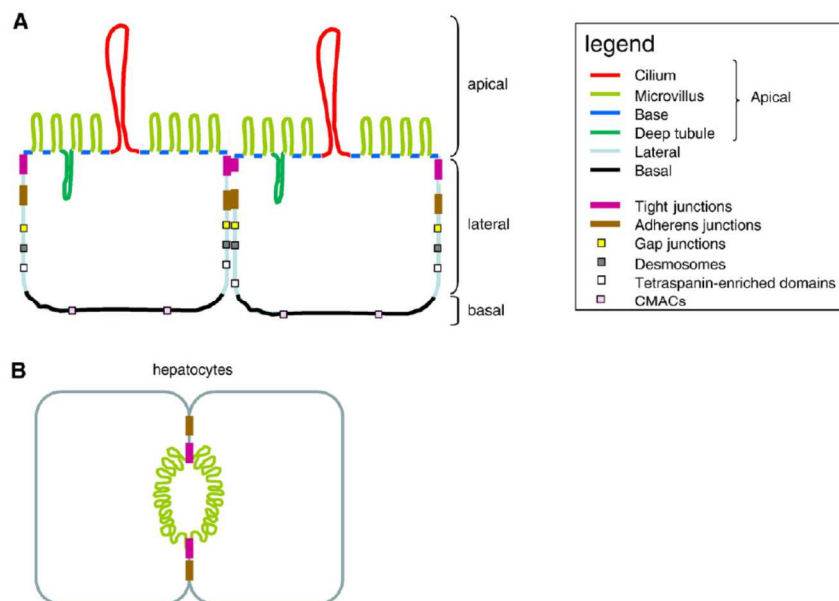


Figure 5: Epithelial cell membrane polarity. (A) Schematic diagram illustrating the different plasma membrane domains in epithelial cells in general. (B) Schematic showing the distinct polarized geometry displayed by hepatocytes [42].

Maintaining the cell surface polarity in *in vitro* cultures is a complex and dynamic process. It is greatly influenced by the cell-cell interaction, cell-extracellular interaction, cytokines and growth factors. In addition, evidences suggest that cell-cell junction protein might have alternate functions at other subcellular sites [43-46]. Comprehensive understanding of such

parameters and interactions will lead to design of an in vitro model that aid to maintain this polarization and help in preventing hepatocytes from de-differentiation. Unfortunately, freshly isolated hepatocytes rapidly lose their polarity after the isolation. However, if they are cultured in the collagen gel sandwich configuration, they can re-polarize in several days [28].

2.4 Co-Culture Systems and the Need for Three Dimensional Models

The adult liver consists of a complex multicellular structure (Fig. 6); which provides a scaffold for many complex cell– cell interactions that allow for the effective and coordinated liver specific functions [47, 48].

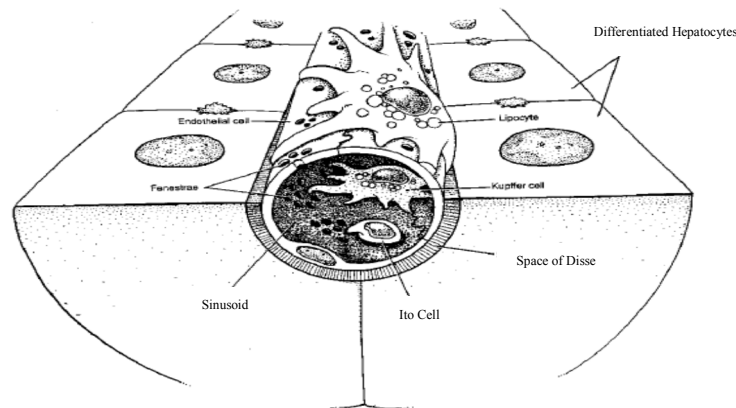


Figure 6: Liver sinusoid. Schematic diagram of the adult liver sinusoid which consists of: differentiated hepatocytes, fenestrated endothelial cells, space of Disse, lipocytes (stellate or Ito cells), bile ductules, and Kupffer cells [47].

It would be of great help in the field of liver tissue engineering to fully understand how different cell types interact together in order to achieve the liver-specific functions and tissue structure. When hepatocytes were grown on Matrigel (a gelatinous protein mixture derived from mouse tumor cells, but it's not a well-defined matrix) with pre-formed endothelial vascular structures, Nahmias et al. [49] noticed that the hepatocytes migrated and adhered towards these

structures and formed a new structure that resembled the in vivo sinusoids. These new structures were able to retain stable cytochrome P450 gene expression and activity and stable albumin gene expression and secretion rate for more than two months period of time. Nevertheless, it is still poorly understood how heterotypic interactions facilitate the maintenance of differentiated hepatocytes. Goulet et al. [43] noticed that microinjecting hepatocytes with Lucifer yellow CH molecules caused a spreading of the dye to the neighboring hepatocytes. In those cultures, hepatocytes were co-cultured with other non-parenchymal cells. On the other hand, this dye spreading wasn't observed in cultures where hepatocytes were cultured alone. The dye spreading indicates formation of gap junctions between hepatocytes; which play significant role in maintaining their phenotype and specific functionality, while no heterologous communication was observed between hepatocytes and endothelial cells. They interpreted these results as due to the fact that these two populations are separated by the space of Disse in the liver.

In liver tissue engineering, investigators should address problems involving microvascular network formation in three dimensional cultures; which showed advantages over the two dimensional ones by mimicking hepatic lobules and sinusoids and hence resulted in better hepatic functional maintenance. The mechanism behind the actual organization of liver sinusoids and how the endothelial vessels are coated with hepatic tissues has never been achieved in vitro. Crucial elements that regulate hepatocytes viability and functionality are the cell-cell interactions and the cell-substrate interactions while to success in developing a functional tissue engineered solution the main obstacles to overcome are closely tied to the high metabolic rate of hepatocytes and the associated limitations in oxygen and nutrient transport. [50-52].

It is well known that the ECM in the liver is similar in structure as other epithelial organs, e.g. kidneys and lungs. The uniqueness of the hepatic ECM comes from the space of Disse where it lacks of any continuous filtration barriers as the basement membrane and the endothelial cells there has the fenestrations feature. This configuration is typical for the functions that this space provides a bidirectional exchange passage for the molecules between hepatocytes and blood stream for a distance that is $< 1\mu\text{m}$. It is also shown that collagen type I in the space of Disse present as a network of cables while other types of collagen, e.g. type III and IV and fibronectin present as discontinuous deposits around collagen fibers (Fig. 7) [53]. Table 2 summarizes the potential of each cell type in the normal liver to secrete ECM components [54].

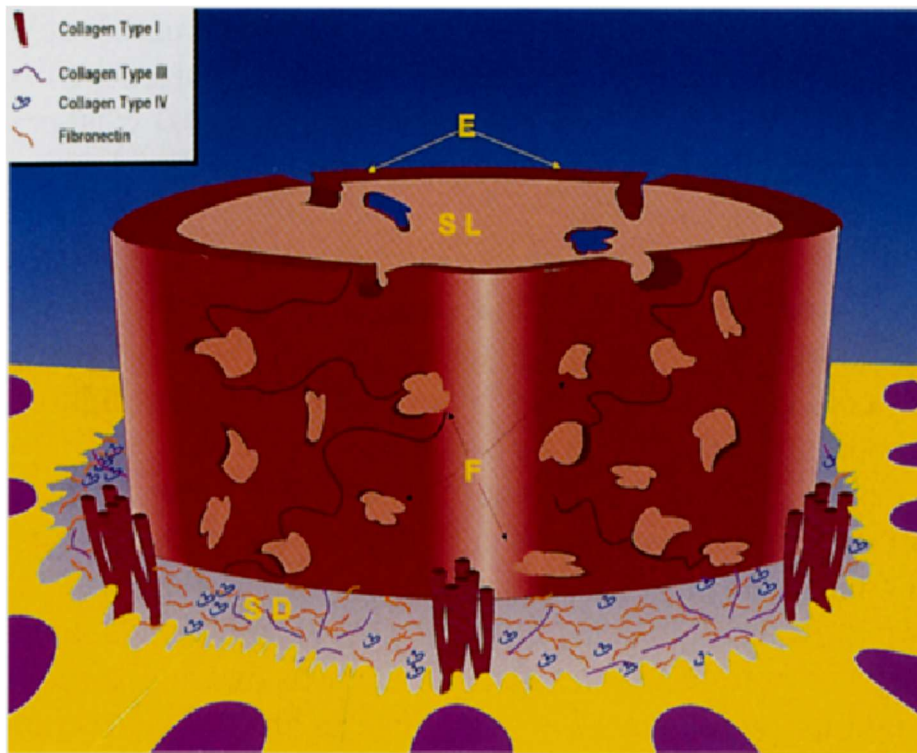


Figure 7: Different ECM components present in the space of Disse; Collagen Type I, Type III , Type IV and Fibronectin (see legend for symbols representation) [53].

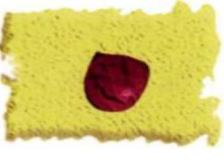




	Hepatocytes Collagen Types I, III Fibronectins Collagen Type IV Laminin Entactin Perlecan
	Ductal Cells Collagen Type IV Laminin Entactin Perlecan
	Ito Cells Collagen Types I, III, IV Tenascin Undulin Laminin Entactin Perlecan
	Endothelial Cells Thrombospondin Undulin Collagen Type IV Laminin Entactin Perlecan
	Kupffer Cells TGF- β

Table 2: The potential of each cell type in the normal liver to secrete certain types of ECM components [54].

Histologically, every hepatocyte cell receives oxygen and nutrients by at least one sinusoid. This vascular network is crucial to both the viability of the hepatocytes and the detoxification of blood. Additionally, most of the hepatic non-parenchymal cells are located near the sinusoids which make vascularization an important focus for further tissue engineering studies.

Several studies investigated the co-culturing of different types of cells with primary hepatocytes [51, 52, 55-57]. Their results indicated that hepatocyte viability and liver-specific functions maintained stable over a culture period of several weeks in vitro. They used different types of cells in their experiments, e.g. biliary epithelial cells, stellate cells, Kupffer cells as well

as non-hepatic endothelial cells and fibroblasts [51, 52, 55-57]. Yamada et al. [58], for example, used lactone-modified Eudragit polymer that contains β -galactose residue; which can act as a ligand of the asialoglycoprotein cell surface receptor expressed by hepatocytes. They mixed equal numbers of hepatocytes and liver non-parenchymal cells and seeded them in tissue culture dishes that were previously coated with the modified polymer. They noticed that hepatocytes rapidly aggregated and formed spheroids and both albumin secretion and 7EC reduction rate were increased by adding the non-parenchymal population compared with hepatocytes cultures alone. In a different study, Sudo et al. [51] tried to approach the co-culture system from a different angle. They tried to create a vascularized liver model by co-culturing primary rat hepatocytes with human microvascular endothelial cells and with rat microvascular endothelial cells in a three dimensional collagen scaffolds. The scaffold was located between two parallel microfluidic chambers where the culture medium was allowed to perfuse through the scaffold with a flow velocity of 27-35 $\mu\text{m}/\text{min}$ (based on the physiological value 36 $\mu\text{m}/\text{min}$). In both co-cultures, hepatocytes formed bile canicular structures and were able to exhibit P450 cytochrome activity which indicates that they maintained their differentiated functions. Another group who also investigated the co-culture systems Lu et al. [55]. They found that the liver-specific functions were significantly enhanced when primary rat hepatocyte spheroids were cultured with NIH/3T3 mouse fibroblasts on galactosylated poly-vinylidene difluoride (PVDF) compared with the hepatocyte spheroids cultured alone. They also found that this PVDF substrate stimulated the hepatocytes to re-organize into spheroids with the fibroblasts coating them which could mimic the liver regeneration. The reason for PVDF to stimulate the spheroid formation was due to the presence of galactose ligands which interact with asialoglycoprotein receptors on the hepatocytes membranes. In an interesting study by Abu-Absi et al. [56], it was

revealed that when culturing primary rat hepatocytes with rat hepatic stellate cells, HSCs proliferated rapidly and exhibited a morphology similar to fibroblasts. They were also able to express some of the cytoskeletal proteins, e.g. α -SMA. This is the same scenario during *in vivo* wound healing; the stellate cells get activated and start producing extracellular matrix proteins, secreting growth factors and proliferating rapidly. The presence of the stellate cells had a positive effect on albumin production. This co-culture system had effects on some liver-specific gene expression, e.g. albumin, CYP2B1/2 and cyclophilin as their mRNA levels were higher than the control.

2.5 Co-Culturing with Mesenchymal Stem Cells

A possible way to achieve the maintenance of basement membrane and the cell polarity is co-culturing with mesenchymal stem cells (MSC). They present important advantages such as: (1) easily isolated, (2) easily expanded *in vitro*, and (3) they are immunoprivileged and immunomodulatory [59]. It has been indicated in the literature that MSCs act in paracrine mechanisms as well as direct cell-cell contact as part of their role in immunomodulation in case of liver injuries [60].

In addition, recent reports of experimental findings have revealed the hepatic differentiation potential of MSCs for *in vivo* cultures (it is still unclear whether MSCs found *in vivo* or a type of differentiated MSCs are involved in hepatocyte maintenance) [61]. This type of cells can provide numbers of cues for hepatocyte development and growth (Fig. 8). For example, membrane-associated liver-regulating protein (LRP) is essential in maintaining the mature hepatocyte phenotype and it is expressed by MSCs [62]. Another example is the Connexin-43 (gap-junction

protein) that correlates with the capacity of fat-storing cell clones in maintaining hepatocytes differentiated state and is expressed by MSCs as well [59].

It has been shown that MSC can deposit a mixture of ECM proteins such as collagen types I & III, fibronectin, and laminin that are identical to those found in native liver [63].

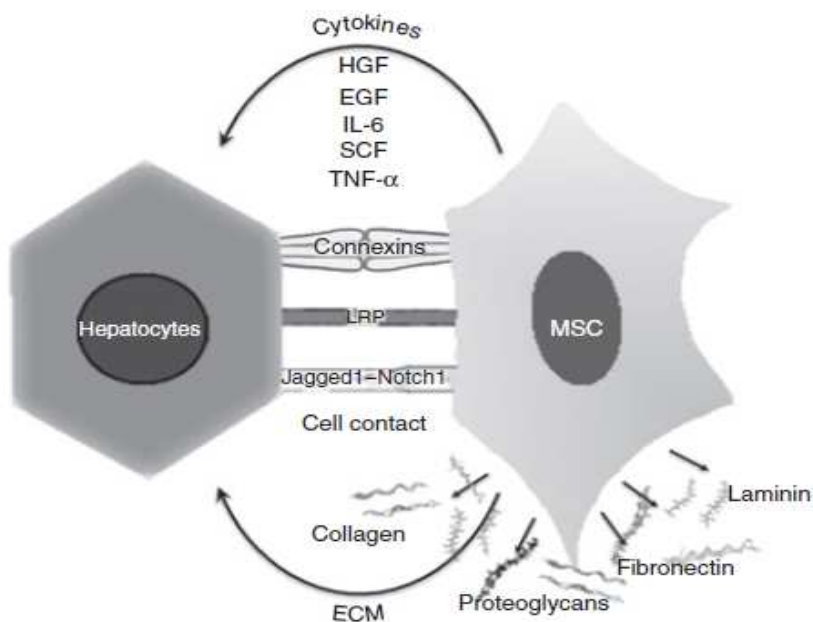


Figure 8: Mechanisms of interaction between mesenchymal stem cells and hepatocytes [59]

In addition, MSCs can be differentiated into endothelial cells. Wang et al. demonstrated the ability of murine embryonic mesenchymal progenitor cell line, C3H/10T1/2 to differentiate into cells that express mature endothelial cell-specific markers such as CD31 and von Willebrand factor [64]. This study used a parallel-plate system of fluid shear stress and concluded that the shear stress significantly induces expression of mature endothelial cells markers at both the mRNA and protein levels. Other researchers demonstrated this capability of MSCs obtained from different tissue sources when vascular endothelial growth factor (VGEF)

was added to the culture medium. Some examples of MSCs tissue sources are: umbilical cord Wharton's Jelly [65], porcine bone marrow [66], kidney [67], human bone marrow [68] and human adipose tissue [69].

Mesenchymal stem cells have been thoroughly investigated in the past decade to be used as potential treatments for acute liver failure and liver cirrhosis [60].

2.6 Porous Constructs and Dynamic Perfusion Systems

In vitro reconstruction of liver tissues is needed to enable the transplantation of tissue-engineered organs. In addition, there is an increasing demand for *in vitro* models that capture complex physiological and pathological events occurring in the liver [70]. Kasuya et al. [70] established a tri-culture model using the main three cell types occupying the space of Disse in their effort to mimic the natural environment for hepatocytes. The model consists of small hepatocytes (SHs), hepatic stellate cells (HSCs) and bovine pulmonary microvascular endothelial cells (ECs). SHs and HSCs formed organoids when cultured on microporous membranes were HSCs penetrated the pores and were distributed to the top surface of the membrane as well as between hepatocytes. After 14 days, ECs were seeded onto the top surface of the membrane and hence forming an architecture that resembles space of Disse where HSCs are located between the layers of hepatocytes and sinusoidal ECs. Their model was established in static conditions and they didn't evaluate the hepatic specific functions.

Dynamic perfusion systems have the advantage of producing an environment that mimics the hepatic sinusoid flow circuit, facilitating a differentiated phenotype, enhancing neo-vascularization and elevating mass transport capacities [25]. Additionally, cultures under continuous flow are more sensitive to hormone induced tissue function and have shown to

improve viability, lifespan, metabolic output and in vivo-like cellular reorganization [11]. Designing bioreactor systems in order to improve mass transfer rates of nutrients and oxygen to the seeded cells is required. It is also important in the process of removing metabolic wastes and acidic degradation products from the biodegradable scaffolds. Chen et al. [71] were able to culture primary hepatocytes within a galactosylated vegetable sponge in a packed-bed bioreactor system. In this study, two flow rates for the medium flow were compared; 18 ml/min and 34 ml/min. They found that at higher flow rates, hepatocytes performed better in terms of albumin and urea secretions over a culture period of one week and the reported rates were higher than other reported rates in the literature for similar systems; high enough to be compared to the normal rat liver secretion rates. They concluded that derivatization with galactose promoted cell-polymer and cell-cell interactions and enhanced differentiated state of the hepatocytes. Although their results showed a promising approach, it was limited due to lack of system tests for longer periods of time and in vivo studies. Also, their system doesn't provide solutions for the vasculogenesis issue for tissue engineered constructs. The major challenge yet to be solved in the dynamic perfusion systems is how to provide protection from excessive shear forces which hepatocytes may encounter; considering that this type of cells is a very sensitive type to very low shear forces.

2.7 Commercially Available Liver Models for Drug Screening

The main hurdle in re-creating liver-like environment is that freshly isolated hepatocytes have limited stability and the lack of hierarchy and structural components of the natural liver. Some existing animal models that use liver slices can maintain the natural structure but they fail to maintain the cell stability for long culture purposes. As it was mentioned before, monolayer

cultures of primary hepatocytes in the collagen sandwich configuration are the most commonly used format for toxicity assessment and provide a suitable model for initial assessment. They are yet severely hindered by the lack of: (1) cell–cell interactions either via direct contact or via paracrine effects, (2) 3D organization, and (3) non-parenchymal cells.

Nonetheless, freshly isolated primary hepatocytes continue to be the most relevant system to study in vitro drug metabolism and hepatotoxicity and provide an initial assessment of drug toxicity and enzyme function [72]. Figure 9 below summarizes six of the most recognized liver models for these purposes. In Figure 9a is a schematic diagram for the RegeneMed[®] model; it uses a transwell approach where non-parenchymal cells were seeded on a nylon screen sandwich insert, stabilized for a week, and then hepatocytes were added to form 3D liver tissue. This model uses near physiological ratio between hepatocytes and the non-parenchymal cells. Figure 9b illustrates the Insphero[®] model; hepatocytes were allowed to form 3D microtissue spheroids using gravity enforced cellular assembly. In this model, hepatocytes and non-parenchymal cells were introduced into a hanging drop in a specifically designed multiwell plate which forms a microtissue spheroid in three days. Hepatopac[®] model (Fig. 9c) features a co-culture of hepatocytes with fibroblasts. The hepatocytes were micropatterned in discrete islands in a 24-well plate surrounded and stabilized by the stromal cells. Figure 9d represents CellAsic[®] microfluidic liver sinusoid model. This model utilizes the lithography techniques to create an artificial endothelial cell like barrier to mimic the porous liver sinusoid. This model is successful in eliminating the need for endothelial cells and replacing them with a structural barrier which shields hepatocytes from shear forces while still allowing nutrient exchange. Zyoxel[®] (Fig. 9e) has the hepatocytes and non-parenchymal cells cultured in poly-carbonate scaffolds in multi-well plate platform. The media will flow from the reservoir to the reactor chamber by pneumatic

controlled underlay. The last example to mention here is the Hurel[®] approach (Fig. 9f); it is also a microfluidic model that incorporates multiple tissues to interact in a physiologically based pharmacokinetic model. This platform has the ability to accommodate multiple microfluidic microscale cell culture units and connect them to media reservoir and a pump. [72]

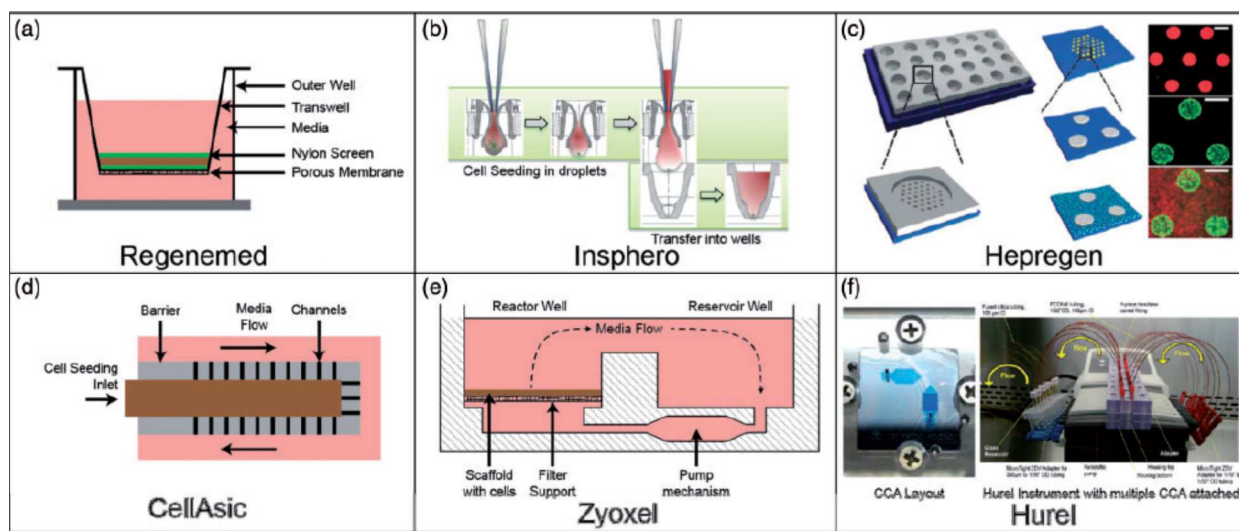


Figure 9: Liver models. Summary of the most recognized liver models to study in vitro drug metabolism and hepatotoxicity. [72]

2.8 Recent Hepatocyte Transplantation Research: Scaffold-less Approach

Because of the limitations on hepatocyte donors, researchers looked into using different types of cells like hepatocyte progenitor cells and stem cells; they injected them as cell suspensions at different injection sites. Injection site is very important to provide extracellular matrix (ECM) for hepatocyte growth and differentiation. This approach is only valid in cases of metabolic diseases and acute liver failure patients where the liver natural architecture is intact and the requirement of homing is avoided. Some injection sites are the portal vein, the inferior mesenteric vein and directly into the liver. It has been shown that the infused hepatocytes dispersed with the host portal blood and translocated into the hepatic sinusoids. A disadvantage

of this technique is that the infused cells were observed in central veins indicating an increased risk of embolization to the lung. It remains an important issue of liver-directed cell therapy; the localization and detection of the infused hepatocytes within the liver parenchyma of the host [73, 74] .

Takebe et al. [75] demonstrated a proof-of-concept of generating vascularized, functional human liver from human induced pluripotent stem cells (iPSCs) liver buds. They first prepared hepatic endoderm cells from human iPSCs by direct differentiation. The yield was about 80% of the treated cells that expressed the hepatic marker HNF-4 α . Then, they cultivated these cells with human umbilical vein endothelial cells (HUVECs) and human mesenchymal stem cells. The presumed human iPSC derived liver buds (iPSC-LBs) were mechanically stable and could be manipulated physically and they have formed endothelial network. To test whether human iPSC-LBs were capable of generating completely functional liver, the group transplanted them in a cranial window model. These buds connected quickly with host vasculature within 48 h of transplantation and formed vascular networks similar in density and morphology to those of adult livers. Moreover, human blood vessels within the transplant became patent (unobstructed) by connecting host vessels at the edge of the transplant. These human iPSC-LB transplants also exhibited hepatic cord-like structures that are characteristic of adult liver after 60 days and were able to produce albumin and metabolize drugs. This study demonstrated a proof-of-concept that organ-bud transplantation offers an alternative approach to the generation of three-dimensional-vascularized organs. In view of this, more in vivo models should be evaluated to prove the feasibility of this approach.

CHAPTER THREE

HYPOTHESES AND SPECIFIC AIMS

Liver transplantation is considered the optimal treatment for end-stage liver diseases. However, this is limited by the high demand for a matching donor which exceeds the availability, the high cost for both the surgery and the annual follow-up, and the need for a life-time immunosuppressant. Current treatments based on non-biological approaches like hemodialysis, hemoperfusion and plasma exchange have limited success in transforming this disease from fatal into treatable disorder. These therapies did not replace the metabolic and synthetic liver functions sufficiently. However, they provided more time for patients waiting for liver transplant and stabilize their medical conditions. The extracorporeal biological approaches such as cross dialysis and liver perfusion are hard to implement, but still provide sufficient solution. In the past two decades, many works have been done toward hepatocyte transplantation and hepatic tissue engineering. It is believed though that a hepatic mass of almost 10% (or even less) [10, 76] of the human liver is able to normalize many hepatic disorders and metabolic diseases. In this case, many liver patients could be treated with only one liver donor with minimal invasive surgery and less cost. The ability to reliably re-assemble isolated hepatocytes into a functional, “neo-organ” would greatly facilitate the development of such systems. However, tissue engineering of sizable implantable liver systems is currently limited by the difficulty of assembling three dimensional hepatocyte cultures of a useful size, while maintaining full cell viability which is closely related to the high metabolic rate of hepatocytes.

The main objective of this project is to develop tissue scaffold designs using biologically active materials and mesenchymal stem cell population for assembling isolated hepatocytes into

a functional, vascularized mini organ. **The proposed work is based on the following general hypotheses:** (A) hepatocytes in perfused porous scaffolds can produce an environment that mimics the hepatic sinusoid with high mass transport capacities, (B) Co-culturing hepatocyte cells with non-parenchymal cells; e.g. mesenchymal stem cells (MSCs) will limit hepatocyte large aggregation in the short term and promote angiogenesis in the longer term as well as shielding them against shear forces generated in the dynamic perfusion systems, and (C) Encapsulating hepatocytes with or without MSCs will protect them from excessive shear forces they will be exposed to under dynamic perfusion conditions; and will provide sufficient cell-ECM contact signal that will maintain hepatocyte polarity in three dimensional cultures.

These hypotheses will be tested in the following proposed experiments in order to develop systems for hepatocyte transplantation at a therapeutic level *in vitro* and *in vivo*. The Specific Aims of the project are to:

- 1) **Examine the effects of different scaffold designs and two cell seeding methods on hepatocyte distribution and viability in three dimensional, high-porous chitosan/heparin perfused scaffolds.** Optimization of cell seeding into three dimensional scaffolds is a major challenge for hepatic tissue engineering. The seeding method must be rapid to minimize the time that hepatocytes spend in suspension in order to maintain their viability. It should also allow highly efficient cell entrapment to maximize donor hepatocyte utilization. In addition, the seeded constructs should retain enough space for perfusion *in vitro* or vascularization *in vivo*.
- 2) **Evaluate the effects of co-culturing hepatocytes (HCs) with bone marrow mesenchymal stem cells (BM-MSCs) on hepatocyte specific functions and examine the effects of the seeding architecture on hepatocyte-MSCs organization and neo-**

tissue formation in-vitro. Recent reports of experimental findings have revealed the hepatic differentiation potential of MSCs in vitro . In addition, MSCs can provide a number of cues for hepatocyte growth and development .It is expected that co-culturing hepatocytes with this specific type of cells will enhance hepatocyte viability and their specific functions, as they will secrete and express certain proteins; connexin-43 and membrane-associated liver-regulating protein (LRP) for example, which are essentials in maintaining hepatocytes mature phenotypic state and their membrane polarity [59].

- 3) Evaluate the effects of encapsulating hepatocytes with or without bone marrow mesenchymal stem cells (BM-MSCs) within chitosan-GAG fibers on hepatocyte viability and metabolic performance under static and perfusion conditions.** Encapsulation will provide means of protection against shear forces under dynamic perfusion conditions. In addition, it will provide means of the required barrier between exogenous cells and the host immune system in the field of bioartificial-implantable organs.

CHAPTER FOUR

THE EFFECTS OF SCAFFOLD DESIGNS ON HEPATOCYTE DISTRIBUTION AND VIABILITY IN THREE DIMENSIONAL, CHITOSAN/HEPARIN SCAFFOLDS

4.1 Introduction

Optimization of cell seeding into three dimensional scaffolds is a major challenge for hepatic tissue engineering. The seeding method must be rapid to minimize the time that hepatocytes spend in suspension in order to maintain their viability. It should also allow highly efficient cell entrapment to maximize donor hepatocyte utilization. In addition, the seeded constructs should retain enough space for perfusion *in vitro* or vascularization *in vivo*. Porous scaffolds and dynamic perfusion systems can be designed to produce an environment that mimics the flow architecture of hepatic sinusoids, and elevates mass transport capacities, while facilitating efficient cell seeding. In this study, we compare two designs that aim to promote cell seeding efficiency by effectively entrapping 100 million cells (~10% of a rat liver) by maximizing either surface area for cell suspension inflow and subsequent perfusion culture, or volume for cell entrapment. Particular pore architectures may also promote vasculogenesis upon *in vivo* implantation if larger surface pores are available for vessel ingrowth.

The objective of this study was to modify the scaffold design developed by Dr. Matthew's group in previous studies, by changing the freezing methods used previously so that the new design will have large pores at the periphery (~500 μm), and small pores at the central (~10 – 20 μm). This new design will allow more vasculogenesis to the scaffold.

4.2 Experimental Work

4.2.1 Materials

Medium molecular weight (MMW) chitosan from crab shells (molecular weight about 190- 310 KDa with 75 - 85% Deacetylated chitin), Trypan blue, FITC-conjugated secondary antibody solution and heparin sodium porcine mucosa were purchased from Sigma-Aldrich (St. Louis, MO). CellTracker™ Green CMFDA Dye was purchased from Life Technologies (by Thermo Fisher Scientific Inc.). ZO-1 Rabbit polyclonal antibody and Rabbit anti-Connexin 32 were purchased from Invitrogen (by Thermo Fisher Scientific Inc.). All other chemicals and solvents were of analytical reagent grade.

4.2.2 Collagen (Type I) Extraction from Rat Tail Tendons

Type I collagen was extracted following the protocols described by Rajan et al. [77] and Elsdale et al. [78] with some modifications. Briefly, the tail was skinned first and then held by two surgical clamps about 5 mm from its thinner extremity (8 tails were used in each extraction). The collagen fibers (seen as white bundles) were then pulled and collected in a beaker with normal saline (0.9% NaCl) and then rinsed twice with deionized (DI) water. The tendons were then moved to a beaker containing 3% acetic acid and stirred overnight at 4°C; at this point the solution turned into more viscous one. The solution was then filtered through 4 layers of cheesecloth and centrifuged at 12,000g for 2 hours at 4°C. The supernatant was collected carefully into 2L beaker and the pellet was discarded. 30% NaCl (volume of 1/5 of supernatant volume collected) was slowly dripped from a burette and the solution was allowed to sit without stirring for 1 hour at 4°C. The solution then centrifuged at 4,000g for 30 min; pellets were collected and rinsed with 5%NaCl-0.6%acetic acid. This step was repeated two times. The pellets were finally

resuspended in 0.6% acetic acid and the solution was stirred for at least 48 hours at 4°C (or until all clumps were dissolved). The solution then dialyzed (in dialysis bags with clamped ends) against 1 mM HCl (10X volume), the 1mM HCl was replaced with fresh one every 4 hours for five times. After that, the collagen solution was collected from the bags and centrifuged at 12,000g for 2 hours at 4°C. 3/1000 of total volume of chloroform then added for sterilization purposes, the solution was stirred for 48 hours at 4°C with loosen cap. The collagen solution concentration was determined by reading the optical density of a sample using spectrophotometer at a wavelength of 280 nm. The OD then was divided by 0.09 to obtain the concentration in mg/ml unit.

4.2.3 Hepatocyte Isolation and Culture in Collagen Gel Sandwich Configuration

Male, *Sprague Dawley* rat weighing 230 to 300 grams was used as cells donor. Hepatocyte cells (HCs) were isolated using the two-step collagenase perfusion procedure described by Seglen [79] and modified by Dunn et al. [28]. HCs viability and cell count were determined by Trypan blue exclusion test and it was 90%. A single isolation typically yields 500 to 800 million hepatocytes with viability around >85% as indicated by Trypan Blue exclusion test of cell viability. The collagen gel sandwich culture was used; in this configuration hepatocyte cells were seeded onto collagen gel pre-coated culture dishes (1 million cells per 60-mm tissue culture dish) and subsequently overlaid with a second layer of collagen gel after few days of incubation at 37°C and 5% CO₂, the protocol suggested applying the second layer after 24 hours of incubation, but longer time was given to allow all dead cells to de-attach and subsequently removed from the culture [28]. The culture medium for HCs consisted of Dulbecco's modified eagle medium (DMEM)- high glucose supplemented with 18.52 mg/L

insulin, 7 mg/L glucagon, 7.5 mg/L hydrocortisone, 40 mg/L L-proline, 50 mg/L gentamicin , 2.5 mg/L Fungizone, 10% fetal bovine serum and 10 ng/ml EGF [80] and it was changed every day. The collagen gel sandwich configuration system was the control for all experiments in this work.

4.2.4 Hepatocyte Membrane Polarization Assessment via Immunofluorescence

Connexin 32 is a gap junction protein expressed in polarized hepatocytes that plays important role in regulating signal transfer and growth control in the liver by constructing gap junction channels and gap junctional intercellular communication [81]. ZO-1 is a tight junction protein that is expressed in the plasma membrane of polarized epithelial cells and plays an important role in sealing together the perimeters of polarized membrane and provides the paracellular barrier necessary to maintain absorption, secretion, and transport [82]. The bile canaliculi can be fluorescently labeled by using CellTracker™ Green CMFDA Dye; 5-chloromethylfluorescein diacetate (CMFDA) is a fluorescent dye that stays in the cell cytosol when hepatocytes are non-polarized and lack the canaliculi network, and is excreted into the bile canaliculi network when it is formed by the polarized hepatocytes [83].

Hepatocytes in collagen gel sandwich were fixed with 10% formaldehyde, washed with cold FBS three times and then incubated with 1% BSA/PBS w/v blocking solution at 4°C overnight. Cultures were then incubated with primary antibody; either rabbit anti-Connexin 32 reactive for rat CX 32 or ZO-1 rabbit polyclonal antibody used as manufacturer directions. The primary antibodies were washed away and a FITC-conjugated secondary antibody solution in added and cultures were incubated overnight at 4°C. DAPI solution was added for nuclei staining in blue color.

CellTracker™ Green CMFDA Dye was applied following the manufacturer directions. Briefly, the dye powder was dissolved in DMSO to make 10 mM stock solution then diluted with serum free culture medium to make 25 μ M working solution. The hepatocytes in cell suspension were incubated with pre-warmed working solution for 30 minutes in 15 ml centrifuge tube, centrifuged at 300 rpm for 5 minutes, resuspended with fresh pre-warmed medium, and finally seeded into the pre-coated culture dish with collagen gel.

Fluorescent images were taken using the phase contrast microscope and Nikon digital camera.

4.2.5 Hepatocyte Metabolic Functions Assays (Albumin and Urea Secretion)

Metabolic performance of cultured hepatocytes was evaluated by measuring: (1) the rate of albumin secretion via Enzyme-linked immunosorbent assay (ELISA) using antibody specific to rat albumin and (2) the rate of urea secretion using diacetyl- monoxime colorimetric method described by Rozet et al. [84] and. Sample collection and medium change was performed every day for the whole period of cultures. These assays were performed in every experiment done in this whole work.

4.2.6 Bulb-Shape Scaffold Fabrication, Cell Seeding and Cell Distribution Evaluation

Chitosan (1.5 wt% medium molecular weight 90% deacetylated) was dissolved in 0.2 molar acetic acid. Then liquid Nitrogen was perfused through a hollow stainless steel rod and immersed in the chitosan solution (Fig. 10). This allowed the chitosan solution to freeze from the inside towards the outside resulting in radially oriented pores with pore size of 20-50 μ m at the

center and 500-800 μ m at the periphery. After freezing, the scaffold was lyophilized, neutralized with 5% ammonia solution and then washed several times with phosphate buffer saline (PBS).

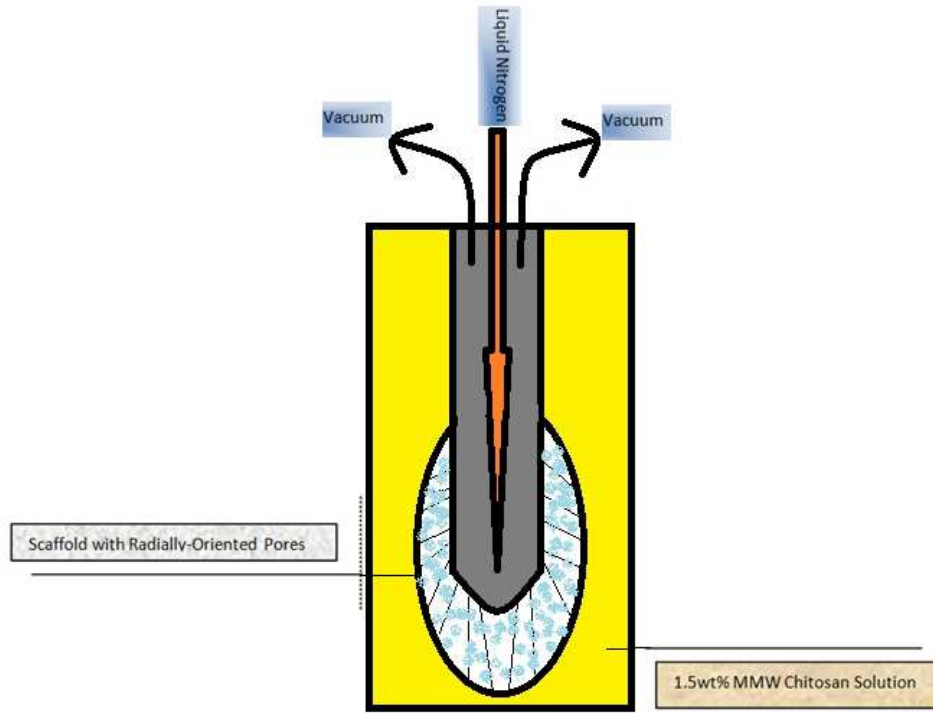


Figure 10: Scaffold fabrication. Schematic diagram of the scaffold fabrication setup.

To have an idea about how the cells were distributed inside the new scaffold microstructure; fixed hepatocytes (in 10% formaldehyde solution) were seeded at a density of 3 million cells /ml using bioreactor setup (Fig. 11) with a peristaltic roller pump at a flow rate of 2 ml/min. As pores at the periphery were larger and got smaller towards the center, the direction of flow was adjusted to be from the outside towards the center, where the cell suspension was drawn into the inside of the scaffold core. The seeded scaffolds were then processed for histology. Briefly, seeded scaffolds were fixed with 10% formaldehyde, dehydrated through a series of graded alcohols (starting with 70% and finishing with 100%), cleared with Xylene (three washes with final one lasts for 24 hrs), and embedded in liquid paraffin under vacuum.

Eight micrometer thickness sections were obtained using the microtome, deparaffinized with Xylene, and rehydrated through a series of graded alcohol (starting at 100% and finishing with 70%). Hematoxylin and Eosin stain (H&E) was applied to get an insight of cell distribution and tissue structure using phase contrast microscopy and capturing digital color images with Nikon digital camera.

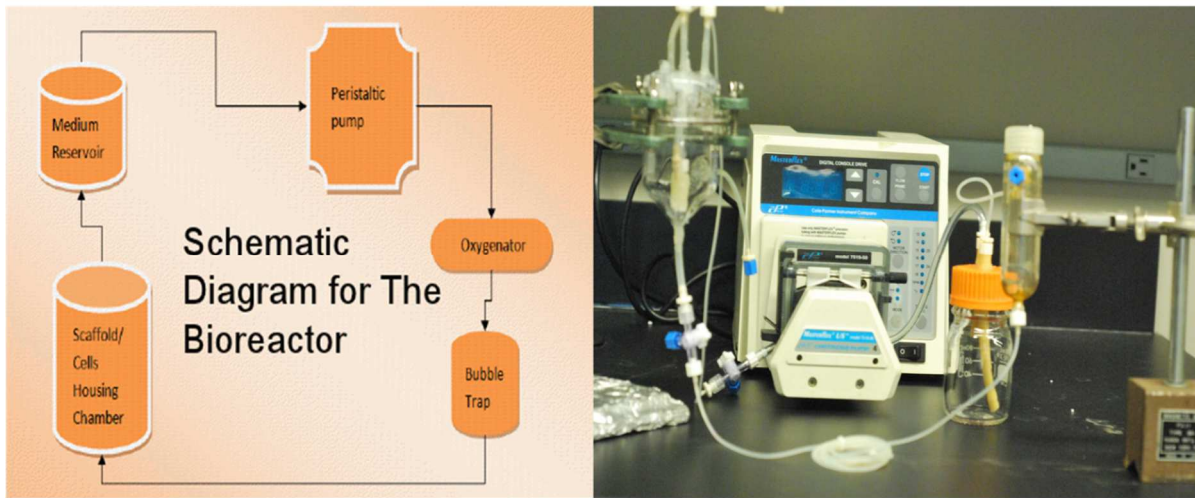


Figure 11: Perfusion Bioreactor System.

4.2.7 Surface Freezing and Central Freezing Scaffolds Fabrication, Cell Seeding and Cell Distribution Evaluation

The old design (surface freezing method) used in our group previously was obtained by filling chitosan solution in annular stainless steel mold and immersing it in isopropanol/dry ice bath allowing the inward radial growth of ice crystals from the surface into the central port (Fig. 12). The new proposed design (central freezing method) was made by filling chitosan solution in the same annular stainless steel mold and then started freezing by perfusing liquid nitrogen through the central channel. This technique allowed the outward radial growth of ice crystals

from the rod into the solution (Fig. 12). The frozen masses were then lyophilized to remove all water crystals leaving behind a network of interconnected microchannels. All scaffolds were derivatized with pre-activated heparin with EDC for 24 hrs, washed three times with PBS to remove excess heparin and incubated with FBS for 24 hrs prior to cells seeding to maximize protein attachment adsorption on the pores' surfaces. All washing steps were carried out in the bioreactor system at flow rate of 5 ml/min.

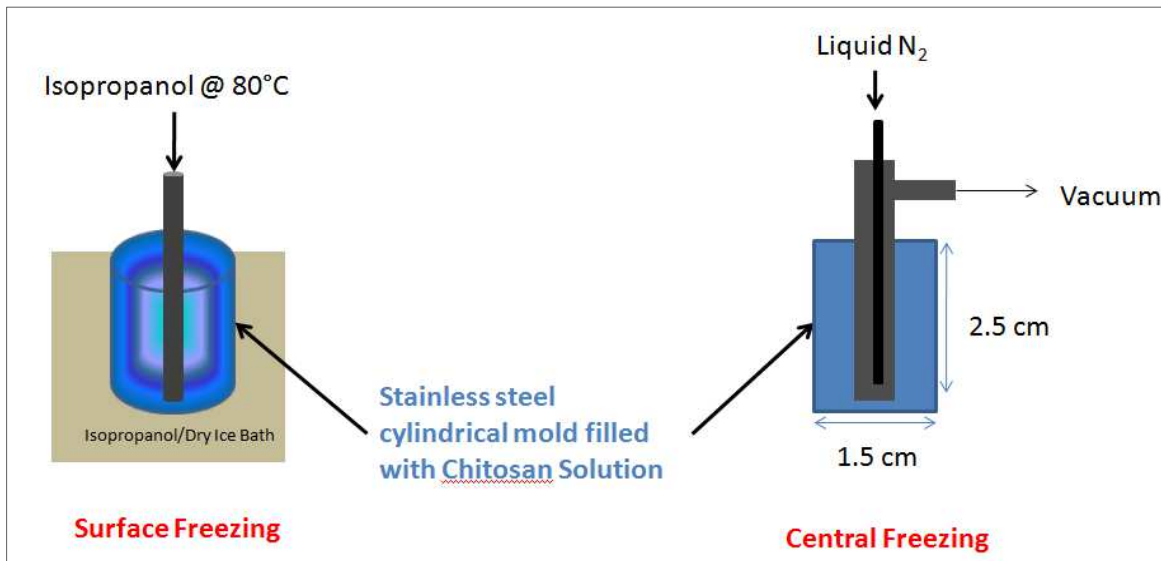


Figure 12: Schematic diagram illustrating the fabrication method for the two scaffold's designs

To estimate the seeding efficiency, the two designs then were seeded with the same cell concentration (5 million cells /ml) as illustrated in Fig. 13. The surface frozen scaffold had the flow directed from central port outwards the periphery and the central frozen scaffold had the flow directed from outside towards the central port. Hepatocyte distribution inside the pores and scaffold loading efficacy were examined by histology methods. The cell concentration used was 5 million cells /ml according to the results of our previous studies [35]. The results showed that higher total cell number with lower seeding concentration yielded higher retention of cells with more homogenous distribution inside the scaffold (i.e. 180 million cells at 5 million cells/ ml).

Seeding time was set to 2 hours and the seeding efficiency was calculated by counting the leftover cells that were not seeded during that time. Digital images from histology sections were extrapolated using ImageJ[®] software to calculate the seeding efficiency based on the number of cells counted in each image, the average volume per photo, and the total volume of the scaffold.

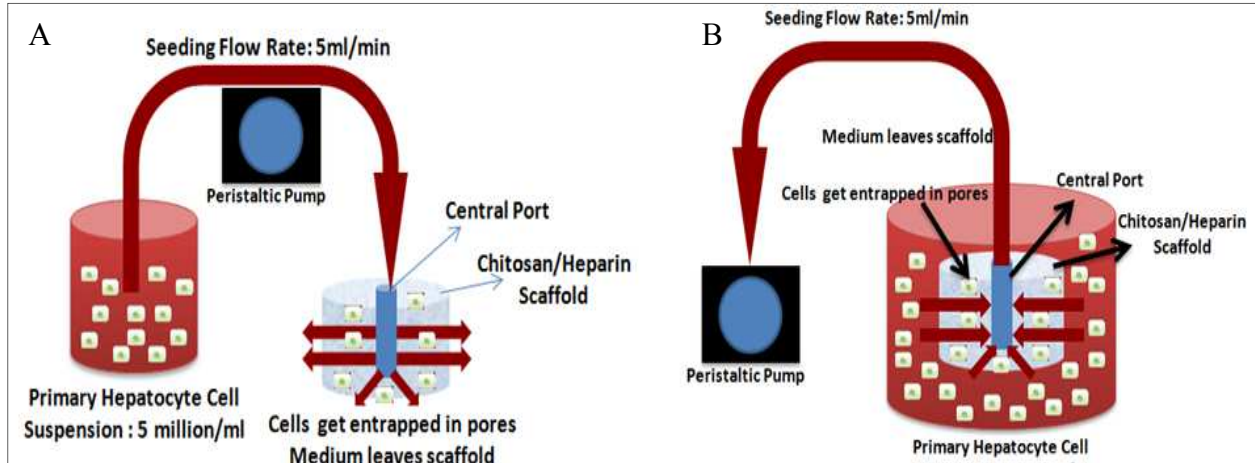


Figure 13: Bioreactor setup for seeding hepatocytes into the scaffolds. Schematic diagram illustrating seeding methods for the two scaffold's designs; (A) surface frozen, and (B) central frozen scaffolds.

4.2.8 Volumetric Flow Rate Calculations

The volumetric flow rate was calculated based on the physiological shear stress and cross-sectional area available for flow for the empty pores for each design. A single pore was assumed to be cylindrically shaped; for the surface frozen scaffold there were two different layers of pore sizes; at outer surface and at inner surface. For the central frozen scaffold there were three layers (Fig. 14).

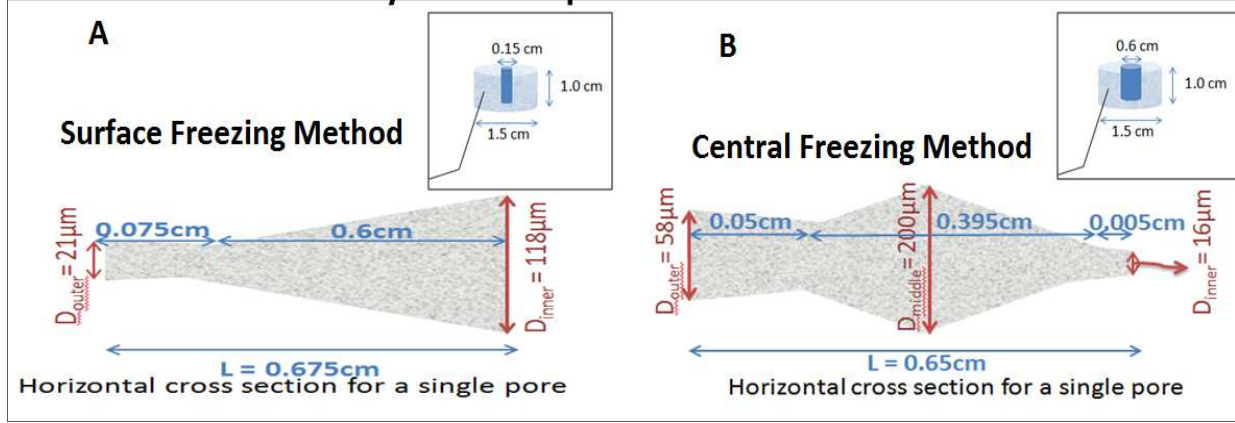


Figure 14: Pores architectures and dimensions. Schematic diagram illustrating the dimensions of all pores in all layers for the two scaffold's designs.

Physiological shear stress ranges between 0.5 Pa (at the sinusoids) up to 2 Pa (5 to 20 dyne/cm²) [85]. By choosing the lowest value $\tau = 5 \text{ dyne/cm}^2$ and applying equation of continuity for a cylinder, the volumetric flow rate in a single pore can be calculated using the following formula:

$$\tau = \frac{6 \cdot \mu \cdot \dot{V}}{\pi \cdot l \cdot r^2}$$

Where;

- l : is the length of a given zone.
- r : is the radius of a pore in a given zone.
- μ : is the viscosity of the blood (~water) = 10 dyne.sec/cm².
- \dot{V} : is the volumetric flow rate (cm³/min).

And the total number of pores at each layer can be calculated using the following:

$$\text{Total \# of pores} = \frac{2 \cdot \pi \cdot R \cdot L}{\pi \cdot r^2}$$

Where;

- L : is the length of the scaffold (1.0 cm).
- R : is the radius of the scaffold at a given zone.

The volumetric flow rate for the **surface frozen scaffold** was calculated to be **1.8 ml/min** for the outer layer and **5.67 ml/min** for the inner layer. And for the **central frozen scaffold** it was **1.2 ml/min** for the outer layer, **6.0 ml/min** for the middle layer and **0.05 ml/min** for the inner layer.

However, and based on oxygen requirements uptake for hepatocytes, the flow rate was calculated using the basic mass transport equation [3, 86, 87]:

$$V = k(P_i - P_o) \left(\frac{Q}{n} \right)$$

Where;

- V : is max. O_2 uptake = 0.38 nmol/s/ 10^6 cells.
- k : is the solubility of oxygen in saline under 21% O_2 and atmospheric pressure = 1.19 nmol/mL/mmHg.
- P_i : is the measured partial pressure (mmHg) of oxygen in the inlet stream of the bioreactor.
- P_o : is the measured partial pressure (mmHg) of oxygen in the outlet stream of the bioreactor.
- n : is the number of cells entrapped in the scaffold (100 million cells).
- Q : is the volumetric flow rate (ml/min).

If P_i was set to be 158 mmHg (partial pressure of O_2 at atmospheric pressure) and P_o was considered to be the typical physiological oxygen partial pressure found in the perivenous zone (25–35 mmHg) [3], then the flow rate should be adjusted to 14.4 ml/min for future cultures to

meet the oxygen requirements uptake for hepatocytes and hence they don't suffer from hypoxia inside the scaffolds.

4.3 Results

4.3.1 Hepatocyte Morphology and Metabolic Functions in the Collagen Gel Sandwich Configuration

The hepatocytes formed a monolayer with a well-connected cellular network and bile canaliculi formation between adjacent cells as seen under the phase contrast microscope (Fig. 15) and when Green CMFDA CellTracker™ dye was used (Fig. 16). They expressed the gap junction protein connexin 32 (Fig. 17) and the tight junction protein ZO-1 (Fig. 18); which indicated that they were able to reconstruct the plasma membrane polarity in this configuration.

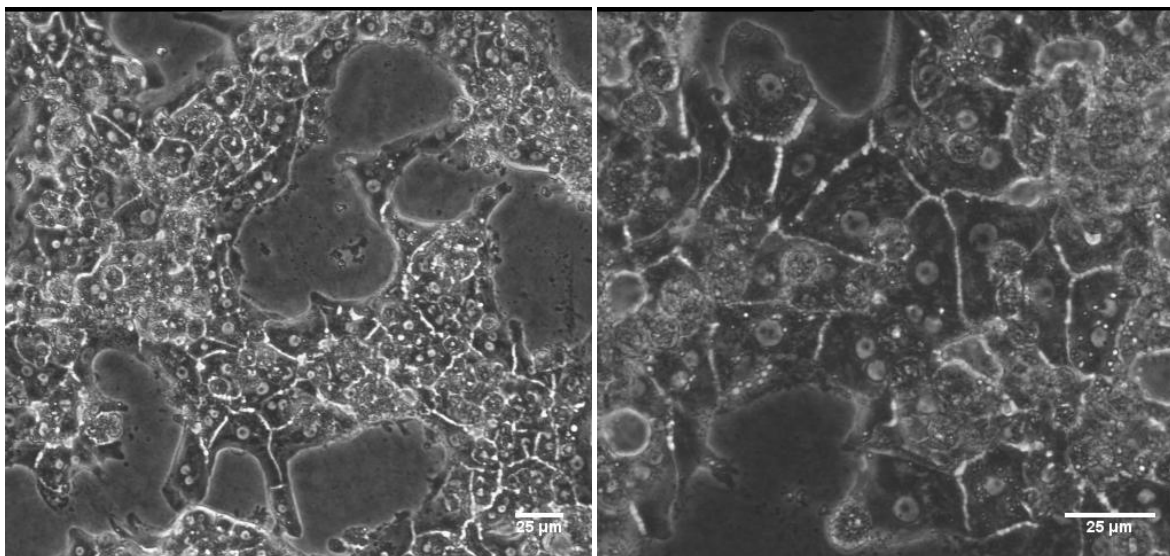


Figure 15: Phase contrast images for hepatocyte in collagen gel sandwich configuration culture.

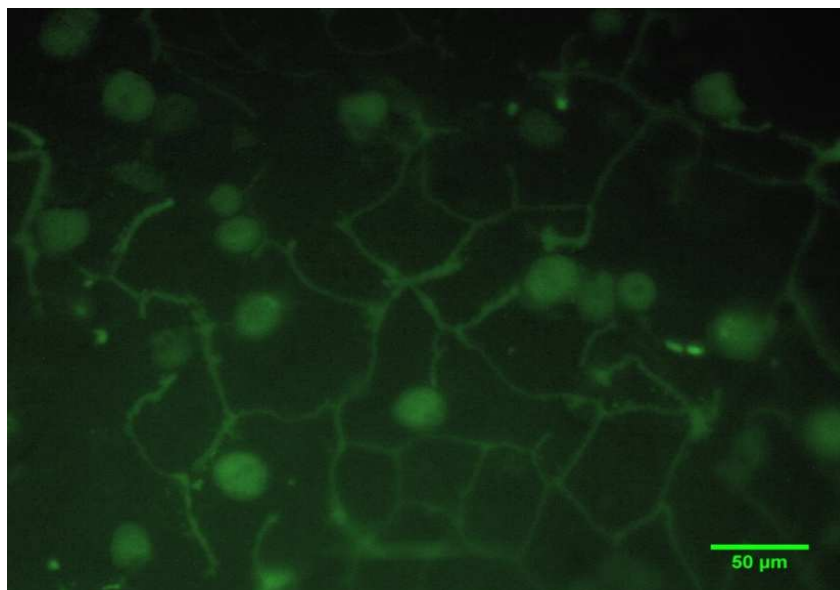


Figure 16: Green CMFDA CellTracker™ labeling. Fluorescent image of hepatocytes in collagen gel sandwich system labeled with Green CMFDA CellTracker™ dye illustrating the formation of bile canaliculi.

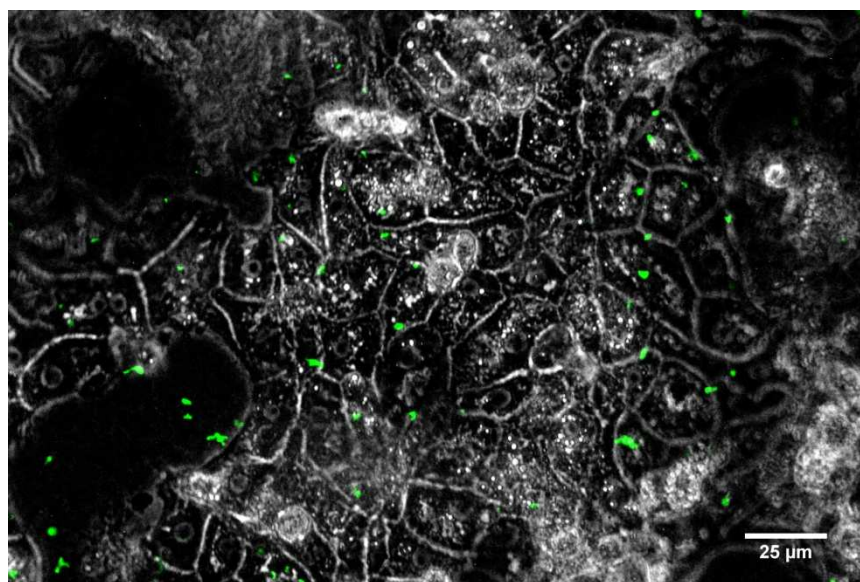


Figure 17: Gap junction Connexin32 labeling. Fluorescence image of hepatocytes in collagen gel sandwich system labeled with anti-Connexin32 - FITC conjugated (green) illustrating the formation of gap junctions between adjacent cells.

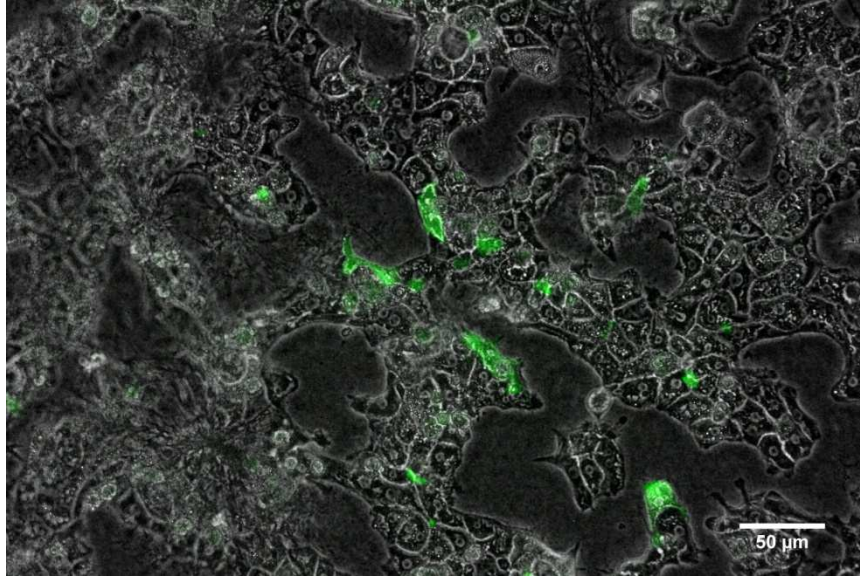


Figure 18: Tight junction ZO-1 labeling. Fluorescent image of hepatocytes in collagen gel sandwich system labeled with anti-ZO-1- FITC conjugated (green) illustrating the formation of tight junctions the membranes of some cells.

Hepatocytes were able to synthesize albumin (Fig. 19A) and secrete urea (Fig. 19B) in levels that match the reported ones in literature for the collagen gel sandwich static cultures [28].

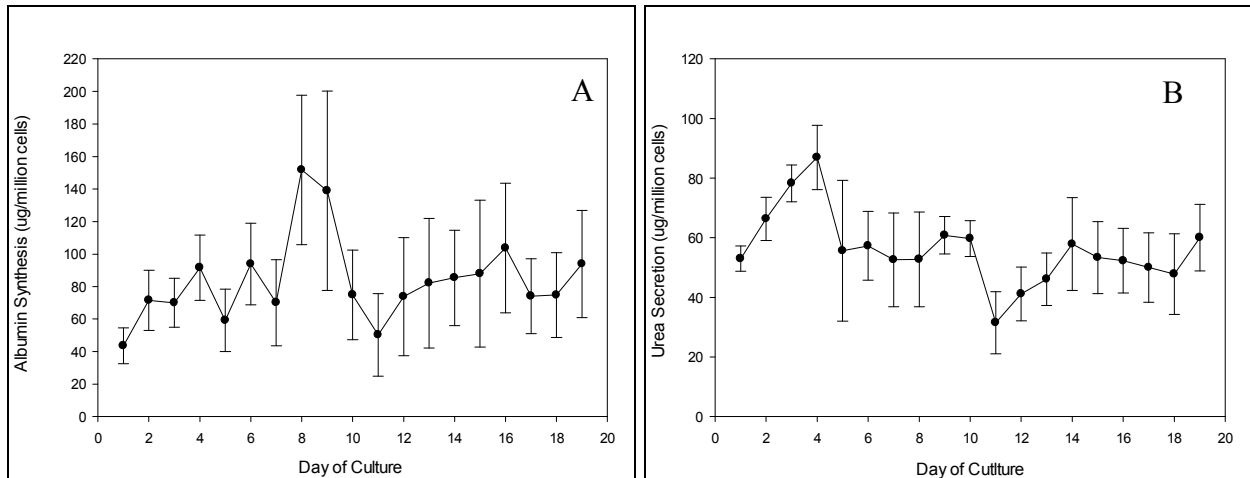


Figure 19: Metabolic assays of hepatocytes in collagen gel configuration. (A) Albumin secretion for hepatocyte culture in collagen gel sandwich configuration. (B) Urea secretion for the same cultures.

4.3.2 Bulb-Shape Chitosan Scaffold Microstructure and Seeding Efficiency

Scanning electron microscopy was performed to evaluate the pore size of the new proposed design and the microstructure architecture (Fig. 20). The pores were tapered- radially oriented with larger diameters at the outer surface ($D_{\text{outer}} = 152.905 \pm 27.101 \mu\text{m}$), and small ones at the inner surface ($D_{\text{inner}} = 49.173 \pm 11.071 \mu\text{m}$) as evaluated using SigmaScan Pro[®] software.

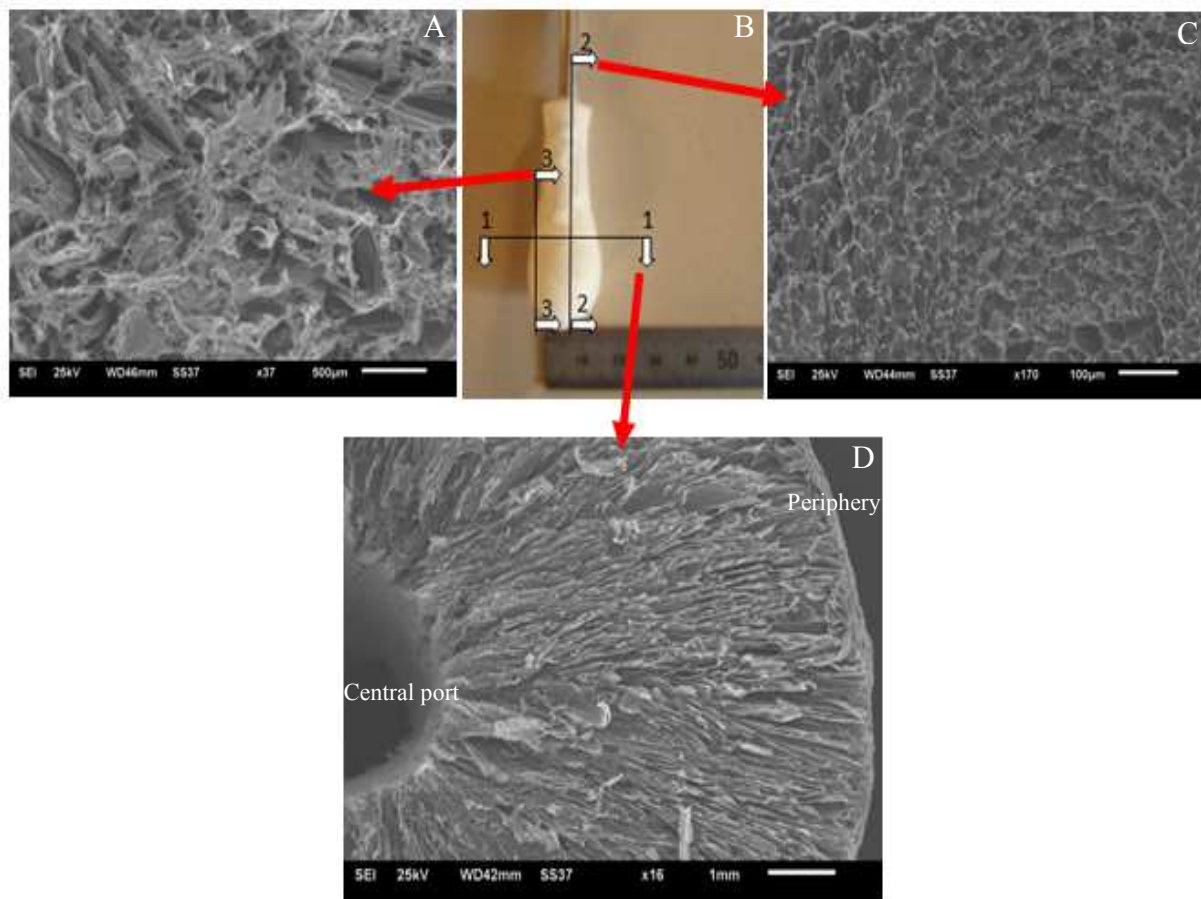


Figure 20: Scanning electron microscopy images for the bulb-shaped scaffold. (A) Periphery of the scaffold (outer pores, view #3), (B) digital image of the actual scaffold where the numbers and connecting lines represent cut sections of the scaffold and the white arrows represent directions of view, (C) inner surface of the scaffold at central port (inner pores, view #2), and (D) cross sectional view of the scaffold showing the radially oriented pores (large at periphery and smaller at center, view #1).

The size of the scaffold can be controlled by controlling the time of liquid nitrogen perfusion. The desired size was estimated to be around 1.5 cm in diameter and 1.0 cm in length.

This size was chosen as a reasonable one for transplanting the target cell quantity (100 million hepatocytes ~10% of rat liver mass) into the peritoneal cavity of a rat weighing approximately 300 grams for in vivo studies. This number of hepatocytes was chosen based on the fact that a rat of these species needs 12% to 23% of the whole liver mass to stabilize metabolic diseases [76]. The seeded cells were more in number at the center of the scaffold compared to the peripheries, but it seems that the central pores were blocked as seen in the histology images (Fig. 21).

One big challenge was encountered in this new design; the scaffold was collapsing due to pressure drop inside the pores and central port during seeding. This maybe because the pores were not successfully evacuated from air before starting seeding or they were blocked. Modification to the fabrication method was applied; before immersing the metal rod in the chitosan solution, liquid nitrogen was allowed to perfuse for few minutes to start the ice crystal formation. This step was important to prevent the formation of thin sheet of chitosan around the central port; which causes the pores to be closed at that site. However, this modification did not yield successful results as expected as the collapsing issue was not resolved.

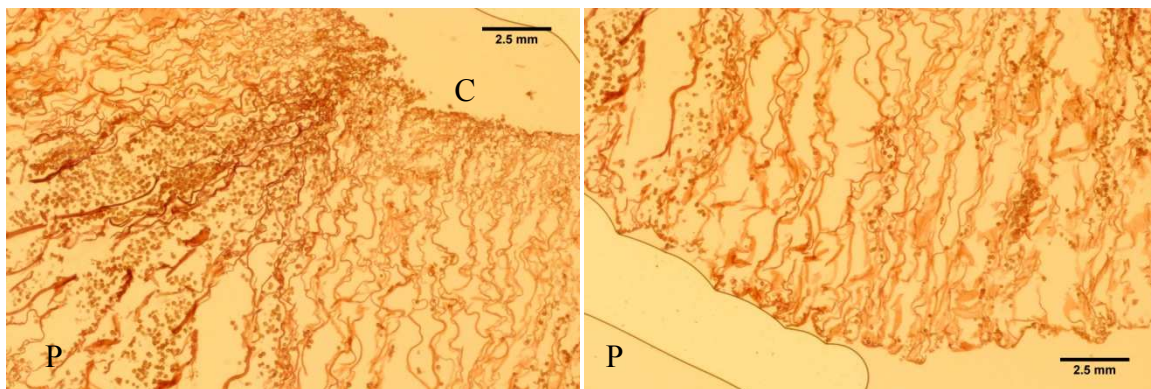


Figure 21: H&E histology images of seeded scaffold. The images show the cells condensed in the center [C] and less at peripheries [P]. It also seems that the central pores were sealed with a thin layer of material.

4.3.3 Comparison between Two Scaffold Designs: Surface Freezing or Central Freezing

The directional freezing and lyophilization technique created highly porous structures with tapered, radially-oriented pores (Fig. 22) with bigger pore diameter at the central port ($D_{\text{inner}} = 118.15 \pm 55.27 \mu\text{m}$) and smaller pore diameter at the outer surface ($D_{\text{outer}} = 21.35 \pm 6.41 \mu\text{m}$) for the surface freezing method. For the central freezing methods the pores have larger diameters at the middle ($D_{\text{middle}} = 201.53 \pm 50.62 \mu\text{m}$), medium diameters at the outer surface ($D_{\text{outer}} = 58.42 \pm 14.14 \mu\text{m}$), and small ones at the inner surface ($D_{\text{inner}} = 16.89 \pm 7.71 \mu\text{m}$) as estimated from the SEM images and using ImageJ[®] software.

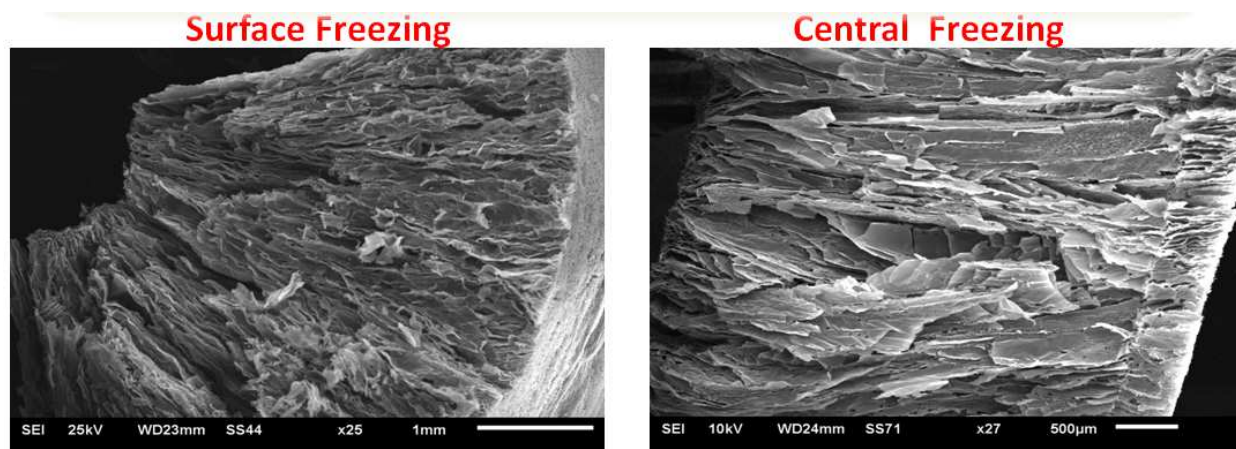


Figure 22: SEM images of two designs. The images show tapered, radially-oriented pores in both fabrication methods

The total volume of the surface frozen scaffold was 1.77 cm^3 and for the central frozen scaffold was 1.48 cm^3 . The seeding efficiency for the surface frozen scaffold was about 78%, with a cell density of $44.1 \times 10^6 / \text{cm}^3$. The seeding efficiency for the central frozen was about 65%, with a cell density of $43.9 \times 10^6 / \text{cm}^3$. The predicted seeding efficiency using ImageJ[®] software for the surface frozen scaffold was 99% and 68% for the central frozen one. The

targeted number of total cells to be loaded to the scaffold was 100 million cells (~10% of rat liver mass).

Histology images showed that the cells were distributed all along the cross sectional area in the surface frozen scaffold (Fig. 23A), while in the central frozen scaffold many pores were empty with cells more condensed at the center (Fig. 23B).

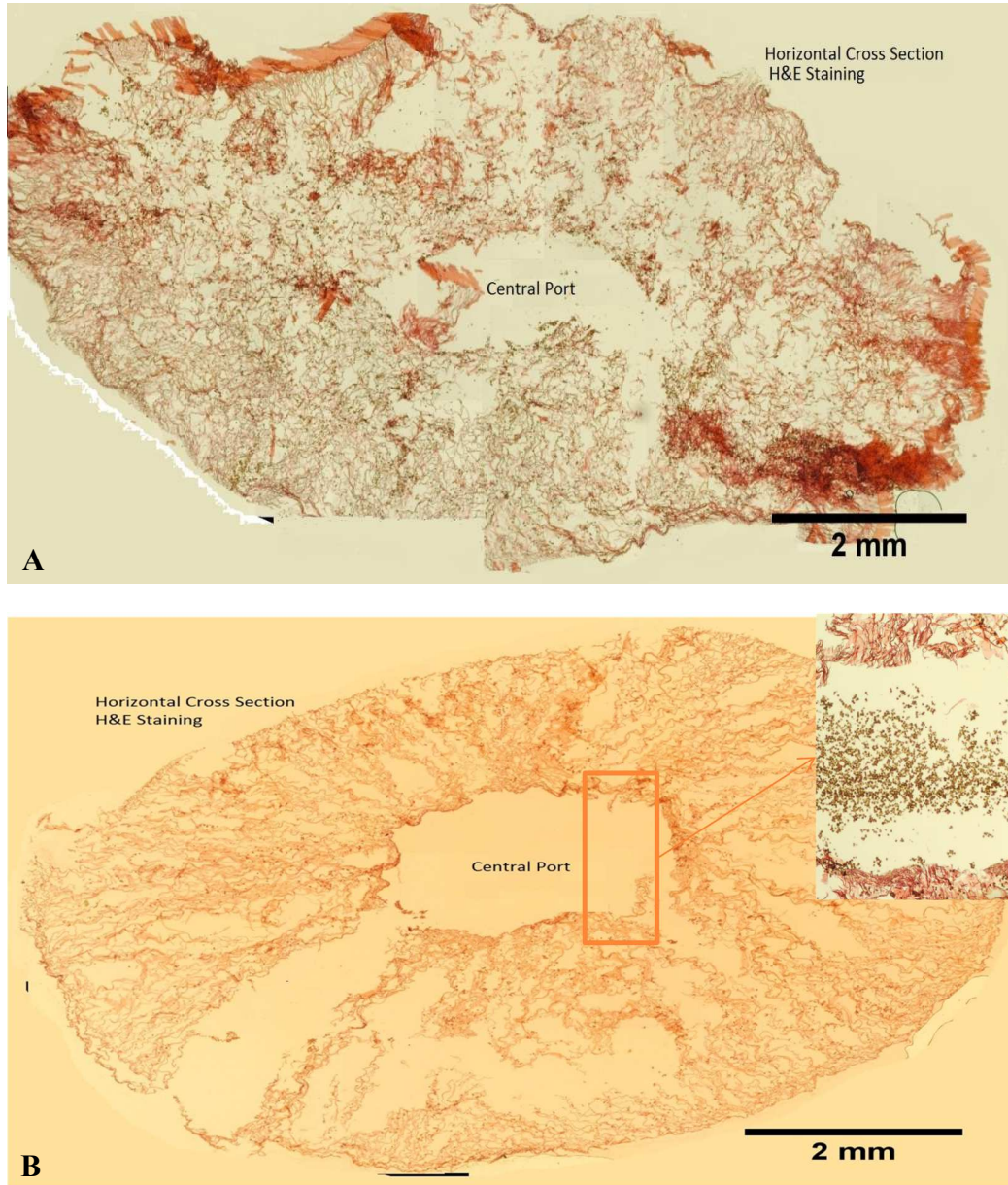


Figure 23: H&E staining images of cross sectional areas for seeded scaffolds. (A) Surface frozen scaffold. (B) Central frozen scaffold.

In yet another modification to the fabrication method to prevent scaffold collapse in the central-freezing method, we adapted the following changes: (1) placing annealed chitosan fibers (as they have high mechanical strength properties) at the center port to keep it open and (2) placing a supportive nylon mesh at the center port. Despite this, the collapsing issue remained unresolved as indicated by the collapse of the scaffold in radial direction, instead of axial. Support to individual pores was needed to reinforce the whole scaffold, which might not be a feasible option.

4.3.4 Metabolic Functions for Hepatocytes in the Surface Freezing Scaffold

In view of the challenges encountered in the central frozen design, the surface frozen design was adapted for the all experiments hereafter in this project.

The chosen 1.8 ml/min flow rate was not sufficient to pull up the cells and circulate them, so the seeding flow rate was changed to 5.6 ml/min. But after seeding, the flow rate was set back to the 1.8 ml/min and the culture was run for five days. Scaffold cultured hepatocytes synthesized albumin (Fig. 24A) and secreted urea (Fig. 24B) but at depressed rates compared to hepatocytes in collagen-sandwich dish cultures, and rates declined with time.

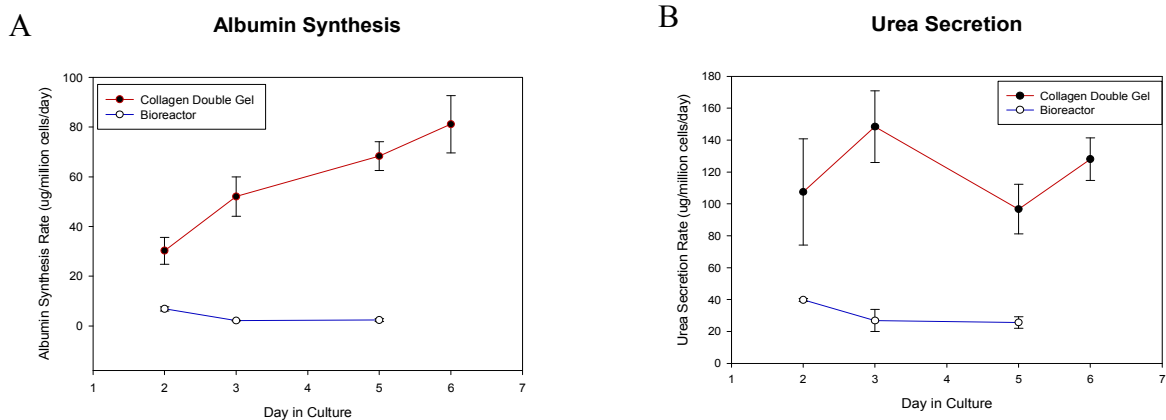


Figure 24: Metabolic functions for scaffold cultured hepatocyte in the surface frozen scaffold at 5.6 ml/min seeding flow rate and 1.8 ml/min culturing flow rate. (A) Albumin synthesis rate. (B) Urea secretion rate.

4.4 Discussion

To successfully design a three dimensional bioartificial liver, one should take into consideration the cell source and the design of the three dimensional scaffold that will create suitable environment for cells to attach and function. The challenges in the field of bioreactor designs for 3D perfusion cultures are focused on the need to provide an appropriate scaffold for tissue morphogenesis. The scaffold design must ensure relatively homogeneous distribution of flow and mass transfer throughout the system. This was important in order to meet the metabolic demands of the cells, as well as the physiological shear forces generated by such flow. In order to achieve the desired cellular structure, hepatocytes must attach preferentially within the pores/microchannels with sufficient strength to withstand both tissue remodeling forces and fluid shear stress forces generated by in the perfusion system [88, 89].

Powers et al [89] suggests that in order to design a sufficient reactor perfusion systems; tissue formation and cell behavior should not depend on the spatial arrangement or location of channels within the microstructure of a given system. In addition, the system should approximate the architectural properties and the perfusion conditions present in the natural hepatic tissue.

Here, we describe the design, fabrication methods, and flow rates calculations for chitosan-heparin scaffolds. The scaffolds were highly porous with tapered, radially-oriented pores and the pores architectures and dimensions can be controlled by controlling the freezing direction to meet a desired design for a specific system. The microstructure of these highly-porous scaffolds provides large surfaces for cells to attach as well as facilitating nutrient and oxygen transportation.

The flow rate of culture medium in the bioreactor was chosen to provide a physiological range of fluid shear stresses within the pore geometry for the surface frozen scaffold design. However, calculations based on hepatocyte oxygen uptake rates suggested that the operating

flow rate (1.8 ml/min) was insufficient to meet hepatocyte oxygen requirements. In addition, seeding with single cell suspensions may have resulted in uncontrolled cell aggregation and poor oxygen and nutrient diffusion within the cell mass.

When Li et al [26] cultured primary rat hepatocyte into chitosan-alginate and chitosan-heparin porous scaffolds, they didn't expose the cells to any kind of flow and the hepatocytes synthesized albumin and secreted urea at higher levels than hepatocytes in monolayer configuration. This suggests that in our system, hepatocytes were exposed to high shear forces that may have lead to cell death.

4.5 Conclusions and Future Work

- With regards to central frozen scaffolds; many issues remain unsolved regarding scaffold collapsing due to pressure drop in the pores during seeding process, so we adapted the surface freezing method.
- Seeding efficiency for surface frozen scaffold was higher than central frozen.
- Operating at flow rate of 1.8 ml/min was insufficient to meet hepatocyte oxygen requirements in the surface frozen design.
- Seeding with single cell suspensions may have resulted in uncontrolled cell aggregation and poor oxygen and nutrient diffusion within the cell mass.
- Modifications to the perfusion system can be made to maintain the hepatic specific functions in vitro; i.e. co-culture with non-parenchymal cells and encapsulation of growth factors into the scaffold.

CHAPTER FIVE

THE EFFECTS OF CELL SEEDING ARCHITECTURE ON HEPATOCYTE DISTRIBUTION AND VIABILITY IN CHITOSAN/HEPARIN SCAFFOLDS

5.1 Introduction

In vitro assembly of functional liver tissue is needed to enable the transplantation of tissue-engineered organs. In addition, there is an increasing demand for *in vitro* models that replicate complex events occurring in the liver. It has been shown that hepatocytes in perfused porous scaffolds can produce an environment that mimics the hepatic sinusoid with high mass transport capacities [25]. Single cell suspensions of hepatocytes may not offer the appropriate cell-cell interaction that is necessary to maintain hepatocyte survival and maintenance of differentiated state. If seeded on non-adherent surface (or in 3D environment), hepatocytes will spontaneously aggregate into spheroids that may exceed 400 μm in diameter and hence develop necrotic center. The advantages of culturing primary hepatocytes as spheroids can be summarized as follows: (1) maintain the structural polarity of cells, (2) maintain the functional bile canaliculi formation, and (3) maintain the differentiated functions of the hepatocytes. Therefore, hepatocyte spheroids are expected to create an efficient 3D tissue models for hepatic studies *in vitro* and can be used as the cell source in many therapeutic, diagnostic and discovery applications as in case of developing bioartificial liver [90].

In the present study, we compared two seeding architectures; single cell suspension and pre-formed spheroids that aimed to promote cell seeding efficiency by effectively entrapping 100 million cells (~10% of a rat liver). Hence, spheroid size can be controlled to produce spheroids of ~100 μm in diameter (which will not develop necrotic center [91]) and then used those to seed

the scaffold. It was shown previously that hepatocytes in aggregates can maintain viability and functional integrity for months [92, 93].

5.2 Experimental Work

5.2.1 Materials

Lactate Dehydrogenase Activity (LDH) Kit was purchased from Sigma-Aldrich (St. Louis, MO). AlamarBlue® Cell Viability Reagent was purchased from Invitrogen (by Thermo Fisher Scientific Inc.). All other chemicals and solvents were of analytical reagent grade.

5.2.2 Seeding with Single Cell Suspension

The bioreactor setup, illustrated in figure 16 from previous chapter, was used to seed the scaffolds with cell suspension (and later to perfuse the culture medium) using different seeding setups. The target number of hepatocytes to be seeded was 100 million per one scaffold. Based on the previous analysis and calculations, three seeding setups were performed to evaluate the effects of seeding flow rate and culturing flow rate on hepatocytes metabolic performance and neo-tissue formation and organization.

1. **Setup #1:** Circulating seeding at 37°C for 2 hours at flow rate of 5 ml/min and culture at 10 ml/min.
2. **Setup #2:** Circulating seeding at 37°C for 2 hours at flow rate of 20 ml/min and culture at 15 ml/min.
3. **Setup #3:** Repeated single-pass seeding at 4°C at flow rate of 20 ml/min and culture at 15 ml/min.

5.2.3 Seeding with Pre-Formed Aggregates

Aggregates of primary hepatocytes were formed based on the intermittent settling /agitation protocol described by Surapaneni et al. [94]. Briefly, 39 million hepatocytes were suspended in 12 ml of hepatocyte culture medium and seeded into 75 cm² culture flask (seeding density of 520,000 cells/ cm²). The flasks were pre-coated with 10 ml of 2% bovine serum albumin (BSA) in phosphate buffered saline (PBS) for at least 24 hrs prior to aggregation at 37°C. The flasks were then placed on a timed controlled linear shaker inside the incubator; 15 sec of mixing at 20 min intervals for 6 hours. This procedure produces spheroids of around 100µm in diameter as this size will not develop necrotic center. One hundred million cells were used to form the aggregates and then seeded into the scaffold as described above using the same three setups in the single cell suspension seeding.

5.2.4 Aggregation Efficiency Analysis and Aggregates Viability

Before seeding the scaffolds, samples of the aggregates were collected at three different time point; 2 hours, 4 hours and 6 hours and fixed with 10% paraformaldehyde in PBS to characterize the aggregation efficiency and the aggregates sizes. Images using phase contrast microscopy were captured and analyzed using ImageJ[®] software. The software calculated the areas of the particles (spheroids) in each image. From the areas, the volumes of the spheroids were calculated and divided by the volume of a single hepatocyte with an average diameter of 20µm and considered to have a sphere shape ($4188 \times 10^{-6} \text{m}^3$) to calculate how many cells were available in each spheroid. SigmaPlot[®] software was then used to generate histograms of number of cells in the spheroids vs. the spheroid count of that amount of cells in. From the histograms, the aggregation efficiency can be estimated at each time point.

To evaluate the viability of the spheroids, Trypan blue exclusion test was performed on the samples collected (before fixing them) and images were captured with Nikon® color digital camera. At least ten images were captured for each time point and the viability was evaluated by counting blue cells and clear cells.

5.2.5 Histology Processing and Hematoxylin & Eosin Staining

To evaluate cell distribution within the scaffolds' microstructure, scaffolds were fixed in 10% paraformaldehyde in PBS for 48 hrs and then processed for histology by embedding in paraffin and cut into semi-thin transverse sections (8 μm) with a microtome. Then the sections were washed with xylene to remove the paraffin. After that, Hematoxylin & Eosin stain (H&E) was applied to distinguish cells from tissue structures using light microscopy. The distribution of cells in the pores was analyzed using the transverse sections by quantitative image analysis of digital light microscopy images.

5.2.6 Lactate Dehydrogenase Activity Assay

The LDH kit is commercially available from Sigma. The following description for the kit is quoted from Sigma website: "Lactate dehydrogenase (LDH) is an oxidoreductase enzyme that catalyzes the interconversion of pyruvate and lactate. Cells release LDH into the bloodstream after tissue damage or red blood cell hemolysis. Since LDH is a fairly stable enzyme, it has been widely used to evaluate the presence of damage and toxicity of tissue and cells. LDH is also elevated in certain pathological conditions such as cancer. Quantification of LDH has a broad range of applications. The LDH Activity Assay kit quantifies LDH activity in variety of

biological samples. The assay is quick, convenient, and sensitive. In this kit, LDH reduces NAD to NADH, which is specifically detected by colorimetric (450 nm) assay”[95].

5.2.7 AlamarBlue Viability Assay

AlamarBlue[®] is a proven cell viability indicator that uses the natural reducing power of living cells to convert resazurin to the fluorescent molecule, resorufin. The active ingredient of alamarBlue[®] (resazurin) is a nontoxic, cell permeable compound that is blue in color and virtually nonfluorescent. Upon entering cells, resazurin is reduced to resorufin, which produces very bright red fluorescence that is measured by a fluorescence spectrophotometer using excitation wavelength of 560nm and emission wavelength of 590nm. Viable cells continuously convert resazurin to resorufin, thereby generating a quantitative measure of viability and cytotoxicity [96].

5.3 Results

5.3.1 Aggregation Efficiency and Aggregates Viability

Hepatocyte aggregates sizes increased as the time progressed. After six hours of aggregation time, spheroids sizes started to grow bigger than the desired size ($>100\mu\text{m}$). Most of spheroids had less than 25 cells after two hours of aggregation (Fig. 25A), between 25- 50 cells/spheroid after four hours (Fig. 25B), and between 25- 100 cells/spheroid after six hours (Fig. 25C). The viability of spheroids was about 70% as tested by Trypan Blue exclusion viability test (Fig. 25D).

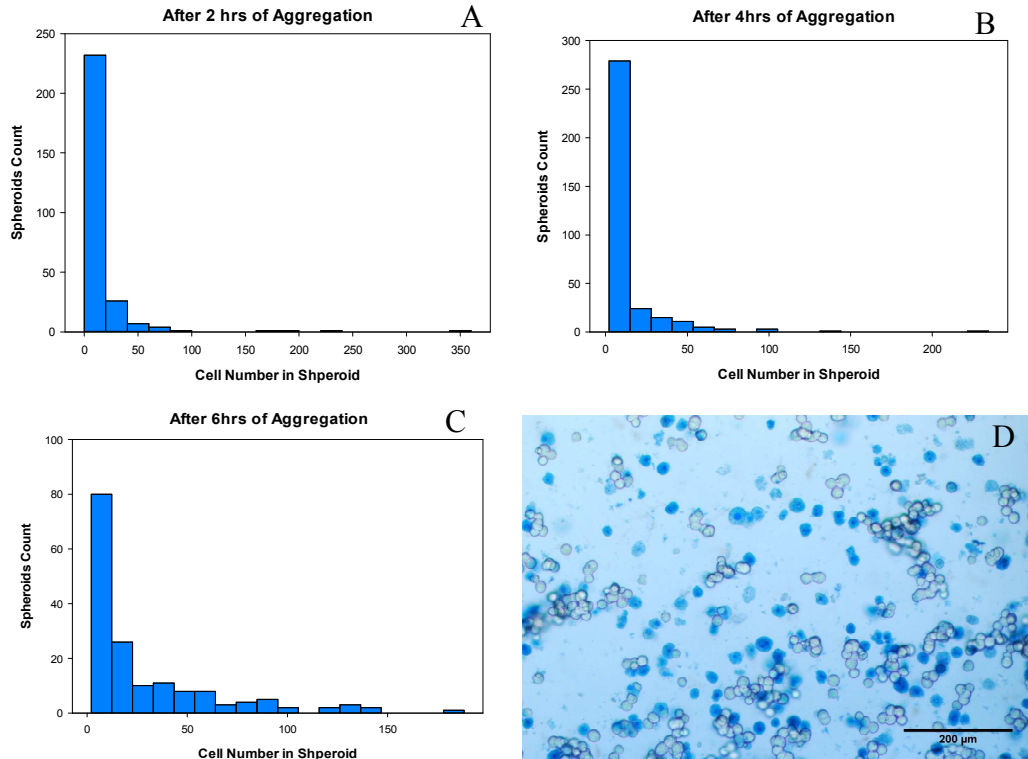


Figure 25: Aggregation efficiency and viability. Histograms for aggregation efficiency after (A) two hours, (B) four hours, and (C) six hours. (D) Digital color image of TrypanBlue cell health indicator showing live cells/aggregates in clear color and dead cells/aggregates in blue color (viability ~70%).

5.3.2 Hepatocyte Metabolic Functions and Viability at Different Seeding/Culturing Flow Rates and Temperatures

For setup #1 (circulating seeding at 37°C for 2 hours at flow rate of 5 ml/min and culture at 10 ml/min) the observations are summarized in Table 3.

	Single Cell Suspension	Pre-Formed Spheroid
Seeding Efficiency	70% (39.55×10^6 cells/cm ³)	85% (48×10^6 cells/cm ³)
Viability (LDH activity)	More stressed	Less stressed
Cell distribution within the microstructure	Homogeneously distributed all over the cross section	At Center
Aggregates size at the end of culture	Not much aggregates noticed (mostly single cells)	200-500µm

Table 3: Summary of observations for setup #1: seeding flow rate 5 ml/min and culture at 10 ml/min at 37°C.

Hepatocytes in both seeding architectures didn't synthesize albumin for the whole period of culture (Fig. 26). On the other hand, they were able to secrete urea (Fig. 26B) but at depressed rates compared to the static collagen gel sandwich configuration; with no significant difference between the two seeding architectures. LDH activity (Fig. 26C) was very high for scaffolds seeded with cell suspension compared to those seeded with pre-formed aggregates.

Histology images showed that most of the cells remained as single cells when scaffolds were seeded with single cells suspension at these flow rates (Fig. 27A), while cells remained in aggregates and the aggregates increased in size (up to 500 μm) from the seeding size (100 μm) which suggests that the spheroids fused together inside the pores. It was noticed that cells were homogeneously distributed all over the cross section of the scaffold when cells were seeded as single cell suspension, while they were concentrated at the center of the scaffold in the case of seeding with pre-formed spheroids (Fig. 27B). However, a number of spheroids were lost during the histology processing and were difficult to locate. In addition, more nucleoli were stained with Hematoxylin in the pre-formed seeded scaffolds; which suggests they were viable at the fixation time (Fig. 27A&B).

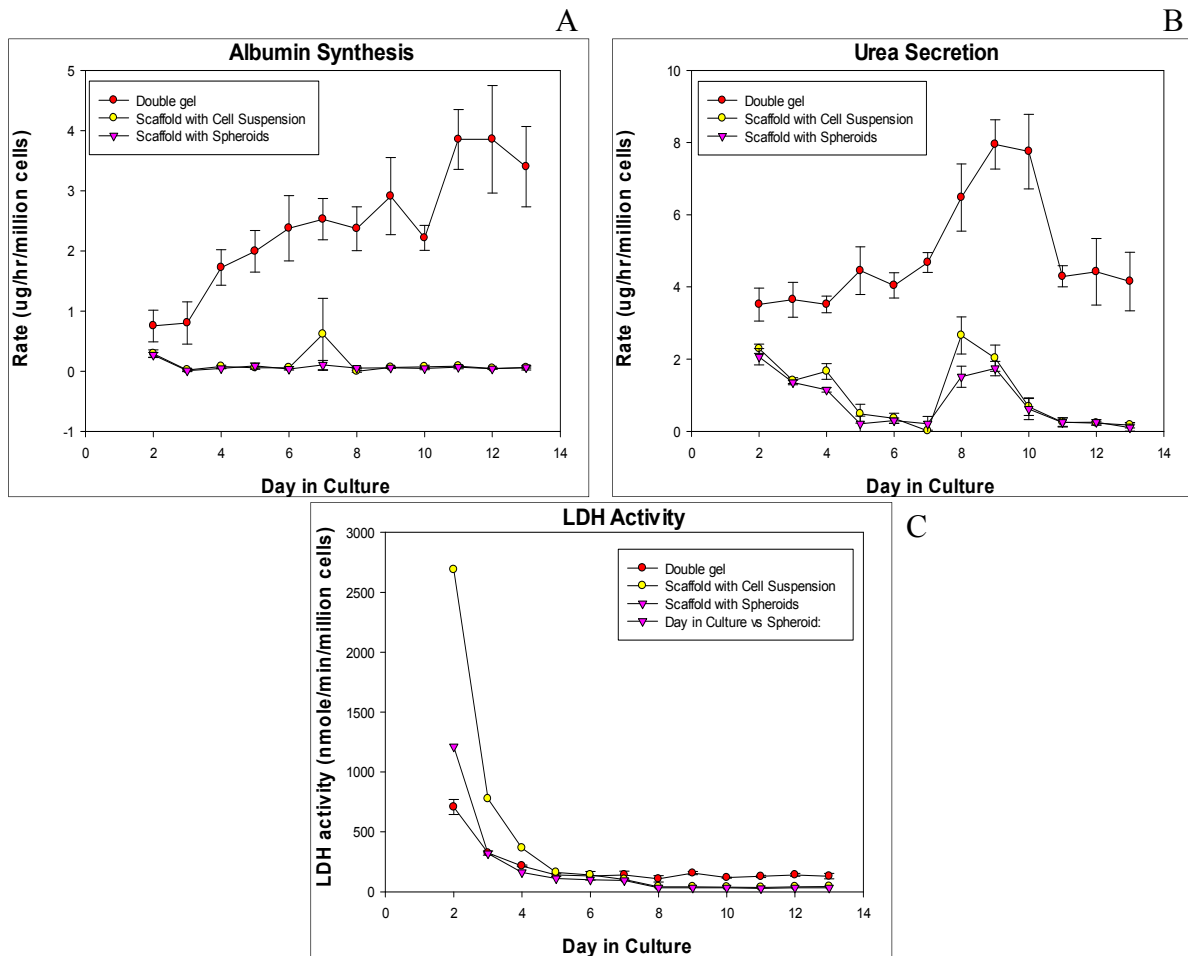


Figure 26: Metabolic performance and viability of perfused, scaffold-seeded hepatocytes (A) albumin secretion, (B) urea secretion and (C) LDH activity at seeding flow rate of 5 ml/min and culture flow rate of 10 ml/min at 37°C.

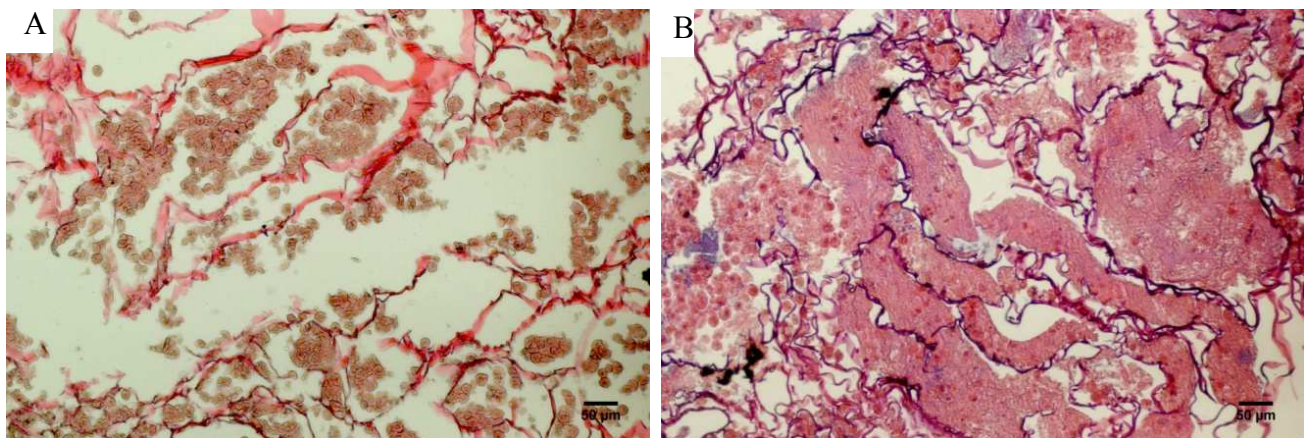


Figure 27: H&E histology images of cross sectional areas for seeded scaffolds with (A) single cell suspension and (B) pre-formed spheroids.

From setup #2 we can conclude that seeding at flow rate of 5 ml/min and culturing at 10 ml/min were not sufficient to seed spheroids homogenously. In addition, culturing at 10 ml/min didn't provide the needed oxygenation.

For setup #2 (circulating seeding at 37°C for 2 hours at flow rate of 20 ml/min and culture at 15 ml/min at 37°C) the observations are summarized in Table 4.

	Single Cell Suspension	Pre-Formed Spheroid
Seeding Efficiency	70% (39.55×10^6 cells/cm ³)	70% (39.55×10^6 cells/cm ³)
Viability (LDH activity)	More stressed	Very stressed (like cells in suspension)
Cell distribution within the microstructure	All along cross section	All along cross section
Aggregates size at the end of culture	40-300µm Mostly single cells, fewer aggregates	40 -300 µm Many single cells, mostly small aggregates (70-100µm)

Table 4: Summary of observations for setup #2: seeding flow rate 20 ml/min and culture at 15 ml/min at 37°C.

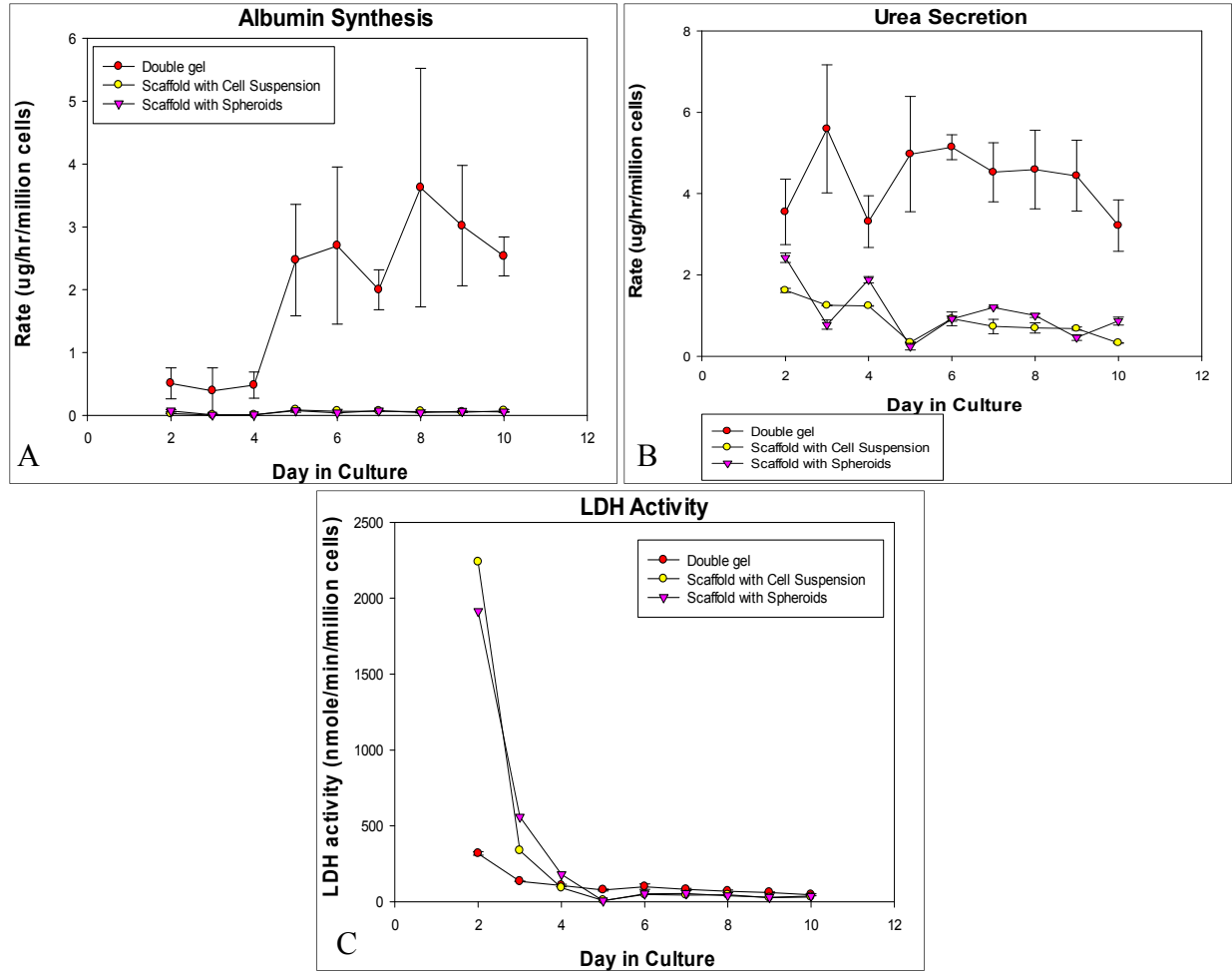


Figure 28: Metabolic performance of perfused, scaffold-seeded hepatocytes (A) albumin, (B) urea secretion and (C) LDH activity at seeding flow rate of 20 ml/min and culture flow rate of 15 ml/min seeding at 37°C.

Hepatocytes in both seeding architectures didn't synthesize albumin for the whole period of culture (Fig. 28A). On the other hand, they were able to secrete urea but at depressed rates compared to the static collagen gel sandwich configuration; with no significant difference between the two seeding architectures (Fig. 28B). It was noticed that the urea secretion rates at these flow rates were higher than the ones from setup#1; where they fluctuated between two and zero while at setup#2 they stayed above zero. LDH activity was very high for both seeding architectures at these flow rates and seeding temperature of 37°C (Fig. 28C).

From histology images, we noticed that the cells were homogeneously distributed all along the cross sectional area in both seeding architectures (Fig. 29A&B). In the single cell suspension seeding, cells remained mostly as single cells with very few aggregates of sizes 40-300 μm ; the spheroids were seen attached at the walls of the pores by SEM (Fig. 30A). In the case of pre-formed spheroids, some single cells were present but mostly there were small aggregates (70-100 μm) and some bigger aggregates (300 μm) also seen attached and spread at the walls of the pores (Fig. 30B). The nucleoli didn't stain with hematoxylin which suggests that most of the cells were dead at the end of the culture.

It is to be noted that in SEM photos the spheroids had rough surfaces with a lot of materials around the cells. These materials might be cell debris from previously dead and deteriorated cells; we can notice such debris in the histology images as well.

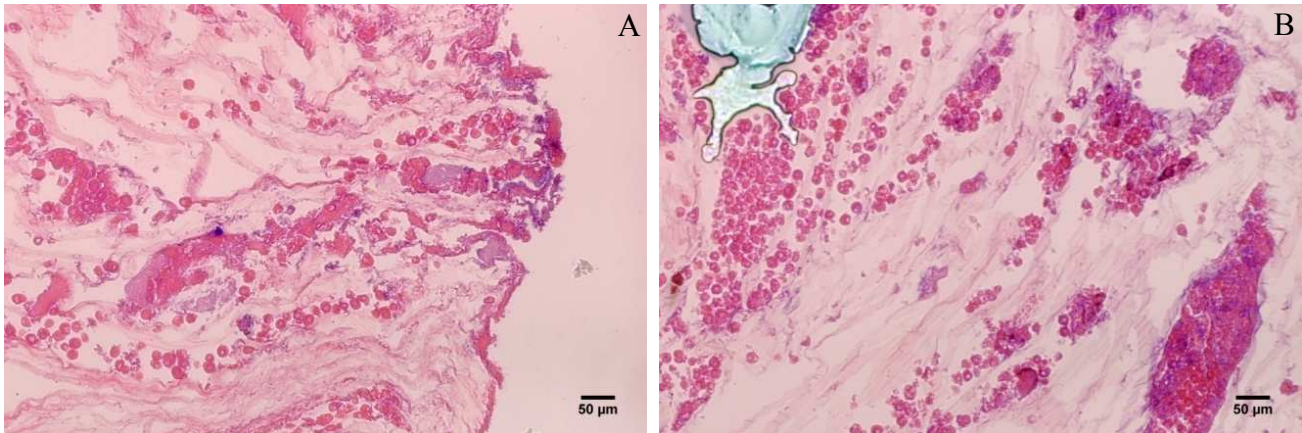


Figure 29: H&E histology images of cross sectional areas for seeded scaffolds with (A) single cell suspension and (B) pre-formed spheroids.

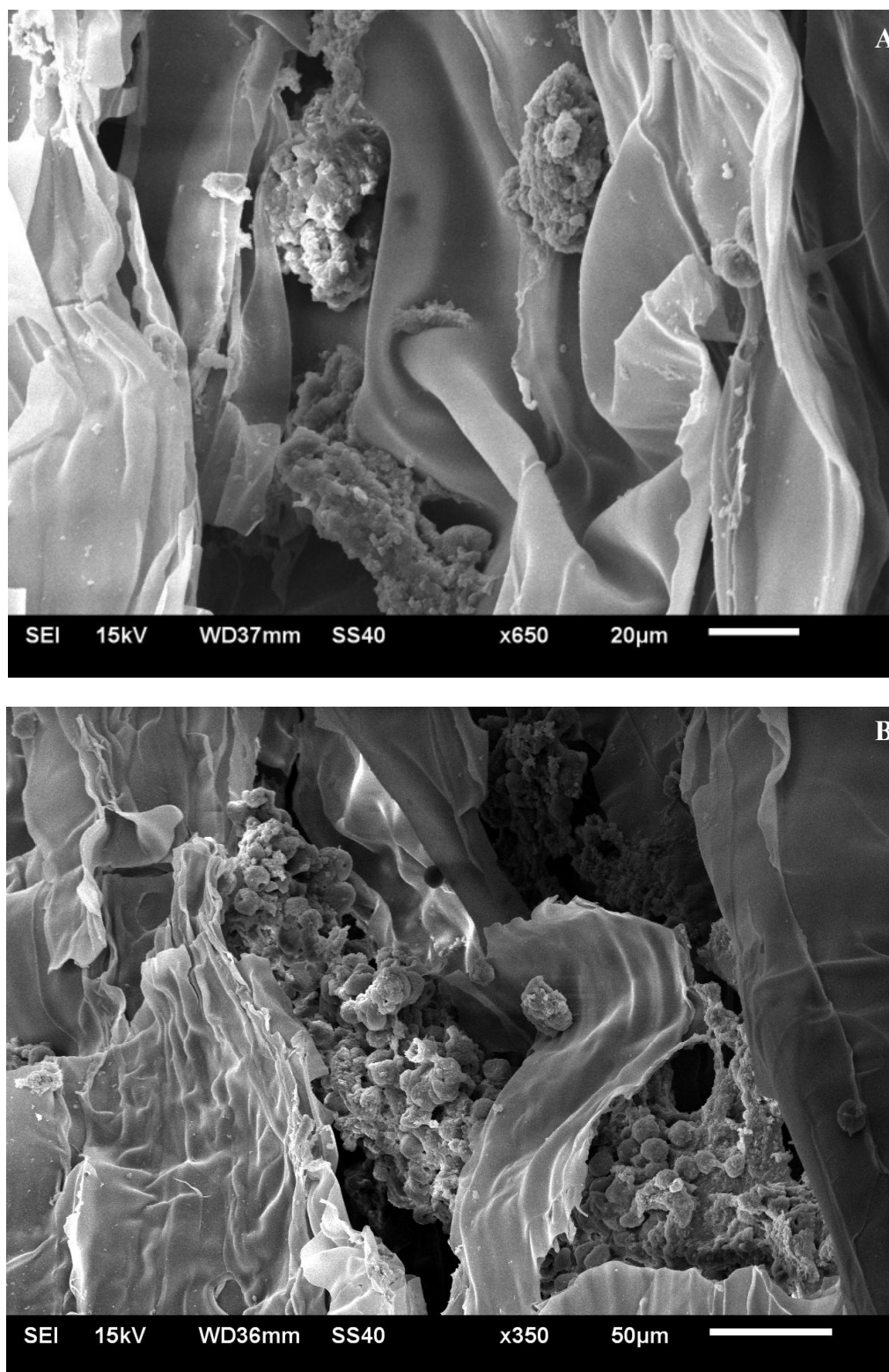


Figure 30: SEM photos of cross sectional areas for seeded scaffolds with (A) single cell suspension with some small aggregates attached to the wall, and (B) pre-formed spheroids with bigger aggregates also attached and spread at the walls.

From setup #2 we can conclude that seeding at 37°C may have contributed to hepatocyte death as their metabolic rate was high at this temperature. While seeding at flow rate of 20 ml/min was sufficient to seed both single cells suspension and spheroids homogenously, it may have generated shear forces that were higher than the levels that hepatocytes can tolerate.

For setup #3 (repeated single-pass seeding at 4°C at flow rate of 20 ml/min and culture at 15 ml/min) the observations are summarized in Table 5.

	Single Cell Suspension	Pre-Formed Spheroid
Seeding Efficiency	88% (49.7 X 10 ⁶ cells/cm ³)	92% (52 X 10 ⁶ cells/cm ³)
Viability (nuclei staining with Hematoxylin)	~50%	~10%
Viability (LDH activity)	More stressed	Less stressed
Cell distribution within the microstructure	All along cross section	Can't be seen (all were at the seeding port and got lost during histology processing)
Aggregates size at the end of culture	Big aggregates filling up the pores.	Many single cells but mostly aggregates of sizes 50 -200 μm.

Table 5: Summary of observations for setup #3: repeated single-pass seeding at 4°C at flow rate of 20 ml/min and culture at 15 ml/min.

Hepatocytes seeded as a single cell suspension and cultured at flow rates of 15 ml/min exhibited higher rates of albumin (Fig. 31A) and urea secretion (Fig. 31B) during the 12-day culture period than hepatocytes seeded as pre-formed aggregates. The albumin rates were at depressed rates compared to hepatocytes in control collagen-sandwich dish cultures but the urea secretion rates were close to the control. LDH activity (Fig. 31C) was low for both seeding architectures at seeding temperature of 4°C compared to the cells cultured in control collagen gel sandwich configuration.

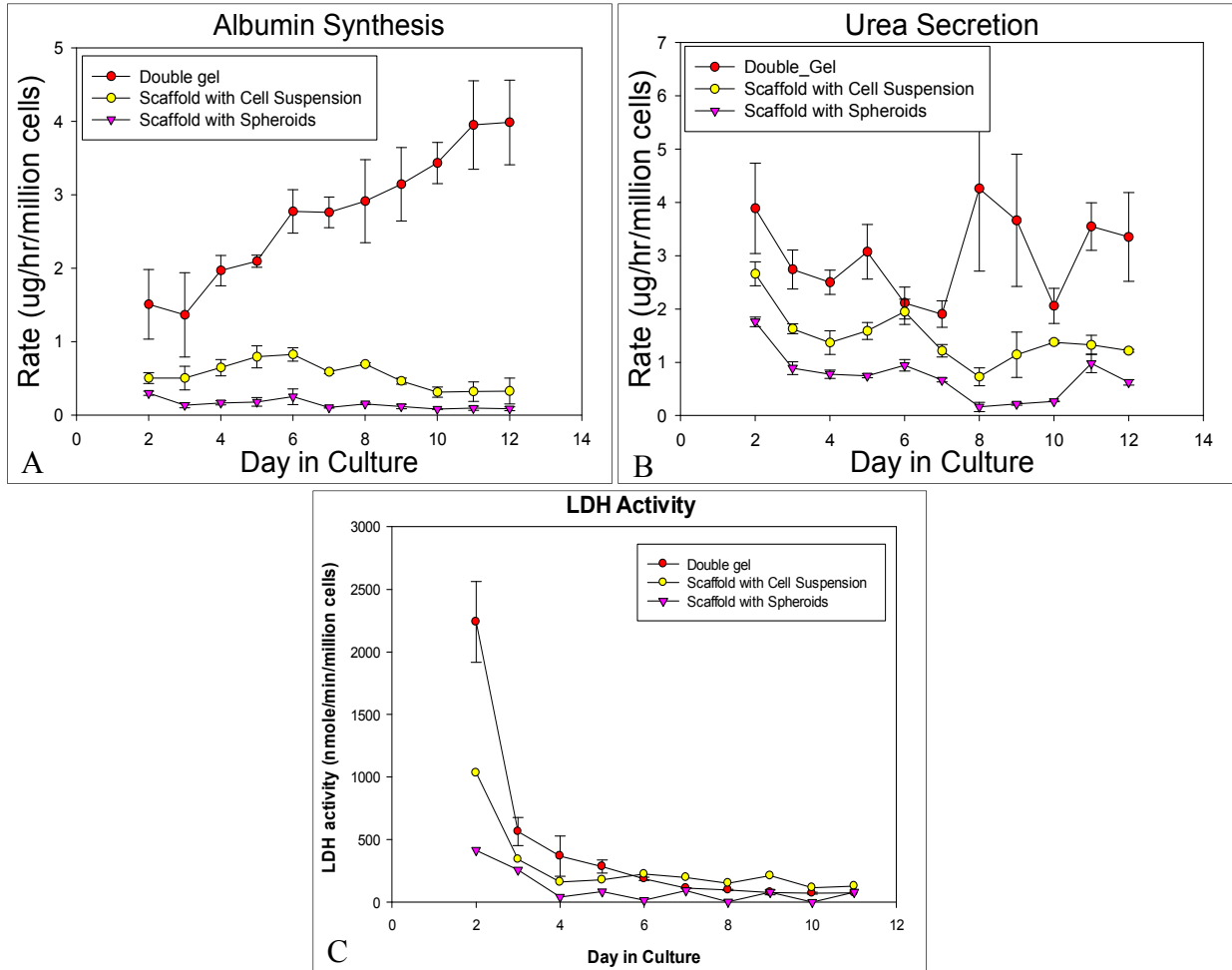


Figure 31: Metabolic performance of perfused, scaffold-seeded hepatocytes (A) albumin synthesis, (B) urea secretion and (C) LDH activity at seeding flow rate of 20 ml/min and culture flow rate of 15 ml/min (seeding at 4°C)

AlamarBlue® cell health indicator assay (Fig. 32) shows that hepatocytes in the scaffold seeded with pre-formed spheroids had very low activity, while those in the scaffold seeded with single cell suspension had higher activity but still lower than the activity of cells in collagen gel sandwich configuration or the static culture of pre-formed spheroids on chitosan-heparin membranes.

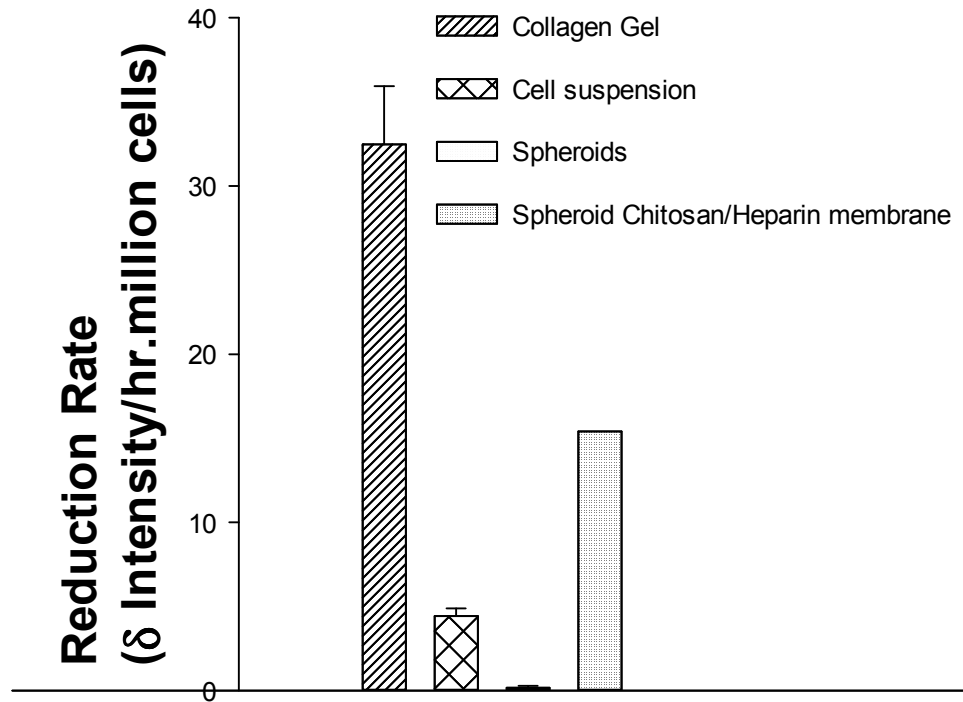


Figure 32: AlamarBlue® cell health indicator assay on day 11 of culture of hepatocyte in perfusion cultures of suspension-seeded and pre-formed spheroid-seeded, hepatocytes in static collagen gel sandwich configuration and preformed spheroids on chitosan-heparin membrane.

Histology sections showed that cells were distributed all along the pores in scaffold seeded with single cell suspension (Fig. 33A). They were more concentrated at the central port of the scaffold in the pre-formed aggregate seeding architecture (Fig. 33B and Fig. 34). It can be noticed from the SEM photos (Fig. 35) that the aggregates were concentrated at the central port forming one large aggregate. Also, cells were spread and attached to the walls of the pores and blocking some of the central pores.

From setup #3 we can conclude that a flow rate of 20 ml/min was adequate for seeding a cell suspension, it was too low to efficiently seed spheroids into the scaffolds. The spheroids settled in the central port and did not distribute into pores, resulting in excessive spheroid

aggregation, diffusion limitations, and cell death. Seeding flow rate of 20 ml/min and culturing at 15 ml/min may have resulted in hepatocyte damage and death due to high shear stress forces.

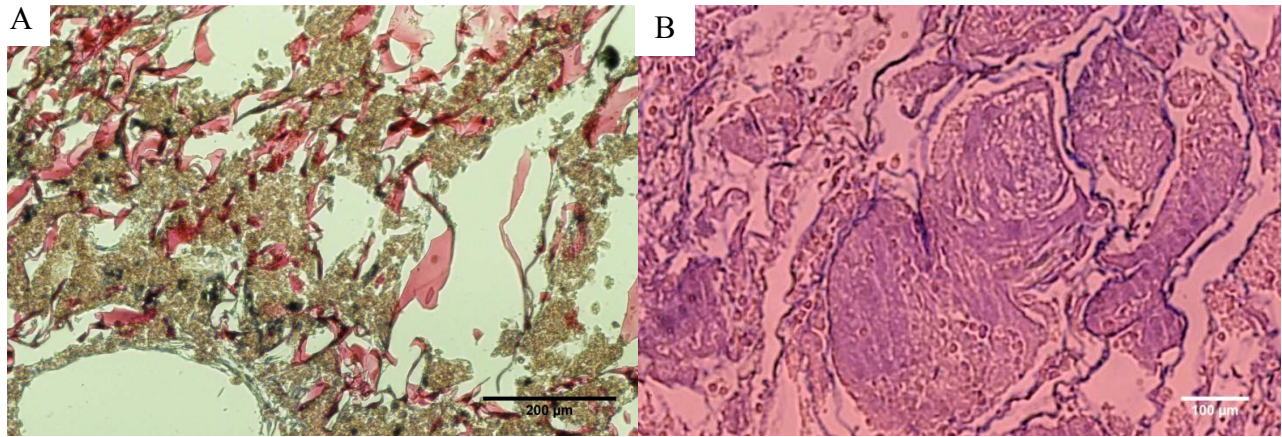
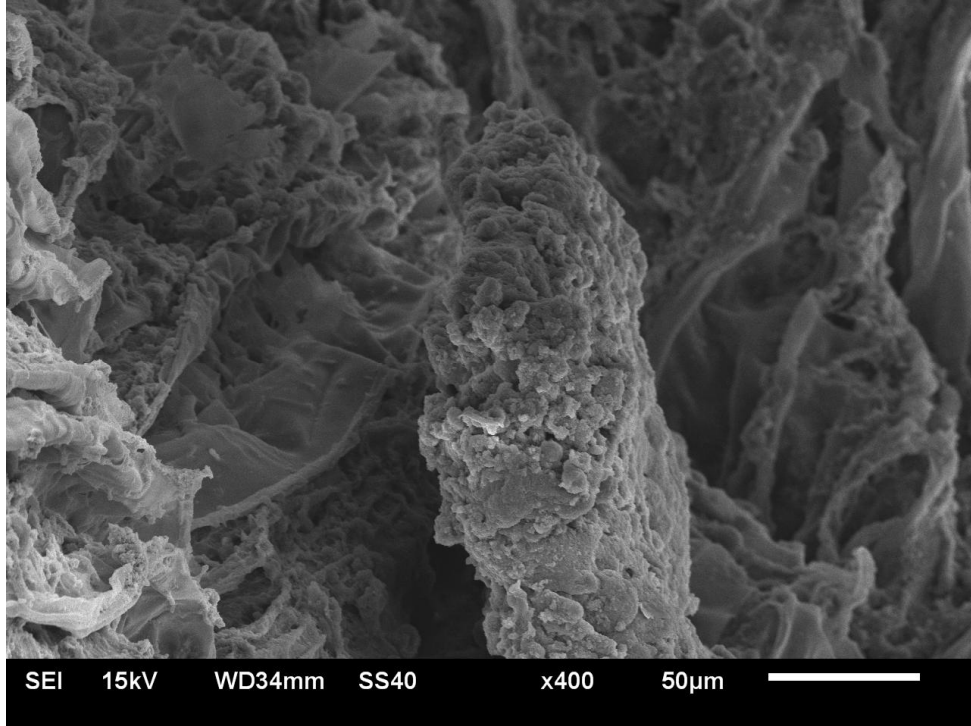
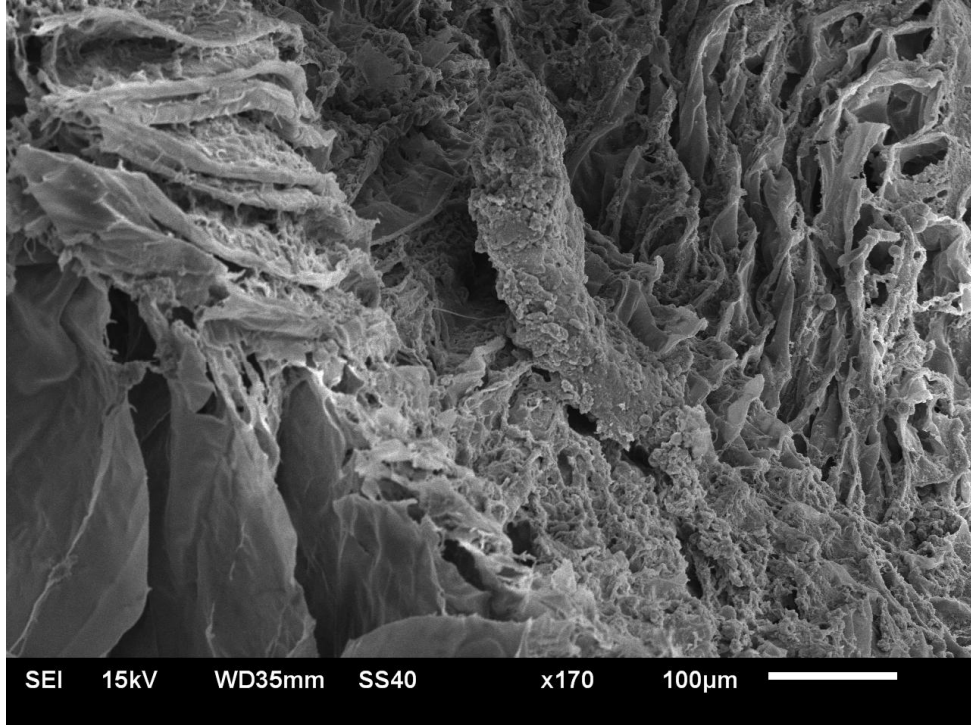


Figure 33: H&E histology images of seeded scaffolds with (A) single cell suspension (cross section) and (B) pre-formed spheroids (longitudinal section).



Figure 34: H&E histology images of a longitudinal section of scaffold seeded with pre-formed spheroids. Notice the large aggregates filling the central port.



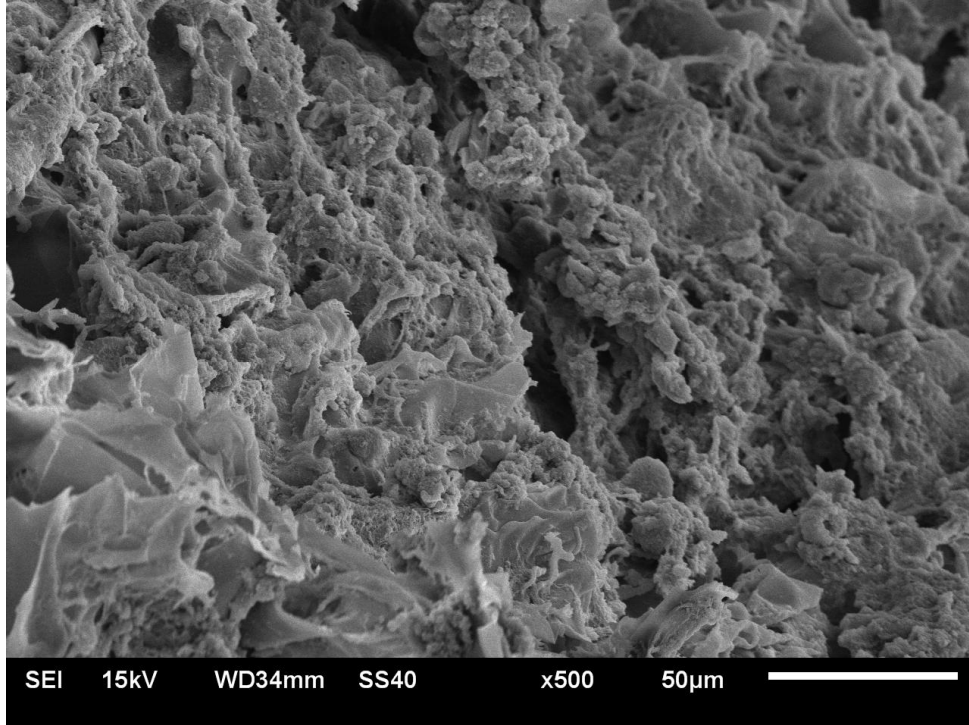


Figure 35: SEM photos of a longitudinal section at the center port of scaffold seeded with pre-formed spheroids showing cells forming large aggregates and blocking the center pores.

5.4 Discussion

Hepatocytes will spontaneously aggregate into spheroids if seeded on non-adherent surface or in 3D environment. The distribution of oxygen and metabolites in these organoids will become critical issue as they are transported by means of diffusion that depends on cells uptake and consumption of these elements, and their excretion to other elements. Hence, the size of these spheroids should be controlled as large ones will have diffusional gradients that will limit the supply of sufficient nutrients and the removal of waste at the heart of aggregates and thus the cells at the center will eventually die [91]. In this work, we sought to control the size of the aggregates by forming them first at the desired size that will not develop necrotic center and then seed them to the limited-adhesion material in 3D environment.

From the experiments performed in this work, we found that the higher the flow rate of seeding, the better the seeding efficiency. On the other hand, it seems that 20 ml/min seeding flow rate was not enough to seed the aggregates while it's efficient for single cell suspension seeding. The spheroids were accumulated in the central port and not evenly distributed into pores; which resulted in one massive spheroid that has poor oxygen and nutrients transport efficiency (specially at the center) and may have resulted in developing necrotic center.

In addition, single pass seeding at room temperature with cold medium (4°C) resulted in better seeding efficiency for both seeding architectures and lower LDH activity. Hepatocytes have high metabolic rates, and by seeding with solutions at 4°C, we lower their activity and make them less sensitive to any oxygen deprivation.

Calculations based on hepatocyte oxygen uptake rates suggests that flow rate should be higher than 14.4 ml/min to meet hepatocyte oxygen requirements (if inlet oxygen partial pressure to bioreactor was considered to be 158 mmHg (O₂ atmospheric partial pressure) and outlet pressure was 35 mmHg (perivevous zone in liver). On the other hand, calculations based on physiological shear stress at the sinusoid (5 to 20 dyne/cm²) and the volumetric flow rate in our porous scaffold suggests that flow rate should not exceed 5.67 ml/min.

While a flow rate of 20 ml/min was adequate for seeding a cell suspension, it was too low to efficiently seed spheroids into the scaffolds. The spheroids settled in the central port and did not distribute into pores, resulting in excessive spheroid aggregation, diffusion limitations, and cell death. Seeding flow rate of 20 ml/min and culturing at 15 ml/min may have resulted in hepatocyte damage and death due to high shear stress forces.

5.5 Conclusions and Future Work

- Available data indicate that effective hepatocyte seeding and perfusion culture requires higher flow rates that raise the risk of shear-induced cell damage. Alternate methods for enhancing diffusional transport in these systems are needed.
- Seeding with pre-formed spheroids has higher efficiency than seeding with cell suspension with higher cell viability, too. On the other hand, hepatocytes performed their metabolic functions at higher rates when seeded as single cell suspension compared to seeding with pre-formed spheroids.
- Poor performance and low viability of hepatocytes seeded as pre-formed spheroids resulted from the spheroids settling down at the central port and forming a one-massive aggregate where most of the cells don't receiving the required oxygen and nutrients and eventually die. Increasing the seeding flow rate beyond 20 ml/min was not a valid option, as this flow rate will expose the hepatocytes to even higher shear forces and they will definitely die from that.
- Modifications to the perfusion system can be made to maintain the hepatic specific functions in vitro by insuring the adequate delivery of oxygen and nutrients and removal of the waste products; i.e. co-culture with MSCs to shield them from excessive shear forces and in the same time initiate vasculogenesis in the spheroids by differentiating MSCs to endothelial cells.

CHAPTER SIX

THE EFFECTS OF CO-CULTURING HEPATOCYTES WITH BONE MARROW MESENCHYMAL STEM CELLS

6.1 Introduction

The vascular network in the liver and the bile drainage system are crucial to both the viability of hepatocyte cells and the detoxification of the blood. Hence, tissue engineered systems should address the need of such networks. Incorporating microvascular endothelial cells to the *in vitro* cultures will help in the vasculogenesis, angiogenesis and anastomosis with the host vascular network. It will enhance hepatocytes viability and their specific functions, as this will mimic the natural environment in the liver as well as protect them from any excessive shear forces they might experience in the dynamic perfusion system. This approach is hindered by the availability of such cell populations and the difficulties in isolating endothelial cells at high yields, specifically sinusoidal endothelial cells (SECs). SECs lose their phenotype rapidly after isolation and their survival depends on co-culturing with primary hepatocytes. There are limited *in vitro* configurations that can accommodate such populations and they can't be passaged and hence they senesce rapidly [97-100].

Mesenchymal stem cells can provide an alternate cell source to substitute for endothelial cells if either differentiated before co-culturing with hepatocytes [65, 101, 102], or differentiated while co-culturing under flow conditions [64]. MSCs might also provide an alternate cell source to substitute for primary hepatocytes [103-106] in hepatocyte transplantation because of their multiple differentiation potential and nearly unlimited availability.

It has been shown that co-culturing hepatocytes with BM-MSCs enabled the restoration of hepatocyte cell polarity due to the ECM secreted by MSCs (e.g. collagen Type-I) as well as

providing a number of cues for hepatocyte growth and development [59]. Also, MSCs can be differentiated into connective tissue cells; i.e. endothelial cells. Wang et al. [64] demonstrated the ability of murine embryonic mesenchymal progenitor cell line, C3H/10T1/2 to differentiate into cells that express mature endothelial cell-specific markers such as CD31 and von Willebrand factor [64, 107].

The objective of this work was to optimize the spatial arrangement of hepatocyte (HCs) and bone marrow mesenchymal stem cells (MSCs) to produce more effective cell-cell contact in 3D environment. This could be achieved by optimizing seeding architecture.

As part of this work, we also examined heterotypic cultures in perfusion system. The premise was that MSCs can provide protection against shear forces by differentiating to vascular phenotypes as well as secreting ECM components that may associate with and hence stabilize the cell membranes of hepatocytes.

6.2 Experimental Work

6.2.1 Materials

CellTracker™ Calcein Red-Orange AM and CellTracker™ Green CMFDA dyes were purchased from Life Technologies (Thermo fisher Scientific Inc.). All other chemicals and solvents were of analytical reagent grade.

6.2.2 Bone Marrow Mesenchymal Stem Cells Isolation and Culture

The same hepatocytes donors rats were used to isolate bone marrow mesenchymal stem cells following a protocol described by Karaoz et al. [108] and slightly modified by our group. Briefly, femur and tibiae were excised then all muscles and connective tissues were detached. The whole bones were then soaked and vortex mixed in ringer solution (without enzymes) for 30

minutes to remove excess soft tissue. After that, the epiphyses were cut away by torsion-twisting off using two Kelly clamps. The diaphyses cavities were then flushed with pre-warmed DMEM (low glucose) supplemented with 10% FBS, 50 mg/L gentamicin and 2.5 mg/L Fungizone (same medium was used for cells culture as well). This flushing was carried out using 18-gauge needle inserted into the shafts to extrude the bone marrow. Marrow plug suspension was then dispersed by pipetting, successively filtered through 70- μ m mesh nylon filter into sterile 50 ml centrifuge tube and then centrifuged 200 x g for 10 min. Supernatant containing thrombocytes and erythrocytes was discarded, and the cell pellet was resuspended in sterile PBS and centrifuged (repeated two times). At the final wash, the cell pellet was resuspended in culture medium and cells from one rat were seeded onto four 10 cm culture dishes (7 ml per dish) and incubated at 37°C in a humidified atmosphere containing 5% CO₂ for 3 days without changing medium. On the third day, red blood cells and other non-adherent cells were removed and fresh medium was added to allow further growth. The adherent cells grown to 70% confluency were defined as passage zero (P₀) cells.

6.2.3 Chitosan-Heparin Disc Scaffolds Fabrication and SEM Imaging

Porous disc scaffolds were prepared by freezing the same chitosan solution in 96-well plate with stainless steel bottom (Fig. 36). Disc scaffolds designated for cell culture were neutralized with 5% ammonia, washed with PBS, derivatized with Heparin, sterilized by soaking in 80% ethanol for 48 hours and finally incubated with medium containing 10% FBS for 24 hrs prior to cell seeding. Discs used for SEM imaging purposes were kept dehydrated and sputter coated with gold for imaging; one of them was cut longitudinally to view the pores directions.

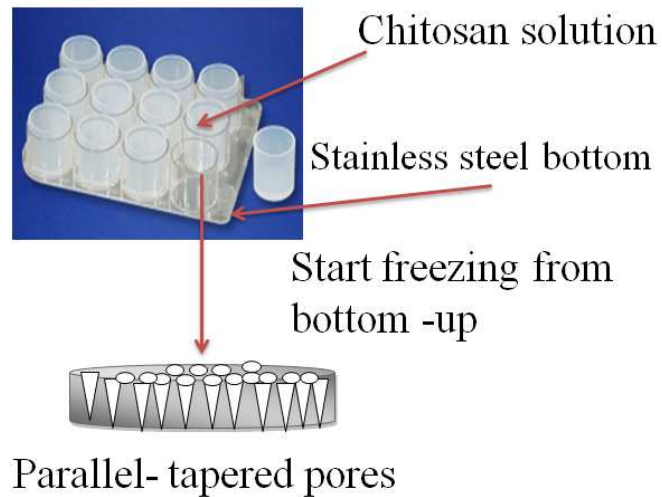


Figure 36: Fabrication of chitosan disc scaffolds.

6.2.4 Cell Labeling with Fluorescent Dyes

For hepatocytes, the CellTracker™ Green CMFDA dye was used as manufacturer's recommended protocol. First, the dye powder was dissolved in 5 μ l sterile DMSO to make 10 mM (molecular weight of dye is 464.8) then diluted in 2 ml culture medium (serum free) to make 25 μ M working solution. The solution was then warmed up to 37°C and used to resuspend the hepatocytes. After that, the suspension was incubated for 30 minutes in 15 ml centrifuge tube in ice (reduce hepatocyte metabolic rate). The cells were then centrifuged at 300 rpm for 5 min and the dye working solution was replaced with fresh, pre-warmed medium. The hepatocytes were now ready to be seeded into the scaffolds.

For MSCs, CellTracker™ Calcein Red-Orange AM dye was used following manufacturer instructions. The dye molecular weight is 789.55; it's dissolved in 6.3 μ l DMSO to make 10 mM stock dye solution then diluted in 2.53 ml culture medium (serum free) to make 25 μ M dye working solution. The dye working solution was added to MSCs growing in a 100 mm dish and incubated for 30 minutes and then was replaced with fresh, pre-warmed medium. The cells were

incubated again for another 30 minutes at 37°C then trypsinized and resuspended in fresh, pre-warmed culture medium to be seeded into the scaffolds.

6.2.5 Cell Seeding and Culture into Three Different Architectures

Three different seeding architectures were examined as illustrated in table 6. Seeding was done with single cells suspensions of either hepatocytes only or hepatocyte with MSCs at 2:1 ratio as described by Gu et al. [109], and cultured on orbital shaker (~50 rpm) to enhance mass transfer in the wells. Culture medium was the same as hepatocyte culture medium mentioned above. Collagen gel sandwich configuration was used as control.

The seeding density was chosen based on the work done by Glicklis et al. [110]. They used a seeding density of 5×10^5 cells/scaffold/ml for scaffolds of 1.5 cm diameter and 1.0 cm height. The disc scaffolds fabricated in our lab were 0.64 cm in diameter and 0.2 cm in height for 96-well plate, and 1.14 cm in diameter and 0.1 cm in height for 48-well plate. The required seeding density was 0.018 million cells per disc scaffold in the 96-well plate and 50,000 cells/cm² in the 48-well plate. Monolayer seeding density based on the unit area was also examined (100,000 cells/cm²).

Four conditions of seeding architectures	Condition #1	Condition #2	Condition #3	Condition #4
	MSC then Hepatocytes	Mixed Suspensions of MSCs and hepatocytes	Hepatocytes then MSCs	Hepatocytes only

Table 6: Seeding architectures. Four different seeding architectures into the chitosan-heparin disc scaffolds.

6.2.6 AlamarBlue® Viability Test in the Chitosan-Heparin Disc Scaffolds

AlamarBlue® cell health indicator assay was performed as described by manufacturer.

Briefly, AlamarBlue® was added to the cultured cells at a dilution of 1:10. The cells were

incubated with AlamarBlue[®] for three hours; where fluorescent was measured by collected samples after one hour (T_1) and after three hours (T_2). The resazurin reduction rates were then calculated for each condition.

6.2.7 Spheroids Sizes Measurement and Statistical Analysis for Spheroids Formed in Disc Scaffolds

Phase contrast images using a digital camera were captured for each condition on days 7 and 17 of culture. At least five images per condition were taken, and the diameters for the spheroids were measured using ImageJ[®] software. The mean diameters and standard deviations were calculated and then plotted using SigmaPlot[®] software. One-way ANOVA statistical analysis was performed to evaluate the spheroid reduction in size between the two measurements per each condition. A p -value < 0.05 was considered to be significant.

6.2.8 Monotypic and Heterotypic Perfusion Cultures in Chitosan-Heparin Scaffolds

Porous scaffolds with a closed ended, annular structure and radial pore architecture (described previously in Fig. 12: surface frozen scaffolds) were used in this experiment. The chitosan scaffolds were modified with heparin, sterilized with 80% ethanol, washed with sterile PBS and perfused with 10% FBS culture medium for 24 hours prior to seeding. The same bioreactor described previously was used (in Fig. 13: surface frozen scaffolds). Cells were seeded as single cell suspensions with cold medium repeated one way (non circulating) passes at 20 ml/min and cell concentration of 35 million/ml. One scaffold was seeded with hepatocytes only (monotypic culture) with 100 million cells suspended in 35 ml cold medium. One scaffold was seeded with mixed cells suspension of MSCs and hepatocytes (heterotypic culture) (70

million hepatocytes plus 27.925 million cells MSCs at 2:1 ration). Seeding efficiency was estimated by counting the cells that were not seeded into the scaffolds after the seeding period). The flow rate used subsequently was 15 ml/min all along the whole culture period. Media samples were collected daily for metabolic function assays (albumin synthesis and urea secretion) and LDH activity assay. Scaffolds were fixed in 10% formaldehyde and processed for histology (H&E staining).

6.2.9 Hepatocyte Metabolic Functions Assays (Albumin Synthesis and Urea Secretion)

Metabolic performance of cultured hepatocytes was evaluated by measuring: (1) the rate of albumin synthesis via Enzyme-linked immunosorbent assay (ELISA) using antibody specific to rat albumin and (2) the rate of urea secretion using diacetyl- monoxime colorimetric method described by Rozet et al. [84] and. Media samples were collected daily for metabolic functions analysis (albumin and urea secretion). Measurements were performed in triplicate (n =3). Data were plotted as means with error bars representing standard deviation.

6.3 Results

6.3.1 Pores Dimensions and Architecture as Shown by Scanning Electron Microscopy (SEM)

The goal was to produce spheroids that were limited in size to $< 100 \mu\text{m}$ by controlling pores sizes. The pore size was controlled by the amount of chitosan solution added to each well as well as the freezing time. For 96-well plate, the amount of chitosan solution added to each well was 0.05 ml. For 48-well plate, 0.1 ml of chitosan solution was added to each well. The freezing time was 15 min in Isopropanol/dry ice bath.

The pores at the bottom of the scaffolds were very small (Fig. 37A) (almost sealed) and the pores opening at the top were of sizes about 100 μm (Fig. 37B). The pores were longitudinally directed and were tapered towards the bottom of the scaffolds (Fig. 37C) so they will hold the spheroids in place and in the same time prevent them from fusing together.

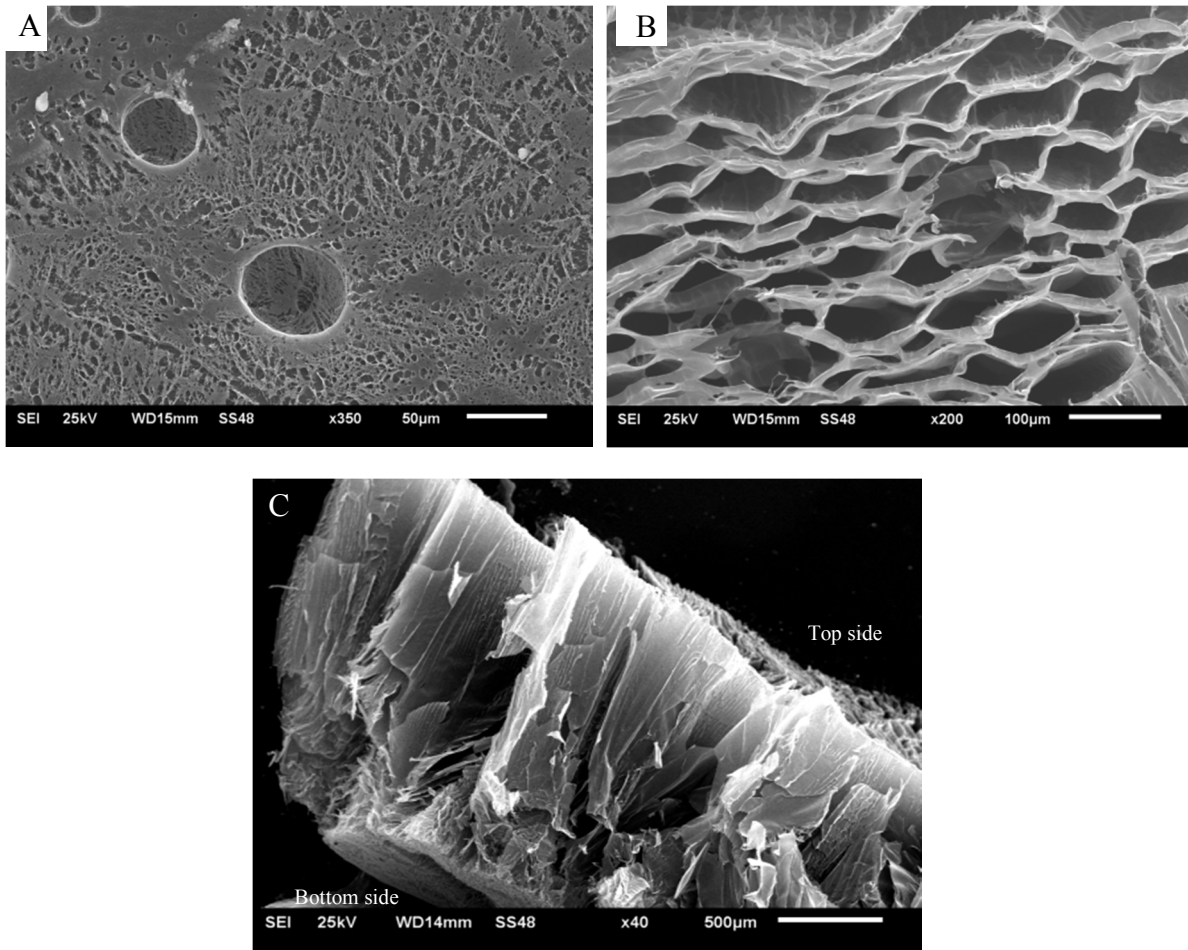


Figure 37: SEM images of chitosan disc scaffolds. (A) Bottom view, (B) top view, and (C) longitudinal cross section.

6.3.2 Cell Morphology in the Disc Scaffolds

MSCs were seeded one day prior to hepatocyte formed spheroids in the chitosan-heparin surfaces (Fig. 38A&B). Hepatocytes in collagen gel sandwich formed one layer of cells with bile canaliculi network formed as evidence of the dye CellTracker™ Green CMFDA secreted to the

bile (Fig. 38C&D). The H&E histology images showed that hepatocyte/MSCs spheroids (Fig. 38E) were smaller in size with tightly-fused cells, while hepatocytes only spheroids (Fig.40F) were bigger in size with less fused cells.

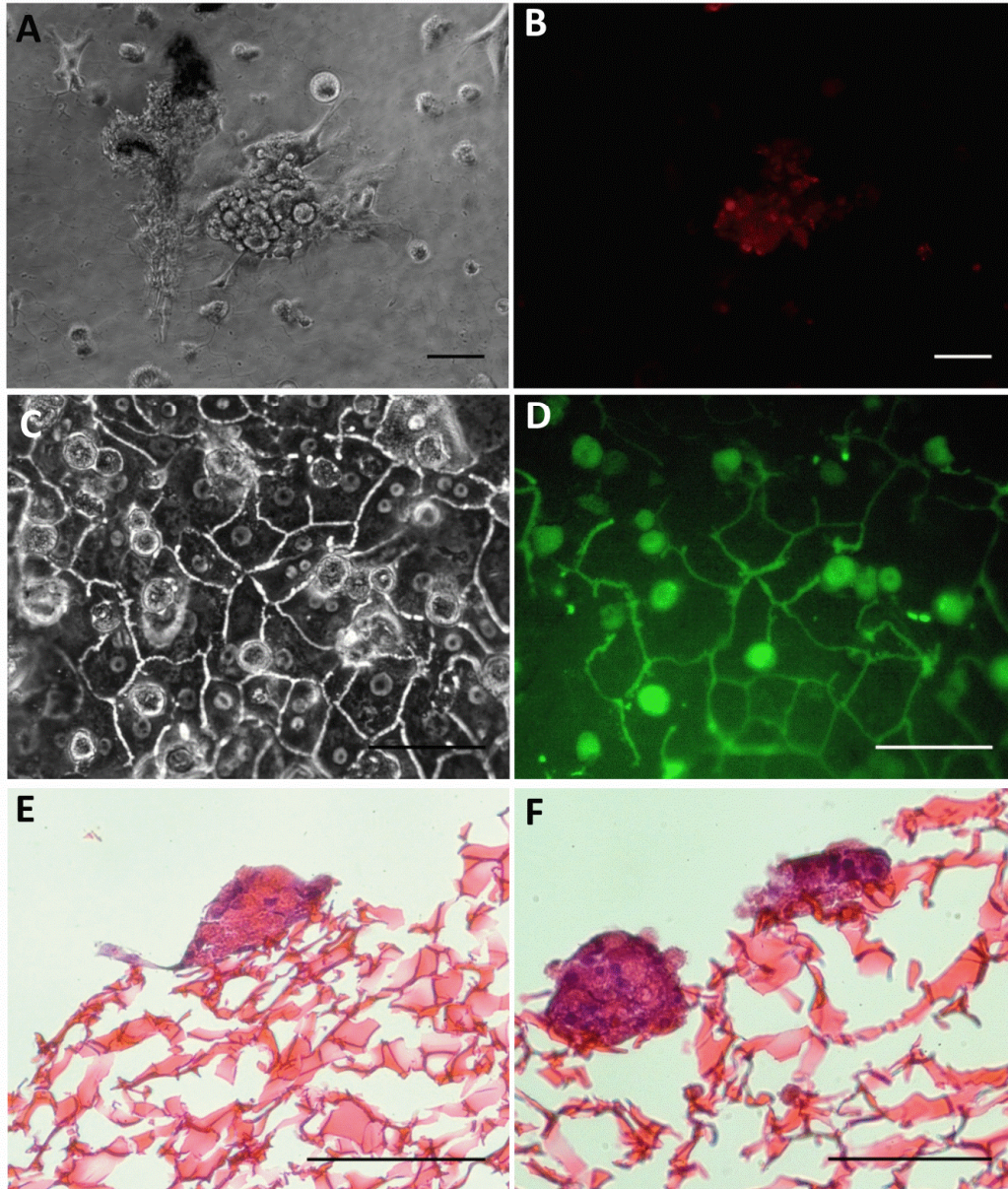


Figure 38: Cell morphology in the disc scaffold system. Phase contrast images (A&C), digital color fluorescent images (B&D) and H&E histology images (E&F) of hepatocyte/BM-MSCs in disc scaffolds cultures. (A&B) MSCs only (day 2 of culture), (C&D) hepatocytes in collagen gel sandwich, (E) hepatocyte/MSCs co-culture, and (F) hepatocytes only after two weeks in culture. Hepatocytes were labeled with CellTracker™ Green CMFDA dye and MSCs were labeled with CellTracker™ Calcein Red-Orange AM dye. Scale bar 100 μ m.

The cells formed compact spheroids with well-defined smooth surfaces in all the mixed co-cultures (Fig. 39A, C, and E). Hepatocytes formed loose spheroids with rough surfaces aggregates in the mono-cultures (Fig. 39G). For condition #1; where MSCs were seeded one day prior to seeding hepatocytes, the MSCs formed spheroids in the center and hepatocytes surrounded them at the peripheries as evidence of fluorescent images (Fig. 39B). For conditions #2 (mixed suspensions of MSCs and hepatocytes) and condition #3 (hepatocytes seeded one day prior to MSCs), the spheroids looked like they were mixed populations of both MSCs and hepatocytes without defined arrangement (Fig. 39D&F). It was noticed from the fluorescent images that the CellTracker™ Green CMFDA dye was not uniformly distributed in the hepatocyte cytosol; which indicates that the bile canaliculi network may have been formed inside the spheroids (Fig. 39B, D, F and H). When fluorescent intensity quantified for each condition (Fig. 40), we noticed that hepatocytes and MSCs had the highest fluorescent activities in condition #2 where they were mixed together as cell suspensions which indicates that more cells were viable at this seeding architecture compared to the other seeding conditions. In addition, as CMFDA dye was expressed more in condition#2, it indicates that the hepatocytes have stronger polarizations expressed as the MSCs were mixed with hepatocytes at the same time before they form the aggregates which may have contributed to better polarization during the aggregation process. We also examined the efficiency of hepatocyte membrane polarization by measuring the fluorescent intensity when labeling with anti-Connexin 32 (gap junction protein) (Fig.41A) and anti-ZO-1 (tight junction protein) (Fig. 41B). Condition #2 (mixed suspensions of hepatocytes and MSCs) had the strongest fluorescent intensity for anti-Connexin 32. When the seeded discs were cultured in an un-agitated condition, there were no significant difference between the gap and tight junctions' expressions. All co-culture conditions expressed higher intensities compared

to the mono-cultures (hepatocytes only) which indicate better membrane polarization in the co-culture systems.

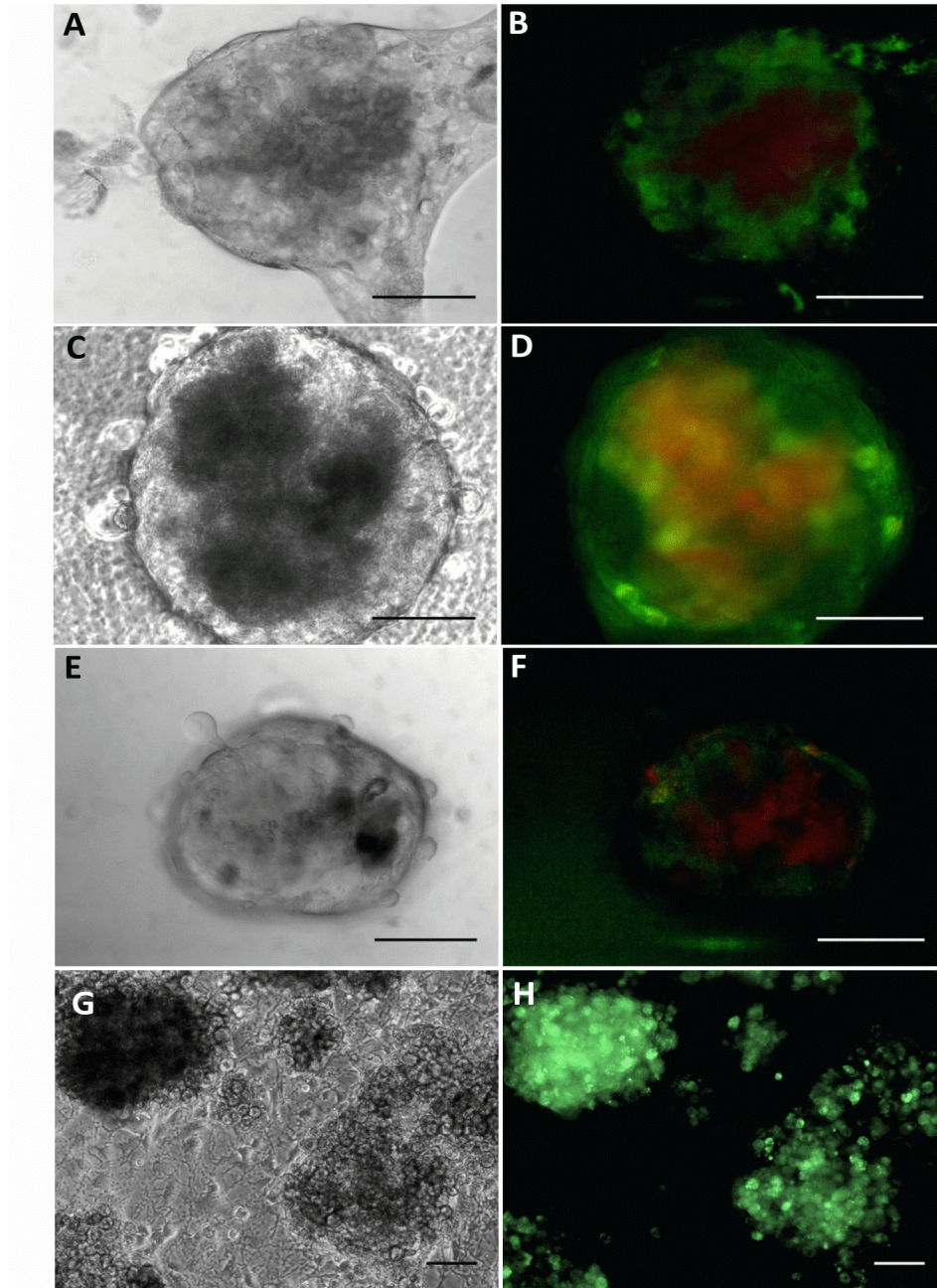


Figure 39: Phase contrast images (A, C, E and G) and digital color fluorescent images (B, D, F and H) of hepatocyte/BM-MSC co-cultures in disc scaffolds cultures after one week of culture. Condition #1: MSCs then hepatocytes (A&B), condition #2: mixed suspensions of MSCs and hepatocytes (C&D), condition #3: hepatocytes then MSCs (E&F), and condition #4: hepatocytes only (G&H). Hepatocytes were labeled with CellTracker™ Green CMFDA dye and MSCs were labeled with CellTracker™ Calcein Red-Orange AM dye. Scale bar 100 μ m.

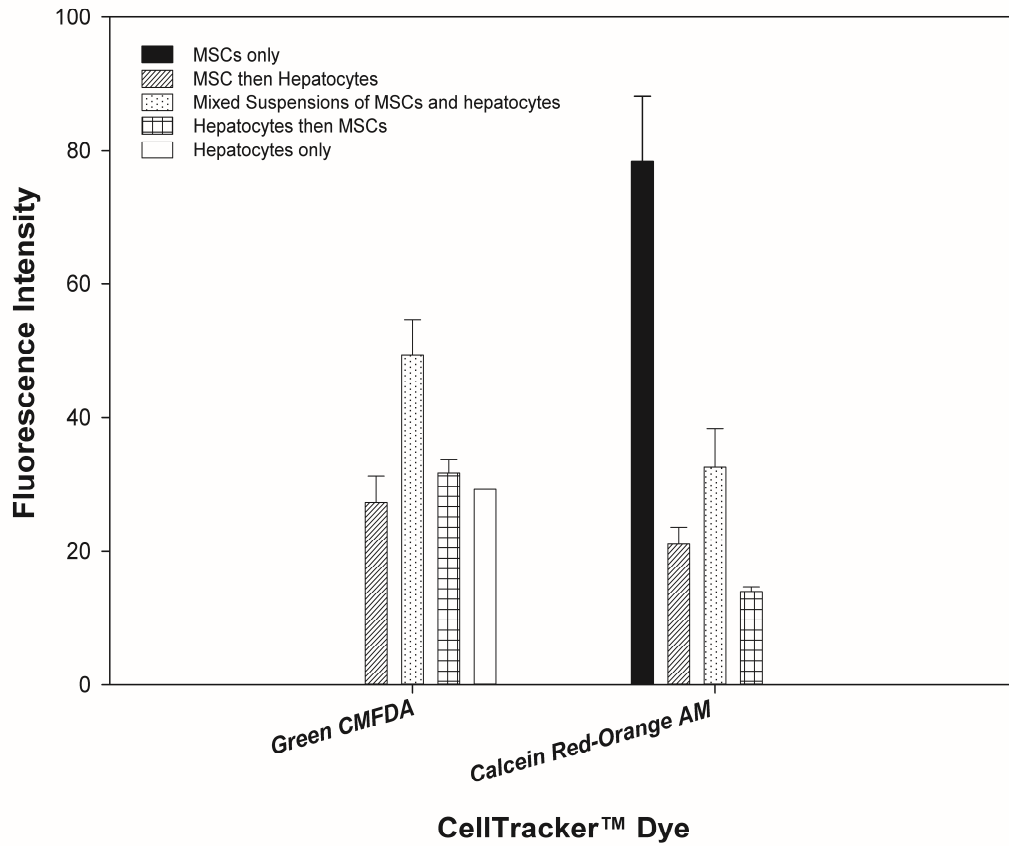


Figure 40: Fluorescent intensities quantification for all seeding architectures for hepatocytes labeled with CellTracker™ Green CMFDA dye and MSCs labeled with CellTracker™ Calcein Red-Orange AM dye (on day 7 of culture). Measurements were performed for different number of spheroids ($n = 5$ to 20). Data plotted as means with error bars representing standard deviation (SD).

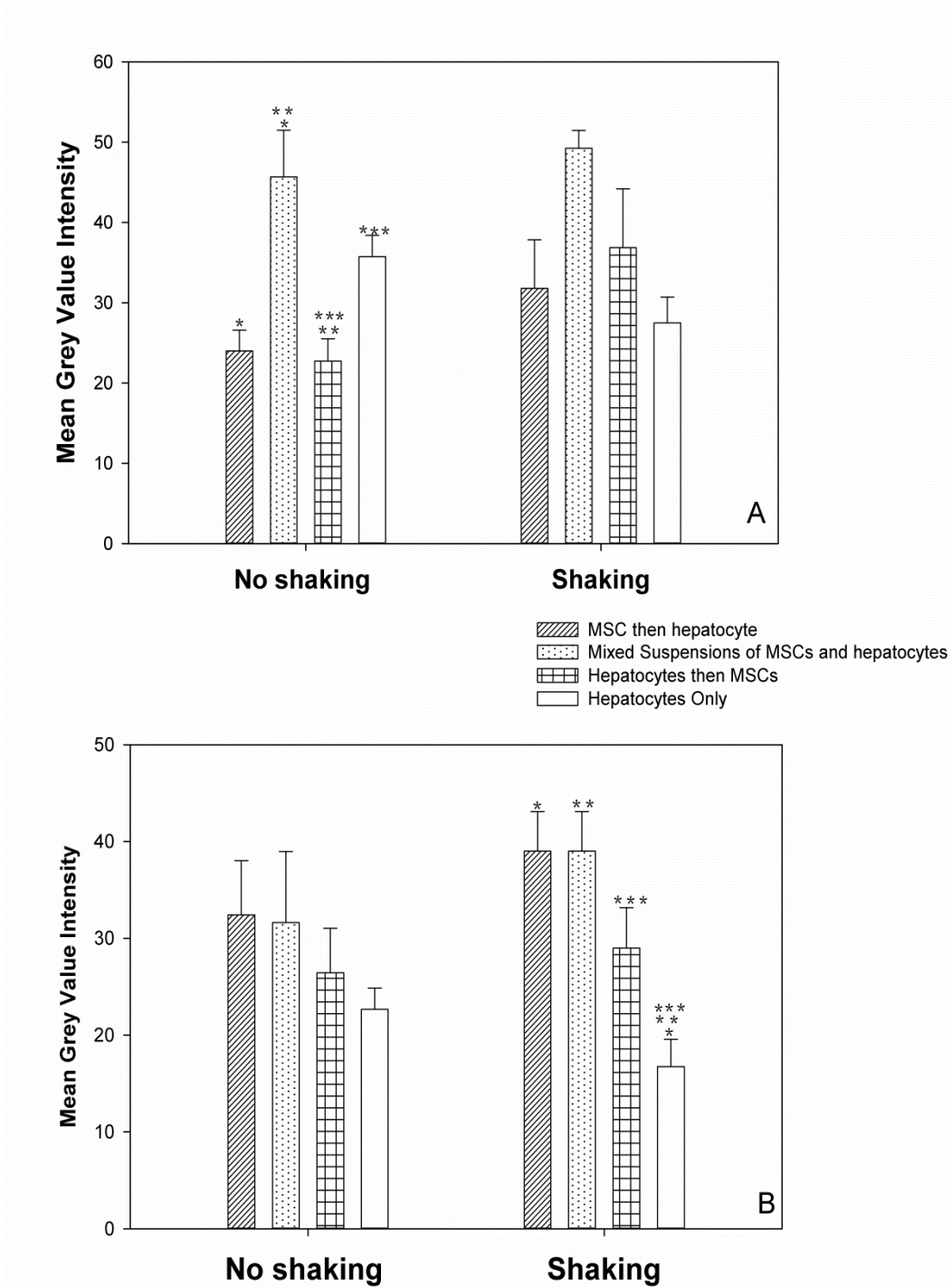


Figure 41: Mean grey value Intensities for (A) anti-Connexin 32, and (B) anti-ZO-1. Measurements were performed for different number of spheroids ($n = 3$ to 16). Data plotted as means with error bars representing standard error of means (SEM). There is not a statistically significant difference between Shaking and Non-Shaking groups ($P < 0.05$).

6.3.3 Spheroids' Sizes at 50,000 cells/ cm² and 100,000 cells/ cm² Seeding Densities

The spheroids formed in the co-culture conditions were smaller in size compared to those in mono-cultures. For seeding density of 50,000 cells/ cm², the spheroids average diameters were about 227± 13, 218± 30, 350± 41, and 341± 35µm on day 7 of culture for all four conditions respectively, and 211± 25, 315± 49, 437±112, and 314± 18 µm on day 17 with no significant difference between the four different seeding architectures (Fig. 42A). The spheroids were larger in size in the 100,000 cells/ cm² compared to the lower seeding density for all seeding conditions, with no significant difference between the groups (Fig. 42B).

For seeding density of 50,000 cells/cm², the conditions #1 and #4 exhibited reduction in spheroids sizes while the other two conditions had increased spheroid sizes (Fig. 42A). On the other hand, for seeding density of 100,000 cells/cm², there were decrease in spheroids sizes from day 7 to day 17 of culture for all conditions, except when MSCs were seeded after one day of hepatocytes there were increase in size (Fig. 42B). We noticed for both seeding densities, spheroids actually got larger for condition # 3 where MSCs were seeded one day after hepatocytes were seeded (Fig. 42A & B). The increase in size though was not large enough to be due to spheroids fusion (about 50 µm increase). This was more consistent with a reasonable increase in cell number due to MSCs growth, given the fact that MSCs were present at the outer surface of the spheroids. In addition, MSCs are known to be not as shear stress sensitive as the hepatocytes, so they were able to proliferate and grow with damages. On the other hand, when hepatocytes were present at the surface of the spheroids (as in conditions #1 and #4), they were more exposed to shear forces and hence shear damage which have resulted in their death and detachments from the spheroids and consequently, reduction of spheroids sizes.

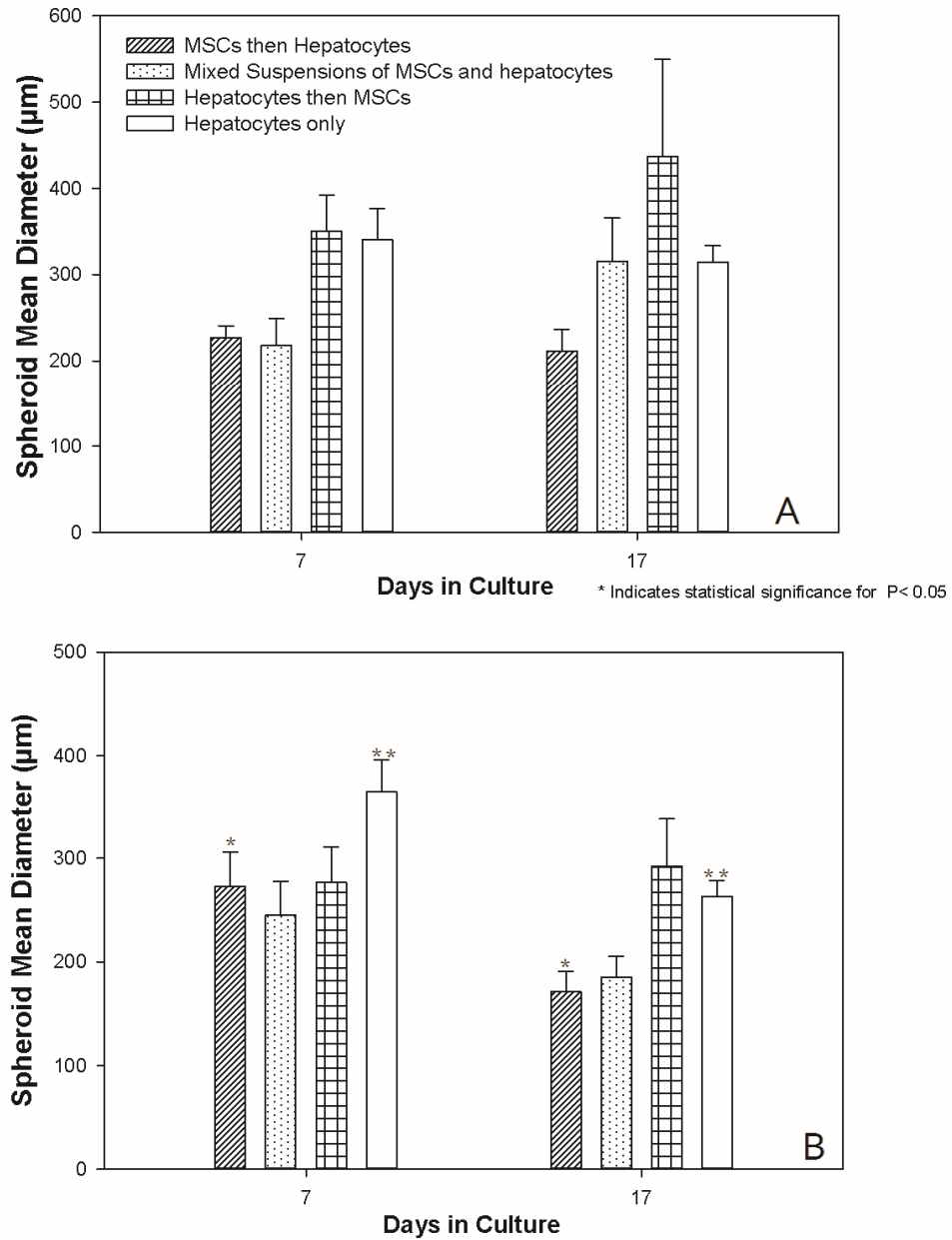


Figure 42: Spheroids mean diameters for (A) Seeding density of 50,000 cells/ cm², and (B) Seeding density of 100,000 cells/ cm². Measurements were performed for different number of spheroids (n =5 to 20). Data plotted as means with error bars representing standard error of mean (SEM).

6.3.4 AlamarBlue® Cell Health Indicator Assay

AlamarBlue® activity for seeding density 100,000 cells/ cm² was lower than the activity of 50,000 cells/ cm² seeding density on day 7 (Fig. 43A) and day 17 (Fig.43B). This observation was in agreement with the hypothesis that more cells were competing for nutrients and supplies, and hence, resulted in lower number of viable cells (as lower AlamarBlue activity indicates less number of viable cells available).

We can notice here that the activity decreases in general from day 7 to day 17 for all conditions (Fig. 44A&B) as hepatocytes were being exposed to damaging shear stresses and hence they lost their viability.

6.3.5 Hepatocyte Metabolic Functions and Viability

For seeding architecture condition # 1 (MSCs seeded one day prior to hepatocyte), the albumin rates were close to those for collagen gel sandwich controls in the first five days of culture and dropped afterwards, while urea secretion rates were fluctuating between either higher rates or similar rates to the collagen gel sandwich configuration (Fig. 44A&B). As MSCs formed spheroids first, then hepatocytes surrounded them at the peripheries, this configuration may have exposed more hepatocytes to the shear forces and caused the rapid decline in their functions compared to the preserved ones in the other two configurations.

For seeding architectures condition #2 (mixed suspensions of MSCs and hepatocytes) and condition #3 (hepatocytes then MSCs), hepatocytes synthesized albumin at rates similar to those in the control collagen gel sandwich configuration in the first week of culture and then it declined in the second week of culture (Fig.44C&E). They secreted urea at rates substantially higher than collagen gel sandwich cultured hepatocytes (Fig. 44D&F). The enhanced hepatic

functions were hypothesized to be due to substrates secreted by MSCs and utilized by hepatocytes that made them more tolerant to shear stresses.

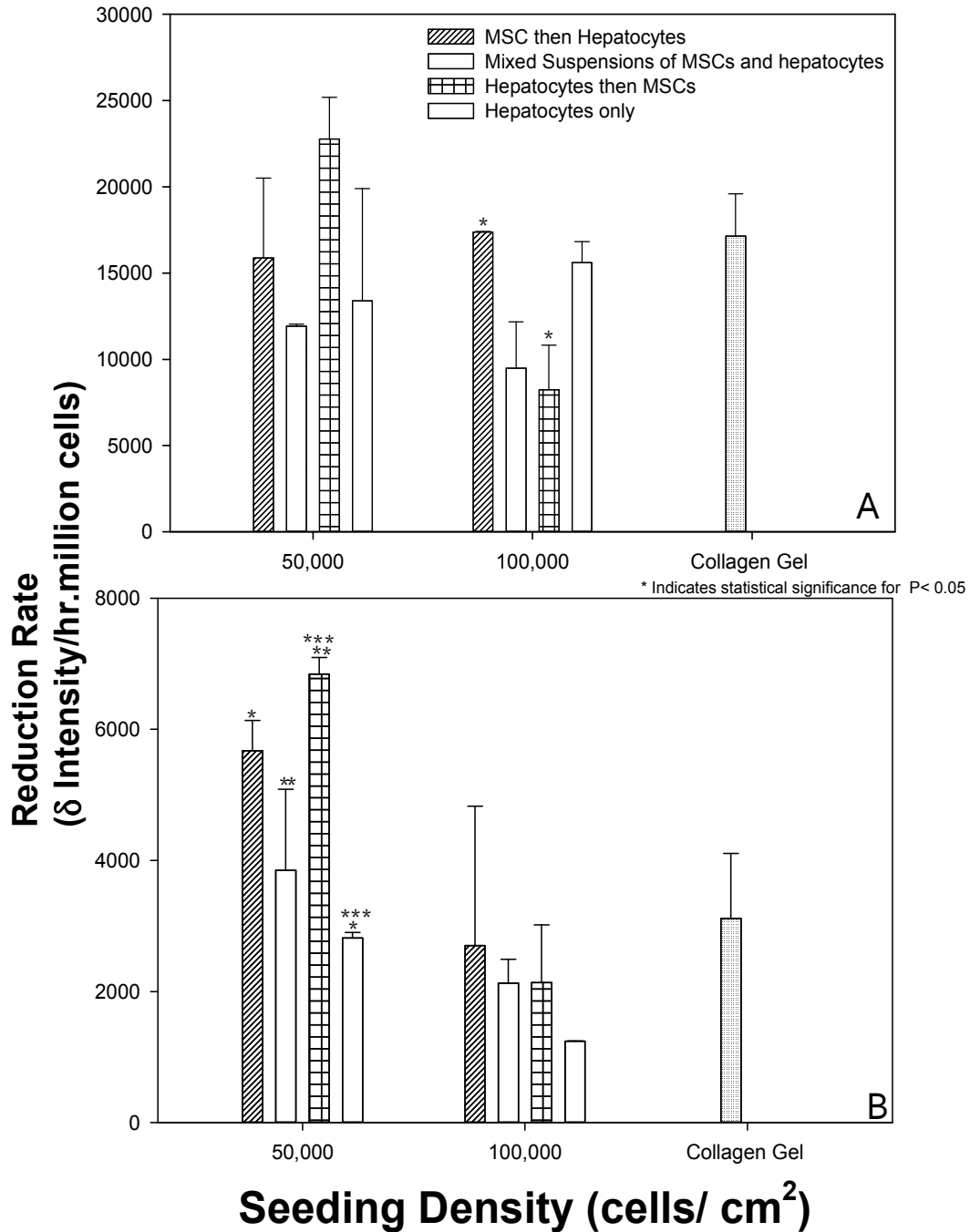
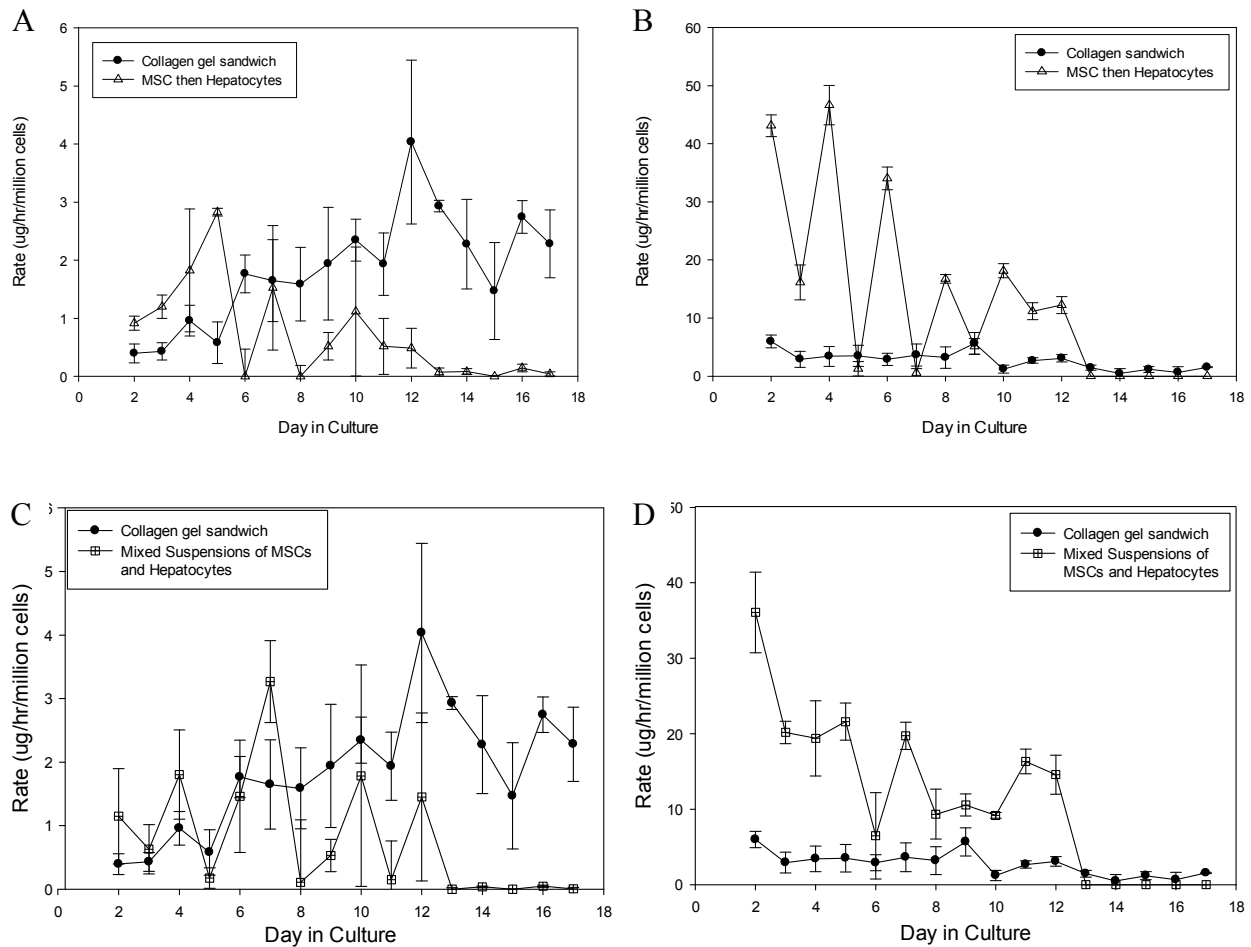


Figure 43: AlamarBlue® reduction rate for both seeding densities 50,000 cells/cm² and 100,000 cells/cm² on: (A) Day 7 and (B) Day 17 of culture time. Measurements were performed in triplicate (n = 3). Data plotted as means with error bars representing standard error of mean (SEM). (P < 0.05)

Hepatocytes cultured without MSCs in the three dimensional environment synthesized albumin at lower rates than collagen gel sandwich configuration (Fig. 44G), while urea secretion was elevated (Fig. 44H). This suggests that monotypic cultures lack necessary signals that MSCs were able to provide in the heterotypic cultures.

After two weeks of culture (~17 days), in all heterotypic conditions, neither albumin nor urea was detected; this suggests that hepatocytes de-differentiated and lost their metabolic functions.



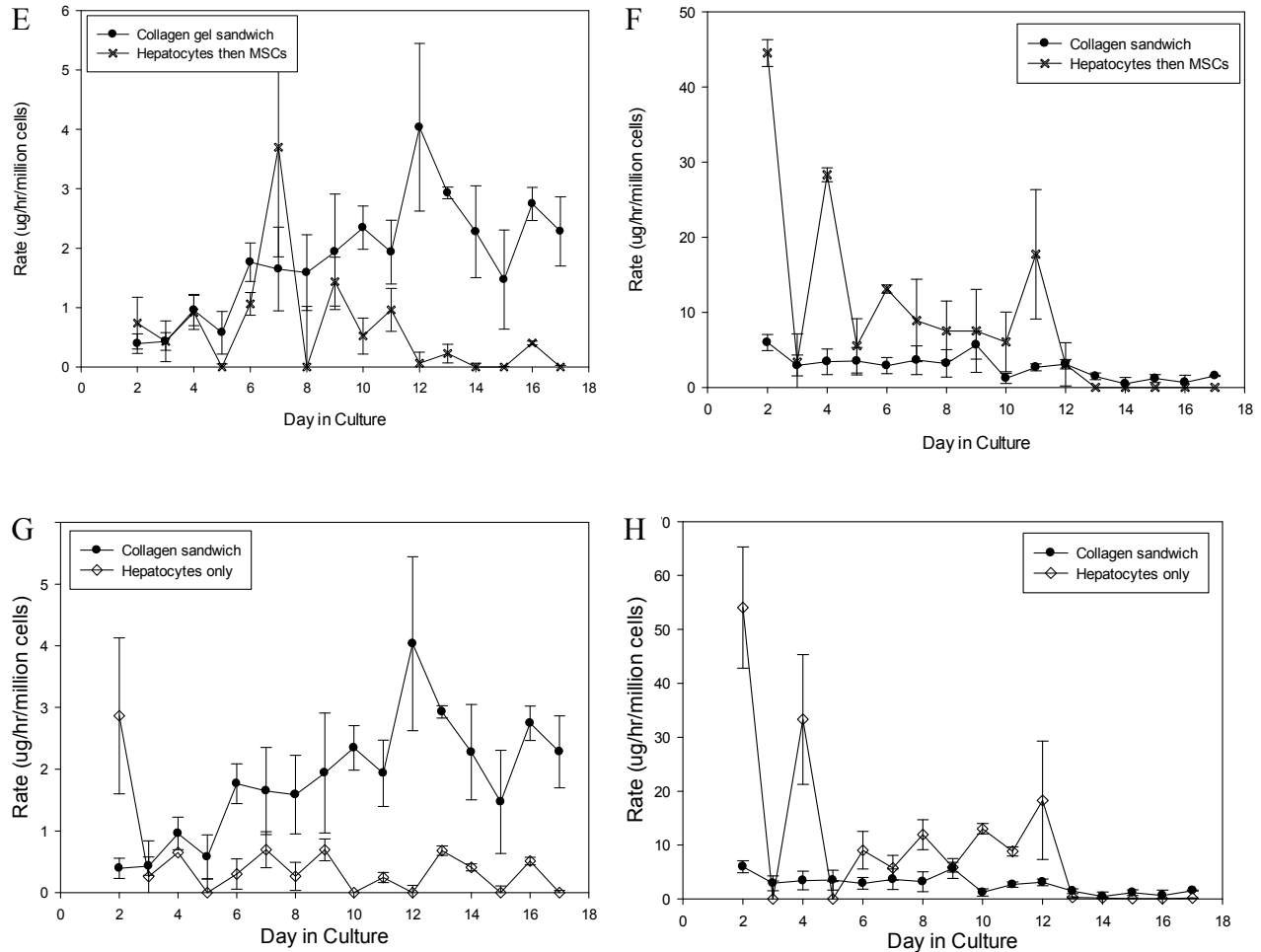


Figure 44: Metabolic functions of hepatocytes/BM-MSCs cultured disc scaffolds. Albumin secretion rates (A, C, E and G) and urea secretion (B, D, F and H) of hepatocyte/BM-MSC co-cultures in disc scaffolds cultures for the four seeding architectures. (A&B) condition #1: MSCs then hepatocytes, (C&D) condition #2: Mixed suspensions of MSCs and hepatocytes, (E&F) condition #3: Hepatocytes then MSCs, and (G&H) condition #4: Hepatocytes only cultures. Measurements were performed in triplicate ($n = 3$). Data plotted as means with error bars representing standard deviation.

6.3.6 Mathematical Model for Urea Production Rate

Since we didn't see continuous decline in the urea production rates, we assume that the aggregates were divided into two zones (outer and inner) that produce urea at two different rates based on their proximity to the nutrients and oxygen source (media). The fluctuation was mostly noted in condition #1 and condition #4; where hepatocytes were arranged at the outer surfaces of

the aggregates. This phenomena was not observed in conditions #2 (mixed suspensions of hepatocytes and MSCs) and condition #3 (MSCs seeded one day after hepatocytes aggregated formed). The outer layer of cells in a given aggregate ($Zone_{OUT}$) was exposed to the agitating medium and hence exposed to high mass transport in addition to high shear forces. The cells in this zone were arranged as one-cell thick layer. The rest of cells were at the inner region of the aggregate which was named $Zone_{IN}$. The aggregates were arranged as hemispheres as they mostly set on top of the material. There were two scenarios suggested (Fig. 45; scenario #1 when the outer layer cells were alive and functioning, and scenario #2 where the outer layer cells were dead, non-functioning but still attached to the aggregate. After one day of scenario #2, the dead cells will de-attach from the aggregate hence the diameter was reduced and we go back to scenario #1 and so forth.

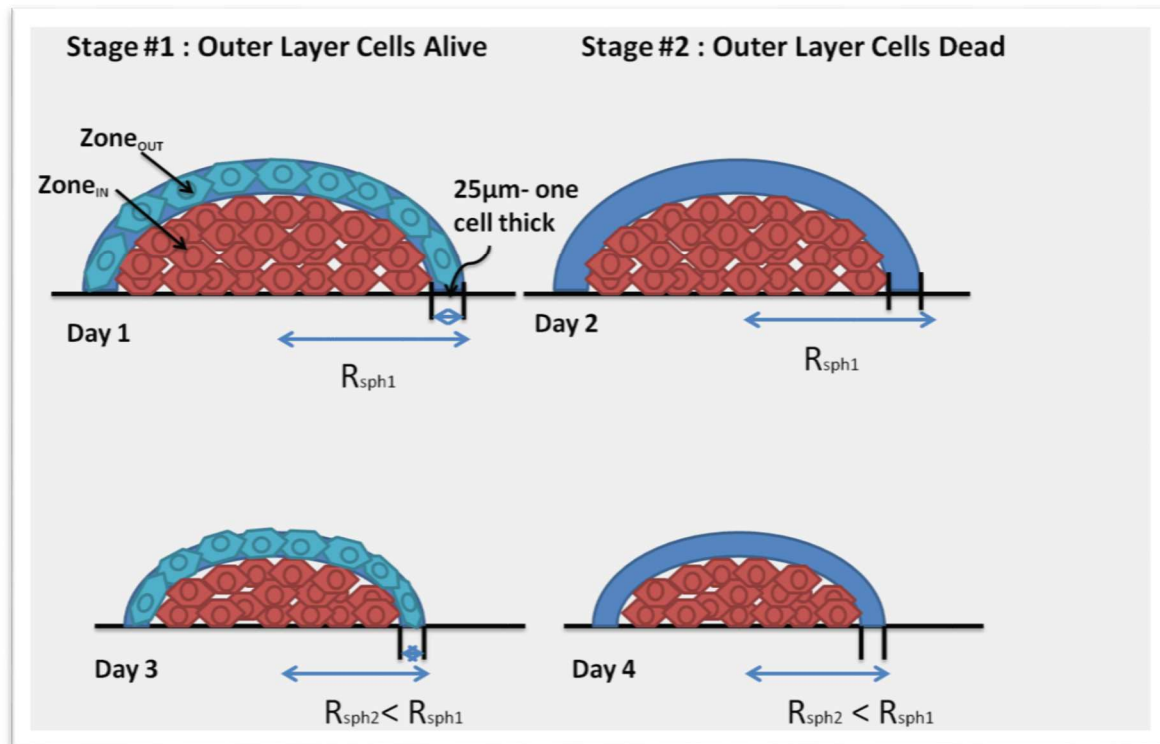


Figure 45: Schematic diagrams represent two scenarios: high and low metabolic functions and the two zones in a given aggregate.

To quantify the urea production rate for each zone, we assume a proportional relationship between production rate and oxygen concentration at that zone [111]. In order to find the oxygen concentration profile for each zone, mass transfer continuity equation in spherical coordinates was applied for steady-state system and constant ρ and D_{AB} [112]. The diameters of the aggregates were extrapolated from the two measurements made on day 7 and day 17; where a linear relationship was generated to calculate the diameters for every day of the whole culture period.

$$0 = D_{AB} \left[\frac{1}{r^2} \frac{\partial}{\partial r} \left(r^2 \frac{\partial C_A}{\partial r} \right) \right] - K \dots \dots \dots (1)$$

Where;

D_{AB} is the oxygen diffusion coefficient in hepatocytes ($3.4 \times 10^{-10} \text{ m}^2/\text{s}$).

K is the oxygen consumption rate (OCR) in hepatocyte spheroids with diameter less than $300 \mu\text{m}$ ($1.5 \times 10^{-5} \mu\text{g}/\text{mm}^3/\text{s}$); which was assumed to be a zero order reaction as OCR reaches plateau value independent from the local oxygen partial pressure at the range of interest (considered as high oxygen concentration) [91].

Solutions for the equation were obtained for the two different scenarios:

Scenario #1: outer layer of cells alive, so both diffusion and reaction terms were considered. The boundary conditions are:

- 1) Radial symmetry around the center

$$@ r = 0 \rightarrow \frac{\partial C_{OUT}}{\partial r} = 0$$

- 2) At the surface of the spheroid it's maximal (bulk) concentration

$$@ r = R_{sph} \rightarrow C_{OUT} = C_{bulk}$$

Where; C_{bulk} is the bulk oxygen concentration, r is the radial coordinate and R_{sph} is the spheroid radius. For Zone_{OUT} the limits are $(R_{sph} - 25) \leq r \leq R_{sph}$.

The oxygen concentration profile at Zone_{OUT} for scenario #1 is given by solving Eq. 1 above for the boundary conditions given:

$$C_{OUT}(r) = C_{bulk} - \frac{K}{6D} [R_{sph}^2 - r^2] \dots \dots \dots (2)$$

The concentration of oxygen in Zone_{IN} was averaged ($C_{av.}$) over a differential volume using the following formula:

$$C_{av.} = \frac{\int_0^R \int_0^\pi \int_0^{2\pi} C_{OUT}(r) \cdot r^2 d\theta d\phi dr}{\int_0^R \int_0^\pi \int_0^{2\pi} r^2 d\theta d\phi dr} \dots \dots \dots (3)$$

The $C_{av.}$ at Zone_{IN} can be calculated by the final equation:

$$C_{av.} = C_{bulk} - \frac{KR_{sph}^2}{6D} + \frac{KR^2}{10D} \dots \dots \dots (4)$$

Where,

$$R = (R_{sph} - 25).$$

Scenario #2: outer layer of cells was compromised due to shear forces damage, so no reaction term was considered, only diffusion and using Eq. (1) above with $K = 0$.

The boundary conditions are:

1) At the surface of the spheroid it is maximal (bulk) concentration

$$@ r = R_{sph} \rightarrow C_{OUT} = C_{bulk}$$

2) Flux at interface is equal from both zones

$$@ r = R_{sph} - 25 \rightarrow N_{Ainner} = N_{Aouter} = -D_{AB} \frac{\partial C_A}{\partial r}$$

The oxygen concentration profile at Zone_{OUT} for scenario #2 was obtained by solving Eq.1 above given by:

$$C_{OUT}(r) = C_{bulk} - \frac{K(R_{sph}-25)^3}{3D} \left[\frac{1}{r} - \frac{1}{R_{sph}} \right] \dots \dots \dots (5)$$

The C_{av} . at Zone_{IN} was calculated using Eq. (2) and Eq. (3) and given by the final equation:

$$C_{av.} = C_{bulk} - \frac{K(R_{sph}-25)^2}{6D} + \frac{KR^2}{10D} \dots \dots \dots (6)$$

Where,

$$R = (R_{sph} - 50).$$

Finally, the rates of urea production (U_{OUT} and U_{IN} $\mu g/ml$) were calculated using a linear equation derived from the urea production rates in collagen dish sandwich at known oxygen concentrations ($\mu g/ml$) by the following equation:

$$U_{OUT/IN} = 2.98 * C_{OUT/IN} \dots \dots \dots (7)$$

The calculated urea rates were then multiplied by the total number of live cells per zone. The total urea production rate was the summation of the urea production rate per zone.

Results of Mathematical Model

Figure 46A illustrates the total urea production rate for condition #1 (MSCs seeded one day prior to seeding hepatocytes) for the first week of culture as predicted by the model versus the actual measured values. In the co-culture system, we have seen higher urea secretion rates than the predicted values based on mono-culture system. The model assumes that a whole layer

of cells at the outer surface of an aggregate was damaged by shear force and removed. While in the actual cultures that might not be exactly the case; some of the cells at the outer layer were damaged and removed not the whole layer of cells. Also, the model predicts the urea secretion values based on a base line of the secretion in the collagen gel mono-cultures. The elevated levels of urea secretion may have been caused by a combination of the 3D culture architecture and substrates or cues secreted by MSCs and used by hepatocytes; e.g., MSC-derived matrix, growth factors, and ammonia. These results are in agreement with previous reports; Isoda et al. [113] found that soluble factors secreted from BM-MSCs had the effect of maintaining liver-specific functions and significantly increase urea secretion and albumin synthesis. Similarly, when culturing porcine hepatocytes with BM-MSCs at a ratio of 2:1, immunocytochemical staining studies by Gu et al. [109] revealed that polarity-restored, organotypic islands of hepatocytes were surrounded with a dense ECM network that was secreted by MSCs. These studies further confirmed the roles of fibronectin, laminin, and collagens assembly within close link between cellular architecture and hepatocyte functions. If we assume a base line of urea secretion as the value in a co-culture system, eq. (7) will change to:

$$U_{OUT/IN} = 6.4 * C_{OUT/IN} \dots \dots \dots (8)$$

And then the predicted values were closer to the measured values (Fig. 46B). But we still see drop of the production on days 5 and 7 (almost zero); this phenomena may have been caused by the release of cellular bi-products from dead cells that were negatively affecting metabolic functions of surviving hepatocytes. Another hypothesis for this drop was that MSCs were proliferating and their nutrients and oxygen demands were increased which caused depletion in their availability for hepatocytes use.

In addition, we have also seen higher magnitude of fluctuation in the conditions where hepatocytes were most likely to be at the outer layers of the aggregates (condition #1 and condition # 4). In the other two seeding arrangements (condition #2 and 3), the hepatocytes were less exposed to shear forces and most likely protected by the MSCs. In condition #3, MSCs were actually seeded one day after seeding the hepatocytes. This seeding arrangement allowed the hepatocytes aggregates to form first, and then MSCs attached to the outer layer which may have provided physical barrier against shear forces. In seeding condition #2, where mixed cell suspensions of hepatocytes and MSCs were seeded at the same day, in which MSCs may have secreted cues that made hepatocyte membranes more shear resistant. Moreover, MSCs contributed to providing some physical barrier by segregating themselves to the outer layer of the aggregates.

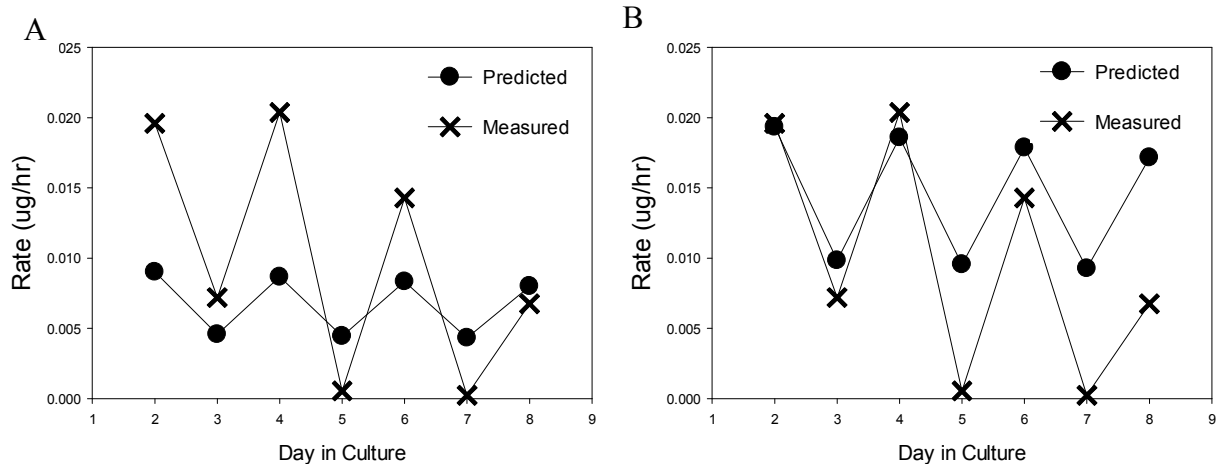


Figure 46: Total urea production rate for condition #1 (predicted vs. measured) when (A) and collagen gel values used as base line for predicted values (B) co-culture values used as base line for predicted values

6.3.7 Metabolic Performance of Heterotypic Cultures in the Perfusion System

The seeding efficiency in both monotypic seeded scaffold and heterotypic seeded scaffold were about 66%. Under dynamic conditions, seeding flow rate of 20 ml/min at 4°C and

culture flow rate of 15 ml/min, hepatocyte-MSC (heterotypic culture) seeded scaffold secreted urea at higher levels than scaffold seeded with hepatocytes only (monotypic culture) (Fig. 47A). Very low albumin levels were detected in the heterotypic seeded scaffold but at very depressed rates compared to the collagen gel sandwich static control (Fig. 47B), no albumin levels detected for the monotypic scaffold. Cells in both scaffolds expressed high levels of LDH activity (Fig. 47C). This suggests that hepatocytes were not functioning maybe due to high shear forces in the system.

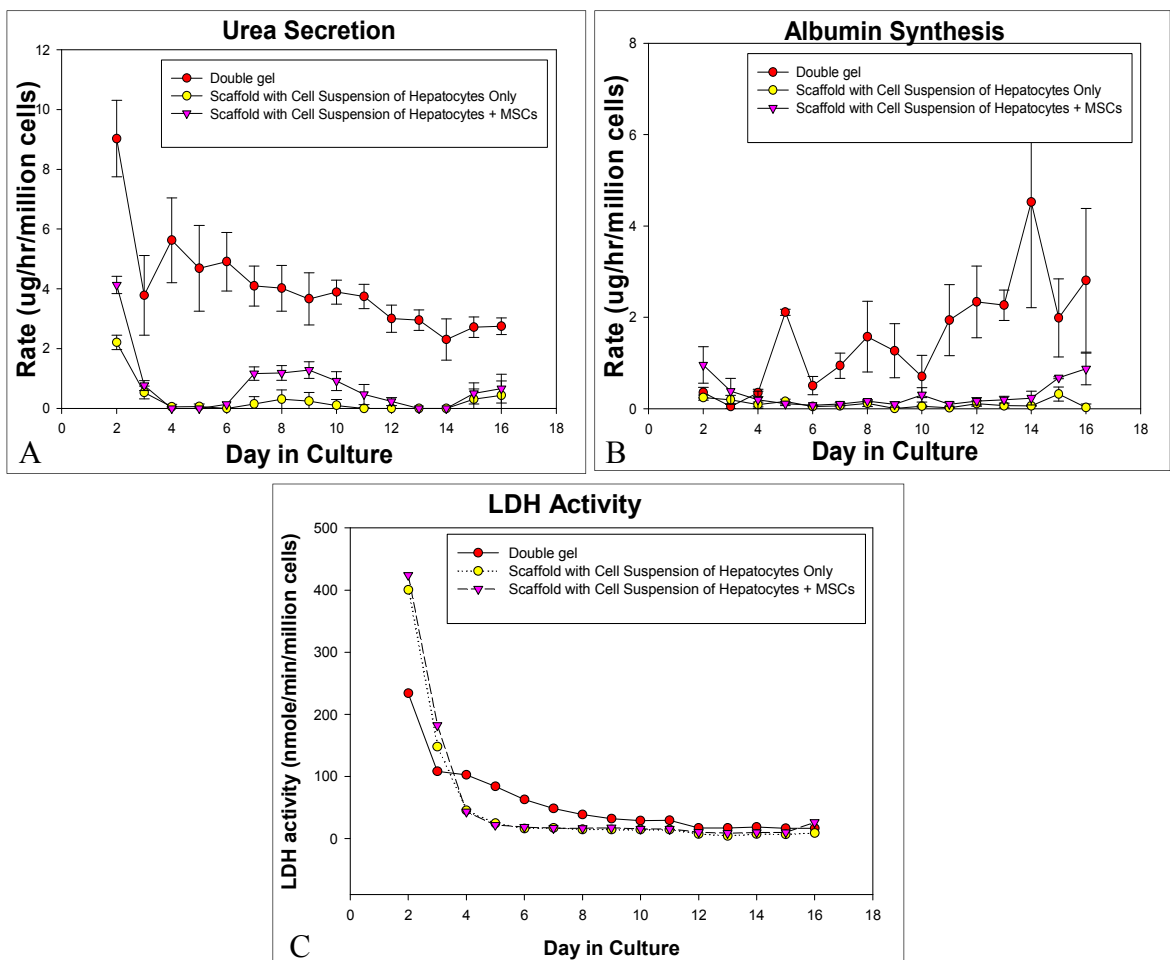


Figure 47: Metabolic performance of perfused, scaffold-seeded with monotypic and heterotypic cells suspension (A) urea secretion, (B) albumin synthesis and (C) LDH activity at seeding flow rate of 20 ml/min at 4°C and culture flow rate of 15 ml/min.

6.3.8 Cell Morphology and Neo-Tissue Formation in Perfused Scaffolds Heterotypic Cultures

MSCs formed layers of cells blocking inner pores (Fig. 48A) and outer pores (Fig. 48B), which may have affected the flow dynamics inside the scaffold (low nutrients supply and high shear forces). The cells look unhealthy and heavily damaged and deteriorated (Fig. 48C), and most of hepatocytes nuclei did not stain purple which indicate they were dead at the time of fixation.

It was noticed that new structures has been formed in the heterotypic-dynamic perfused scaffolds. Fat droplets appeared in some new tissues (Fig. 48D), formation of blood vessels like structures and hollow spheroids were noticed in the heterotypic seeded scaffold and not noticed in the monotypic culture (Fig. 48E & F). Some positive staining for CD31 marker was observed in the neo-tissue (Fig. 48G). Platelet endothelial cell adhesion molecule (PECAM or CD31) is found on the surface of endothelial cells and function as intercellular junction protein [107] (positive control Fig. 48H).

When the H&E histology sections were exposed to blue color light, hepatocytes appeared to fluoresce a green color with dark circles within the cytoplasm indicating the nucleolus (Fig. 49A). MSCs didn't fluoresce any colors, which gave us better idea how the two types of cells re-arranged themselves (when the fluorescent images compared side by side with the color images for the same sections) (Fig. 49B). We can conclude from both types of images that MSCs form mono layers around hepatocytes spheroids, with some cells embedded inside the spheroids (yellow arrows in Fig. 48B). It was also noticed that MSCs seem to segregate to the surfaces (Fig. 48A-B and E-F). The hollow structures formed appeared to be lined with single cell layer of MSC with hepatocytes aggregates built up around the holes (Fig. 49C-H).

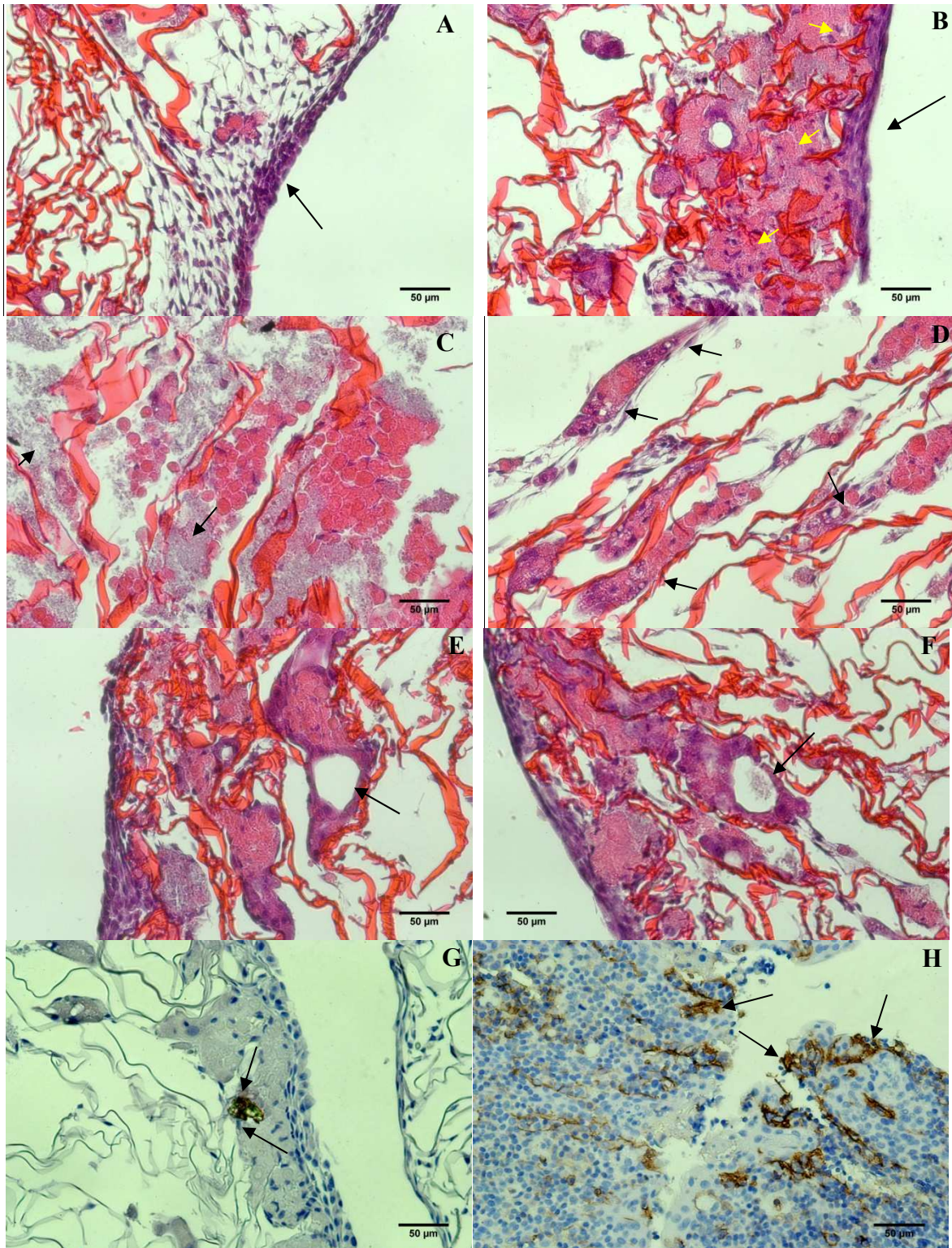


Figure 48: H&E histology images of cross sectional areas for MSCs-hepatocytes perfused scaffolds illustrating: (A) layers of cells blocking central port pores, (B) layers of cells covering the outer surface of the whole scaffold, (C) cell debris, (D) Fat droplets, (E & F) Blood vessels-like structures (arrows), and (G&H) Immunohistochemistry images for CD31 (H is control).

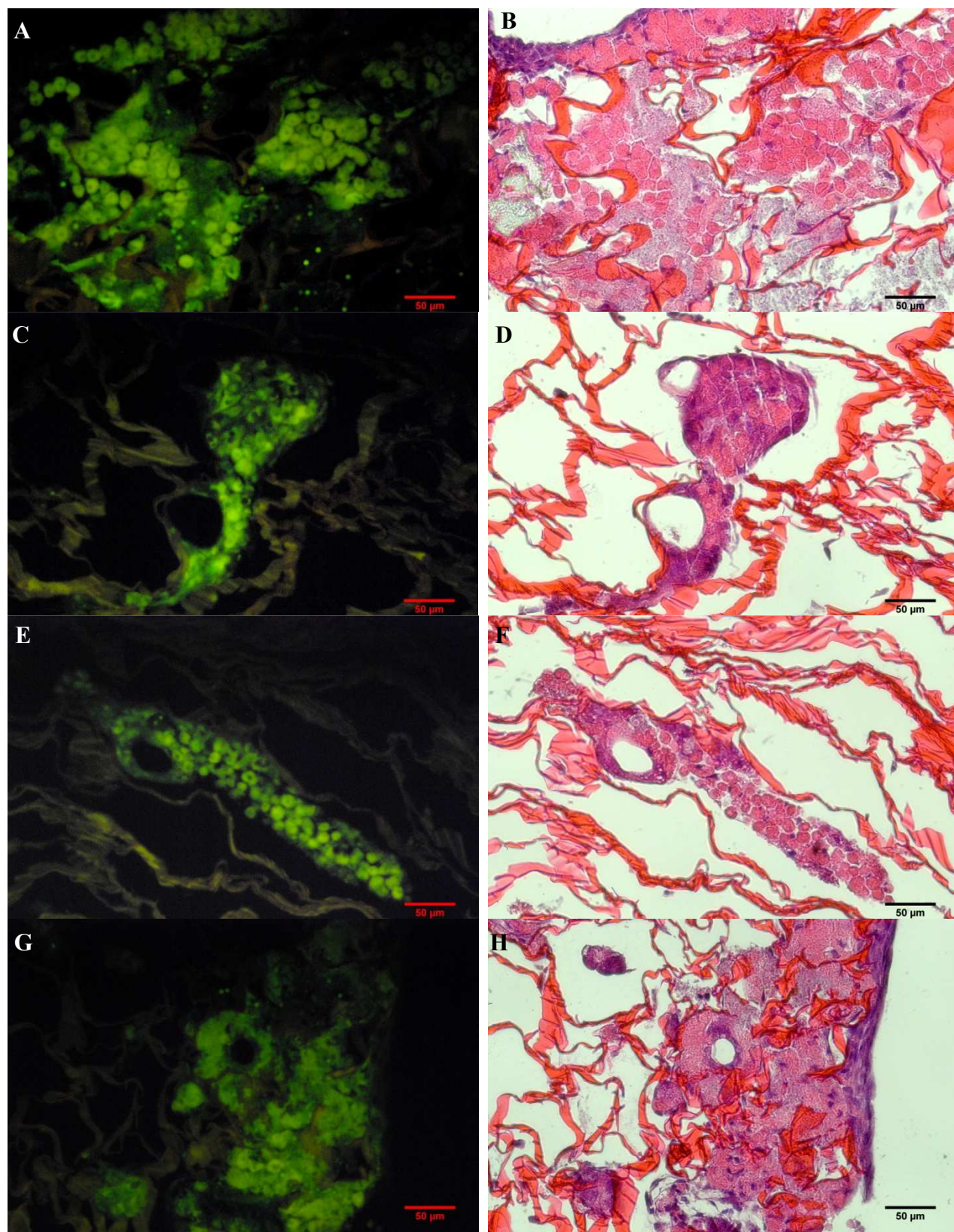


Figure 49: H&E histology images of cross sectional areas for MSCs-hepatocytes perfused scaffolds (A, C, E and G) under blue-color light, and (B, D, F and H) under normal-white light.

The hollow structures diameters range from 15.27 to 57.42 μm , which could be any type of blood vessel (from a vein to a capillary).

Masson Trichrome histology images revealed that some collagen was deposited in these cultures, but at very small quantities (Fig. 50).

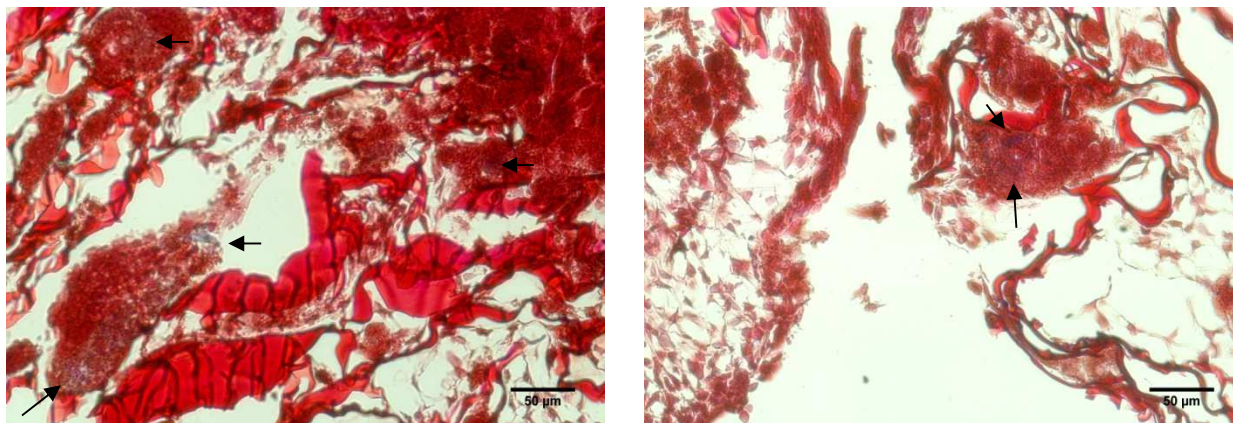


Figure 50: Masson Trichrome staining images of cross sectional areas for MSCs-hepatocytes perfused scaffolds. Arrows are pointing to faint blue-colored collagen.

6.4 Discussion

Culturing hepatocytes with MSCs on weakly-adhesive surfaces resulted in forming small-very compact spheroids. While culturing them without MSCs results in larger and looser aggregates. These very compact spheroids may have prevented adequate mass transfer and hence resulted in hepatocyte death in the long term culture.

Hepatocyte-MSC 3D disc scaffold culture results show enhanced metabolic functions in the first week of culture (short term cultures). This suggests that the elevated levels of urea secretion may have been caused by a combination of the 3D culture architecture and substrates or cues secreted by MSCs and used by hepatocytes; e.g., MSC-derived matrix, growth factors, and ammonia. In effect, MSCs and their heterotypic signals may have partially protected hepatocytes

from hypoxia in a three dimensional environment with limited circulation. These results were in agreement with previous reports; Isoda et al. [113] found that soluble factors secreted from BM-MSCs had the effect of maintaining liver-specific functions and significantly increase urea secretion and albumin synthesis. Similarly, when culturing porcine hepatocytes with BM-MSCs at a ratio of 2:1, immunocytochemical staining studies by Gu et al. [109] revealed that polarity-restored, organotypic islands of hepatocytes were surrounded with a dense ECM network that was secreted by MSCs. These studies further confirmed the roles of fibronectin, laminin, and collagens assembly within close link between cellular architecture and hepatocyte functions.

The heterotypic cultures in 3D disc scaffolds didn't perform well in terms of albumin synthesis in the long term culture. Prior studies suggest that albumin synthesis by hepatocyte spheroids was not affected by the oxygen tension, it was rather influenced by other factors such as the greater extent of heterotypic cellular interactions at the lower co-culture ratios and the number of viable hepatocytes in the formed spheroids [110]. It has also been shown that when hepatocytes were exposed to shear forces higher than 5 dynes/cm² albumin synthesis rate was significantly decreased. Therefore, increasing medium flow rate will provide higher supplies of nutrients and oxygen to the cells, but it also damages them [3, 114]. Given our orbital shaking system for the disc scaffolds, we speculate that there was a cyclic effect of shear forces due to shaking. The wall shear stress (τ_w) in the orbital shaking system can be estimated using Stokes' approximation [115]. For a constant rotational speed ($\Omega = 50$ rpm) and an orbital radius of agitation ($R_g = 3.175$ cm), the wall shear stress was estimated to be constant over the plate bottom surface and has a value of ~ 0.25 dyne/cm². This value was calculated for an empty well, while the wells in the experiments conducted here were filled with high porous chitosan scaffolds seeded with spheroids and culture medium. In addition, Salek et al. [115] results showed that τ_w

varies with different volume fills of the wells, the higher the volume the higher the shear forces will be. Hence, the fluid flow was turbulent in the wells as velocity vectors in the perpendicular planes varies along the bottom surface of the well, which would have increased the wall shear stress magnitude in the radial direction for values much higher than 0.25 dyne/cm^2 (Fig. 51). Tilles et al. [116] results showed that hepatocytes functions noticeably decreased when the flow conditions resulted in wall shear stresses higher than 0.33 dyne/cm^2 . We offer this scenario to explain the fluctuation in urea rates we observed in this set of experiments: the outer layers of hepatocytes were exposed to the moving medium and hence express high rates of urea and albumin. Due to the shear forces they were exposed to, these layers were damaged and they no longer able to produce urea and albumin. The next day, the layers of dead cells were removed exposing new-fresh layers of hepatocytes that secretes urea and synthesizes albumin.

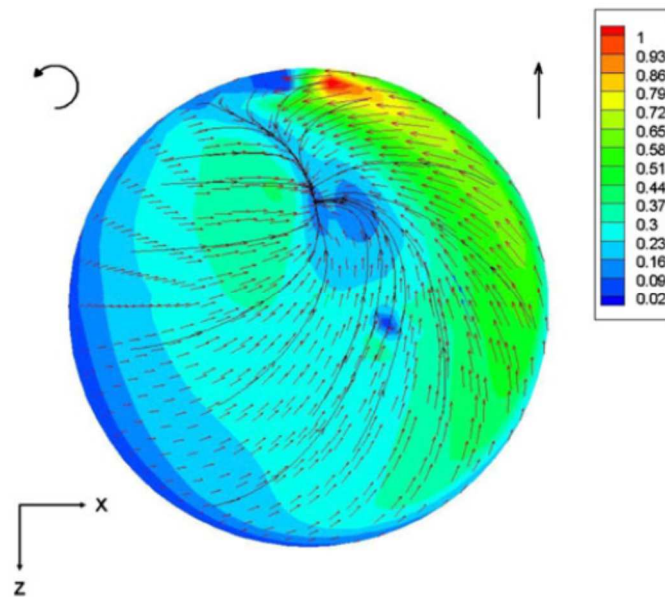


Figure 51: Wall shear stress magnitudes on the bottom surface of rotating well at 100 rpm filled with 2 ml medium. The magnitude of reference vector is in Pa ($1 \text{ Pa} = 10 \text{ dyne/cm}^2$). [116]

In the heterotypic perfusion system, MSCs blocked the pores which may have caused poor circulation in some pores and elevated shear forces in others. This may have contributed to hepatocyte death and overall poor metabolic functions. In addition, seeding MSC at the same time of seeding hepatocytes (mixed cell suspensions of MSCs and hepatocytes) may have interfered with the formation of cell-cell junctions between hepatocytes themselves and hence didn't allow them to form the required junction for their survival.

It was noticed that new structures were formed in the heterotypic-dynamic perfused scaffolds. Some blood-vessel like structures (suggests vasculogenesis) and fat droplets formation inside cells (suggests adipogenesis and lipocytes) were noted. This was due to the capability of MSCs to differentiate into other phenotypes of supporting cells that will be beneficial for hepatic neo-tissue formation in the field of bioartificial liver, i.e. endothelial cells or adipocytes.

6.5 Conclusions and Future Work

- Hepatocyte-MSC 3D disc scaffold culture results suggest that elevated levels of urea secretion may have been caused by a combination of the 3D culture architecture and substrates or cues secreted by MSCs and used by hepatocytes; e.g., MSC-derived matrix, growth factors, and ammonia. In effect, MSCs and their heterotypic signals may have partially protected hepatocytes from hypoxia in a three dimensional environment with limited circulation.
- In heterotypic perfusion system, MSCs blocked the pores which may have caused poor circulation in some pores and elevated shear forces in other poor. This may have contributed to hepatocyte death and overall poor metabolic functions.

- Co-culturing with MSC is a potentially useful approach for hepatic neo-tissue formation in the field of bioartificial liver.
- Further studies are required to investigate enhancement of intra-aggregate diffusion by using ECM-based microparticles to assemble mixed spheroids of hepatocytes and vascular-differentiated mesenchymal stem cells.
- Shear protection is required in these scaffold based microstructures. One possible method is to encapsulate the cells with ECM material; e.g., shrink wrapping method based on established soft lithography techniques describe by Palchesko et al. [117]. Or the microencapsulation technology used at Dr. Matthew's lab; a technique that is based on the complex coacervation principle [118]. The use of chemical additives to protect cells from fluid-mechanical damage is another possible solution. These additives are believed to have two different protection mechanisms that act upon on the cell. The first mechanism is of biological effect; the additive changes the cell itself to make it more shear resistant by its physical incorporation into the plasma cell membrane. The other mechanism is a physical protection; which means that the factors that are affecting the level/frequency of transmitted shear forces to the cell in a given culturing system have changed so that less cell damage is observed while the resistance of the cell to shear remains unchanged. This can be achieved by changing the viscosity of the fluid the cells are exposed to [119].

CHAPTER SEVEN

THE EFFECTS OF ENCAPSULATING HEPATOCYTES WITH OR WITHOUT BONE MARROW MESENCHYMAL STEM CELLS (BM-MSCS) WITHIN CHITOSAN-GAG FIBERS ON HEPATOCYTE VIABILITY

7.1 Introduction

As noted in the previous chapters, hepatocytes lose their functions and de-differentiate upon excision from their natural environment and cultivated in biomaterial matrices. Further, it was concluded from the studies on the chitosan-heparin scaffolds that the shear forces have great effects in hepatocytes viability and cause subsequent death upon perfusion in the dynamic system. Hence, we sought other alternatives to shield the cells from these forces.

One promising approach is the encapsulation system. Microencapsulation has shown to produce high density cultures when cells are encapsulated in ionic complexes between cationic chitosan and anionic GAG. This encapsulation method can protect from shear damage in flow or stirred cultures. Anchorage-dependent cells like hepatocytes can be provided with suitable surfaces by co-encapsulating microcarriers or other ECM attachment materials. In addition, microencapsulation will provide convenient method of cell handling and reduce cell damage that can be caused by pipetting. This method can also allow microcapsules to retain and concentrate secreted cellular products if the appropriate membrane permeability is achieved. Finally, microencapsulation methods are examined as means of providing the required barrier between exogenous cells and the host immune system [118]. Microencapsulation can be in the form of microcapsules or fibers. In this work, fibers were being investigated as possible approach for hepatocytes encapsulation. When primary rat hepatocytes were encapsulated in HA-collagen capsules and perfused with medium in a perfusion bioreactor system in previous work at Dr. Matthew's lab, they were able to maintain their metabolic functionalities for one week [120].

The Objective of this work was to optimize fiber conditions for hepatocytes culture by evaluating cell morphology and organization as well as metabolic function (albumin and urea secretion). The GAGs investigated in this work were: Chondroitin Sulfate A (CSA), Hyaluronic Acid (HA) and Heparin (HEP). HA-CHI formula has been shown to produce the thickest walls without swelling of the capsules and on the other hand, CSA-CHI has a high attachment-enhancing effect where hepatocytes exhibited extensive aggregation [118, 121, 122].

7.2 Experimental Work

7.2.1 Materials

High molecular weight (HMW) chitosan from crab shells (molecular weight about 600 KDa with 75 - 85% Deacetylated chitin), Hyaluronic acid (HA) sodium salt from *Streptococcus equi* (molecular weight about 15,000– 30,000 Da), Heparin sodium porcine mucosa, Chondroitin sulfate A (CSA) sodium salt from bovine trachea (molecular weight about 50–100 kDa, polygalacturonic Acid (PGA) sodium salt and carboxymethylcellulose (CMC) sodium salt (medium viscosity with molecular weight about 250 kDa) were all purchased from Sigma-Aldrich (St. Louis, MO). Type I rat-tail collagen (2 mg/ml) prepared in house as described elsewhere in this document was used. All other chemicals and solvents were of analytical reagent grade.

7.2.2 GAG-Chitosan Polyelectrolyte Complexes Formation into Fibers

Different compositions of GAGs with double strength collagen (2 mg/ml) were tested to evaluate the wall thickness of the membranes formed using phase contrast microscopy and evaluate their physical appearance in terms of stretching, snapping, rupturing and the ease of handling.

The formulations of polyanionic solutions examined for fibers formation were as follows:

- 1) 8%CSA, 3%CMC, double strength collagen, 0% heparin.
- 2) 8%CSA, 3%CMC, double strength collagen, 0.5% heparin.
- 3) 8%CSA, 3%CMC, double strength collagen, 1% heparin.
- 4) 2%HA, double strength collagen, 0% heparin.
- 5) 2%HA, double strength collagen, 0.5% heparin.
- 6) 2%HA, double strength collagen, 1% heparin.
- 7) Mixture of 8%CSA and 2%HA with double strength collagen, 0% heparin.
- 8) Mixture of 8%CSA and 2%HA with double strength collagen, 0.5% heparin.
- 9) Mixture of 8%CSA and 2%HA with double strength collagen, 1% heparin.

All polyanionic solutions were made by dissolving each GAG separately in Sorbitol-HEPES buffer contains: 0.4 g/L KCl, 0.5 g/L NaCl, 3.0 g/L HEPES.Na, and 36 g/L sorbitol in de-ionized (DI) water with pH adjusted to ~7.4 [121]. The fibers were formed following the microencapsulation protocol described by V. Lin and H. Matthew 2002 with double strength collagen (2 mg/ml) interior [121]. The fibers were formed by extruding the GAG-collagen solution through a 24G catheter using a syringe pump at flow rate of 0.34 ml/min. The fibers were extruded into a beaker containing chitosan-sorbitol solution (final concentrations were 0.6

wt% chitosan and 5.6 wt% sorbitol). The chitosan-sorbitol solution was made by mixing two solutions prepared separately: (1) chitosan solution that was made by dissolving 3g of high molecular weight chitosan in 250 ml DI water with 0.6ml acetic acid added after 24 hrs, and (2) sorbitol solution made by dissolving 28.4g sorbitol in 250 ml DI water. After fibers were extruded, they were allowed to set in the chitosan-sorbitol excess bath for two minutes, the fibers were then washed with 0.9 wt% NaCl, then poured into beaker containing PGA (0.1 wt%) in Sorbitol-HEPES buffer used for surface stabilization of the fibers.

For wall thickness evaluation study, the fibers were crushed under cover slips and phase contrast images were collected.

7.2.3 Culturing Hepatocytes in Chitosan-GAG-Collagen Fibers

Based on the results from previous experiment, the formula of 2 % HA + 1 % heparin + double strength collagen (2 mg/ml) composition was chosen to carry on cell culture experiments. Hepatocytes only and MSCs with hepatocytes were encapsulated in the fibers as previously described. 0.2 ml hepatocyte volume (~8 million) and 0.2 ml of GAGs + collagen solution were extruded through a 24G catheter using a syringe pump at flow rate of 0.1 ml/min and the fibers were pulled manually into chitosan-sorbitol excess bath and cut with a surgical blade into 1 cm fiber long (Fig. 52A); into which each segment has about 1 million hepatocytes. The fibers were then poured into beaker to be washed with 0.9 wt% NaCl for three times with shaking, poured into another beaker filled with 0.1 wt% PGA and shook once and again rinsed with 0.9 wt% NaCl. Finally, the fibers with cells were transferred to the culture wells in 6-well plate with 1 ml of medium added to each well (without FBS) (Fig. 52B). For heterotypic cultures, 4 million hepatocytes were mixed with 8 million MSCs (1:2 ratio) and the fibers were cut into pieces of 1

cm length that contain about 1 million hepatocytes. Media samples were collected daily for urea and albumin analysis and digital images were captured.



Figure 52: Hepatocytes encapsulated in fibers. (A) one-cm long fibers in chitosan-sorbitol bath. (B) Each fiber was poured into a well of 6-well plate tissue culture plate with 1 ml hepatocytes medium.

7.2.4 Cell Distribution in a Bundle of Chitosan-Hyaluronic acid- Heparin- Double Strength Collagen Fibers

Twenty million fixed hepatocytes (1:1 volume ratio of cell volume to GAGs solution volume) were encapsulated in the fibers (2% HA with 1% heparin and double strength collagen at 2 mg/ml concentration). To form a bundle of fibers, the fibers were wrapped around a stainless

steel rod that was attached to a rotating motor at fixed speed of 30 cm/min. The bundle was then washed with 0.9 wt% NaCl, stabilized with 0.1 wt% PGA solution, and washed again with 0.9 wt% NaCl. The wrapping was performed in a certain procedure: wrap the first layer at certain angle and the second layer at the opposite angle and hence ensure a porous scaffold will form (Fig. 53).

The seeded bundle scaffold was then processed for histology and H&E staining.

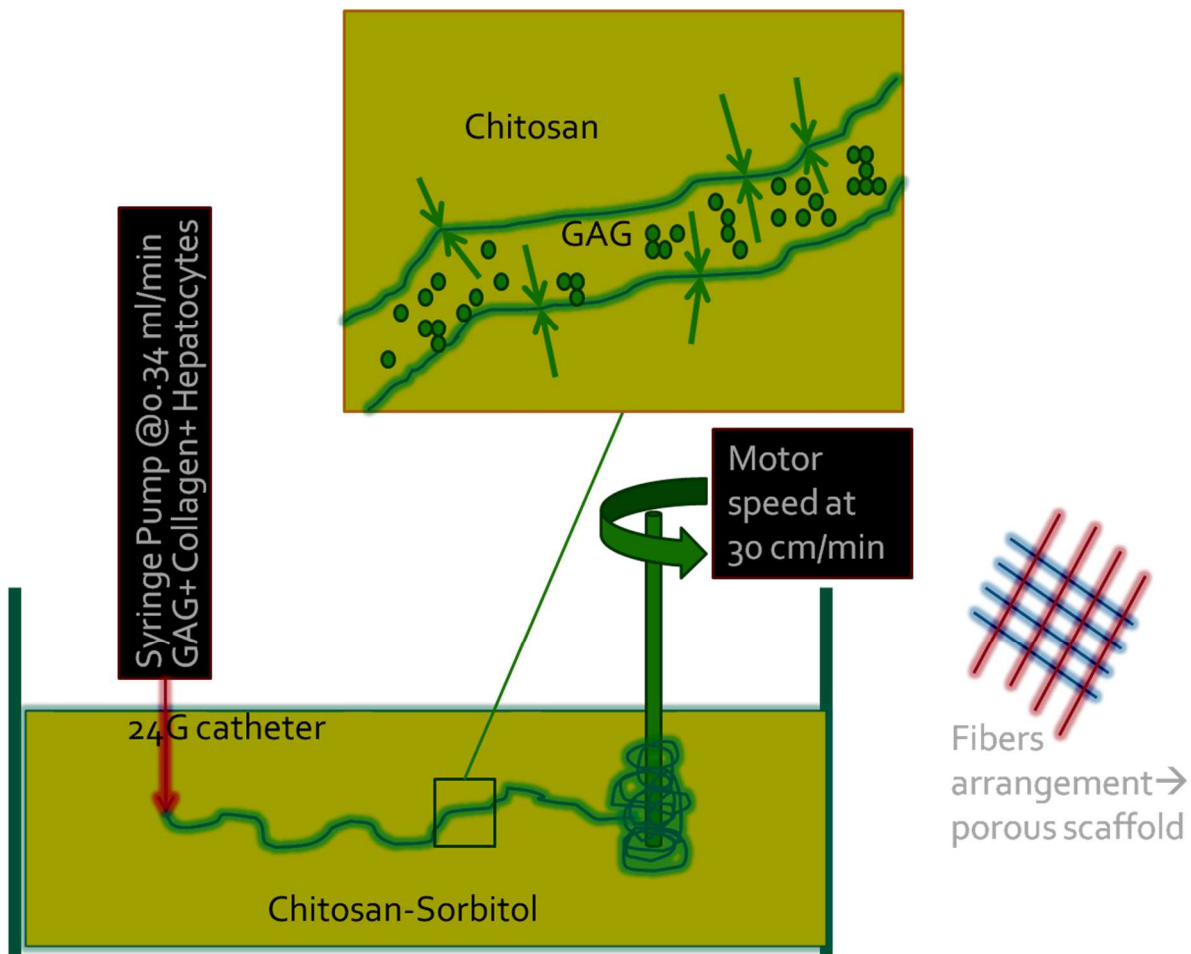


Figure 53: Fiber bundle fabrication method. Schematic diagram of bundle scaffold fabrication process of hepatocytes encapsulated in 2 % HA + 1% heparin + double strength collagen.

7.3 Results

7.3.1 Membrane Thickness for Different Formulas of GAG-Chitosan Polyelectrolyte

Complex Fibers

The phase contrast imaging observations were summarized in the table below (table 7) with noticeable remarks for each formula. 2% HA with 1% heparin and double strength collagen formed the thickest membrane with fibers that didn't snap while formation and stayed as continuous fibers which made them easy to handle. The dehydrated fibers membranes were very thin (Fig. 54.A) with thickness of about 1 μm (Fig. 54B). We can notice here that the membranes have smooth surface from inside and rough surface from the outside, as the chitosan acting with the GAG from outside and building up towards the outside.

	8%CSA+3%CMC+ double strength collagen (2mg/ml neutralized)	8% CSA +2%HA+ double strength collagen (2mg/ml neutralized)	2%HA+ double strength collagen (2mg/ml neutralized)
No heparin	<ul style="list-style-type: none"> • Continuous fibers. • While washing rupture. • Thin walls 	<ul style="list-style-type: none"> • Snapping. • Very thin walls 	<ul style="list-style-type: none"> • Snapping • Very thin walls
0.5% heparin	<ul style="list-style-type: none"> • Snapping • Rupture • Thin walls 	<ul style="list-style-type: none"> • Continuous fibers • Moderate thickness 	<ul style="list-style-type: none"> • Continuous fibers • Very thin walls
1% heparin	<ul style="list-style-type: none"> • Snapping • Moderate thickness 	<ul style="list-style-type: none"> • Continuous fibers • Very thin walls 	<ul style="list-style-type: none"> • Continuous fibers no snapping. • Easy to handle • Thick walls

Table 7: Summary of observations for fibers made from different GAG formulations.

The fiber membranes formed with this technique have porous network as seen via scanning electron microscope (Fig 54C & D); this will allow small molecules to pass through the membranes in and out the fibers but in the same time provide means of protection against flow. This architecture resembles the space of Disse at the hepatic sinusoids. The inside pores were in the range of 119.6 ± 24 nm diameters (Fig. 54C) and the outside pores were in the range of 178.3 ± 33 nm diameters (Fig. 54D) as estimated using ImageJ (Feret diameter).

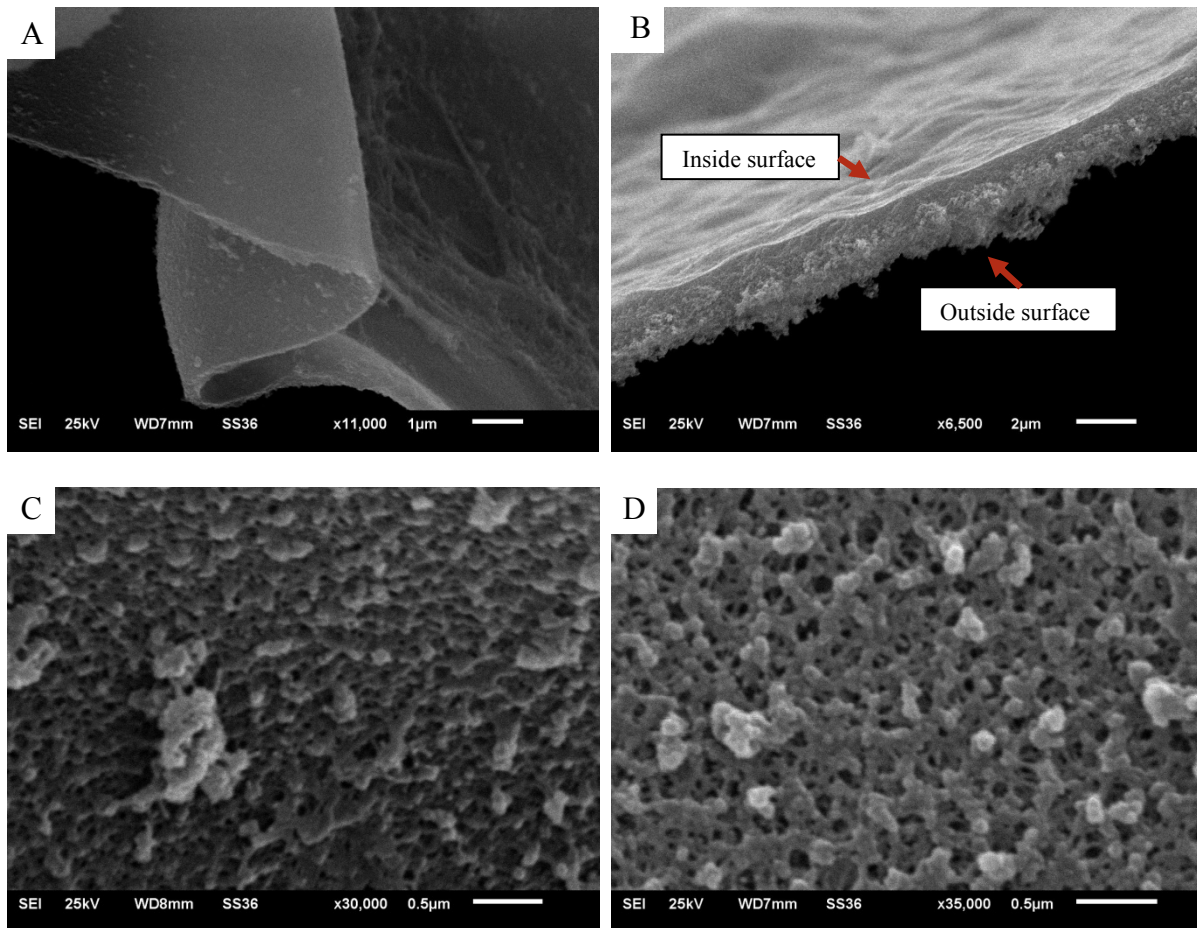


Figure 54: SEM photos of the fiber's membrane. (A and B) is an edge of a fiber membrane. The membranes have high porosity from inside (C) and outside (D).

When fixed hepatocytes were encapsulated in the 2% HA with 1% heparin and double-strength collagen, and then flattened by crushing them under glass cover slip, the wall thickness was 25.90 ± 9.87 μm (Fig. 55A&B), while the dehydrated membranes had thickness of ~ 1 μm

(as seen via SEM images Fig. 54A). This is in agreement with the fact that the membranes were basically hydrogels with water as the main content.

We can see from the SEM images (Fig. 55C&D) that the fixed cells were connected to each other with the ECM material used in the encapsulation (collagen) which will provide the basic ECM from the start of the culture until the live cells secrete their own ECM material. This is of high importance for anchorage-dependent cell types like hepatocytes.

For the other formulations, the walls were very thin to be measured for wall thickness. Even at high magnification, the edges of the walls can't be focused properly to distinguish the start and the end of the membrane wall. The other formulations tested either formed thin-walled capsules, or very fragile (snapping), or were rupturing while washing out the excess polymer, or a combination of these remarks. Figure 57 lists phase contrast images for each formulation tested.

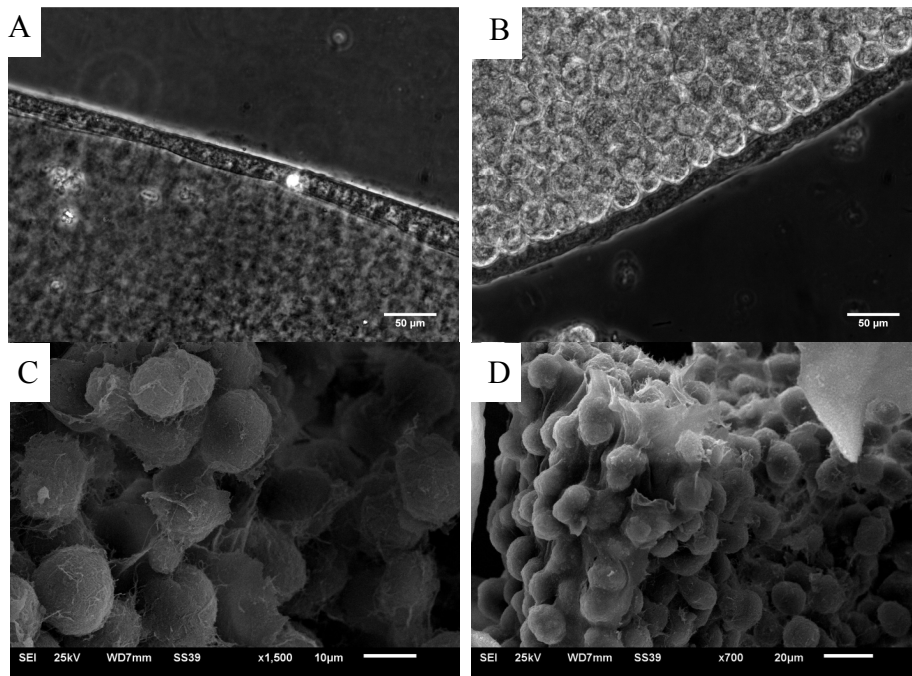


Figure 55: Phase contrast images (A&B) and SEM images (C&D) of encapsulated hepatocytes in chitosan- 2% HA with 1% heparin and double strength collagen fibers.

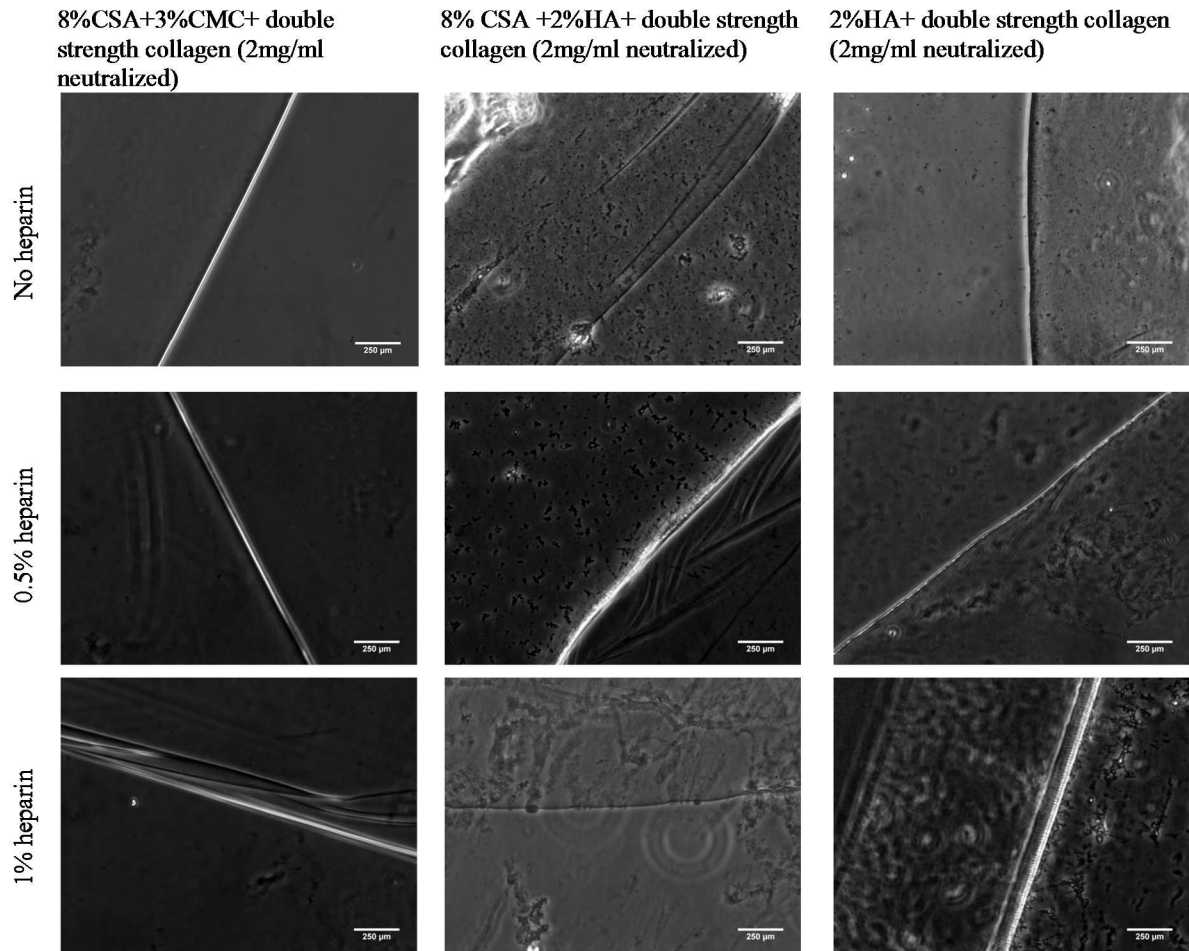


Figure 56: Phase contrast images illustrating the membranes formed in each of the listed formulations.

7.3.2 Encapsulated Hepatocytes (with and without MSCs) Morphology

The cells aggregated into large cylindrical aggregates (following the shape of the fibers) that were floating inside the fibers. They aggregated as one big aggregate in monocultures (Fig. 57A & B). In the heterotypic cultures, they appeared as several smaller separate aggregates (Fig. 57C&D). The fibers were about 0.65 ± 0.13 mm thick.

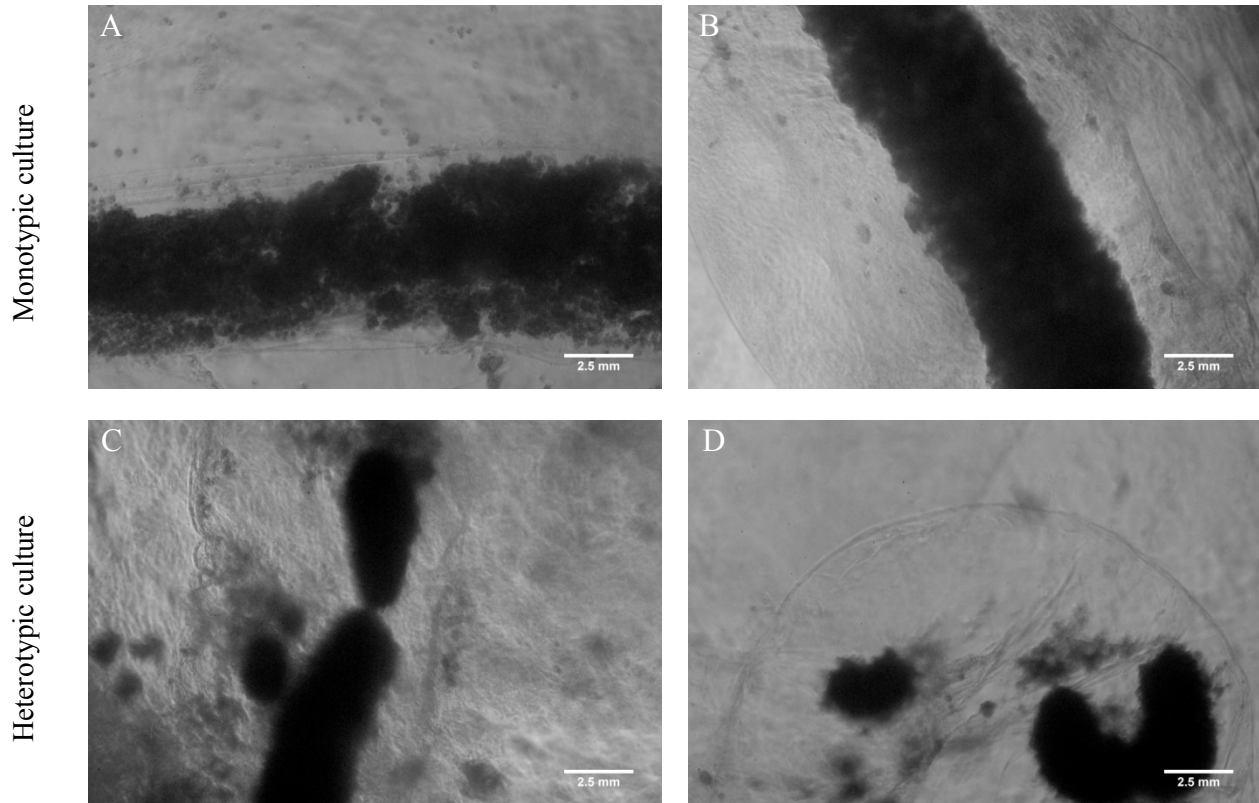


Figure 57: Phase contrast images of encapsulated hepatocytes in chitosan- 2% HA with 1% heparin and double strength collagen fibers. (A & B) Monotypic cultures, (C & D) Heterotypic cultures.

While the fibers looked intact, were easy to handle, and survived the washing and shaking steps on the fabrication day (Fig. 58A), they swelled on day 2 (Fig. 58B) and eventually ruptured and released all aggregates by day 4 of culture (Fig. 58C).

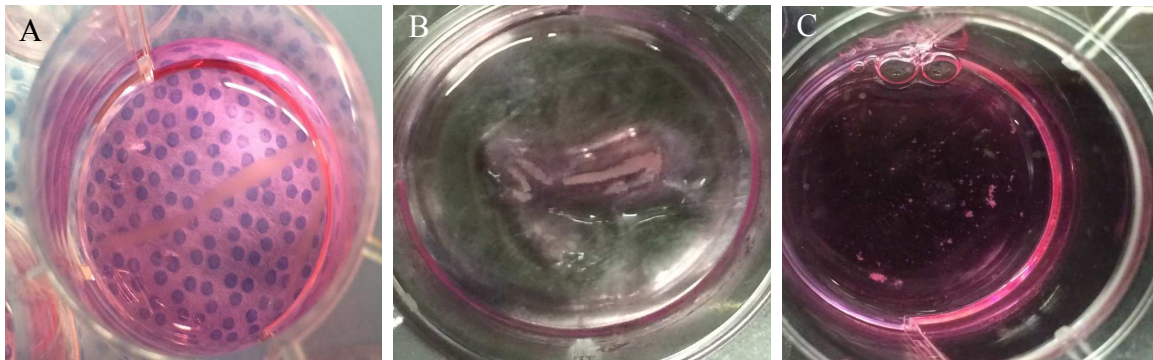


Figure 58: Digital images of encapsulated hepatocytes in chitosan- HA- heparin fibers. Digital color images of the fibers on (A) day 1, (B) day 2, and (C) day 4.

7.3.3 Metabolic Performance of Encapsulated Hepatocytes with/without MSCs

No statistically significant differences in urea secretion between cultures of encapsulated hepatocytes only and cultures of mixed hepatocytes and MSCs. The urea secretion rates were at depressed rates compared to collagen gel sandwich controls (Fig. 59A). On the other hand, no albumin detected at all in both cultures (Fig. 59B).

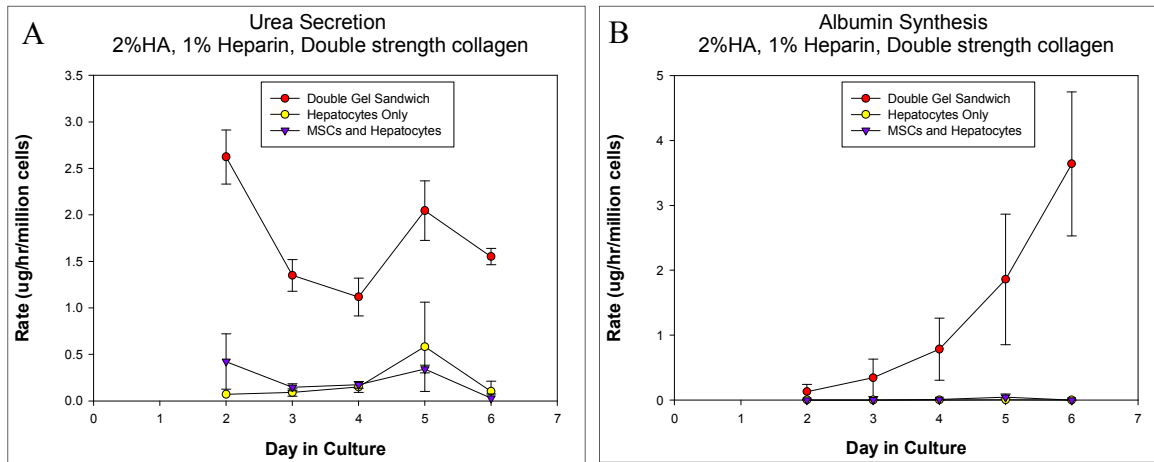


Figure 59: Metabolic performance of monotypic and heterotypic cells suspension in chitosan-2% HA with 1% heparin and double strength collagen fibers. (A) Urea, and (B) albumin secretion rates.

7.3.4 Cell Distribution in Fiber Bundle Scaffold

Fibers could not be easily wrapped around the connector and form a bundle of fibers in the intended way of wrapping procedure illustrated in figure 53 above. Instead, they wrap around each other at a concentric bundle dragging the whole scaffold downward (Fig. 60). The wrapping was performed to generate the required spacing between the fibers by moving the wrapping rod up and down. Histology images revealed that the fibers have spacing between them inside the bundle (porous scaffold) (Fig. 61 black arrows), but it looks like there was a membrane at the periphery sealing the whole bundle (Fig. 61 red arrows).



Figure 60: Digital image of fixed hepatocytes in fiber bundle scaffold.

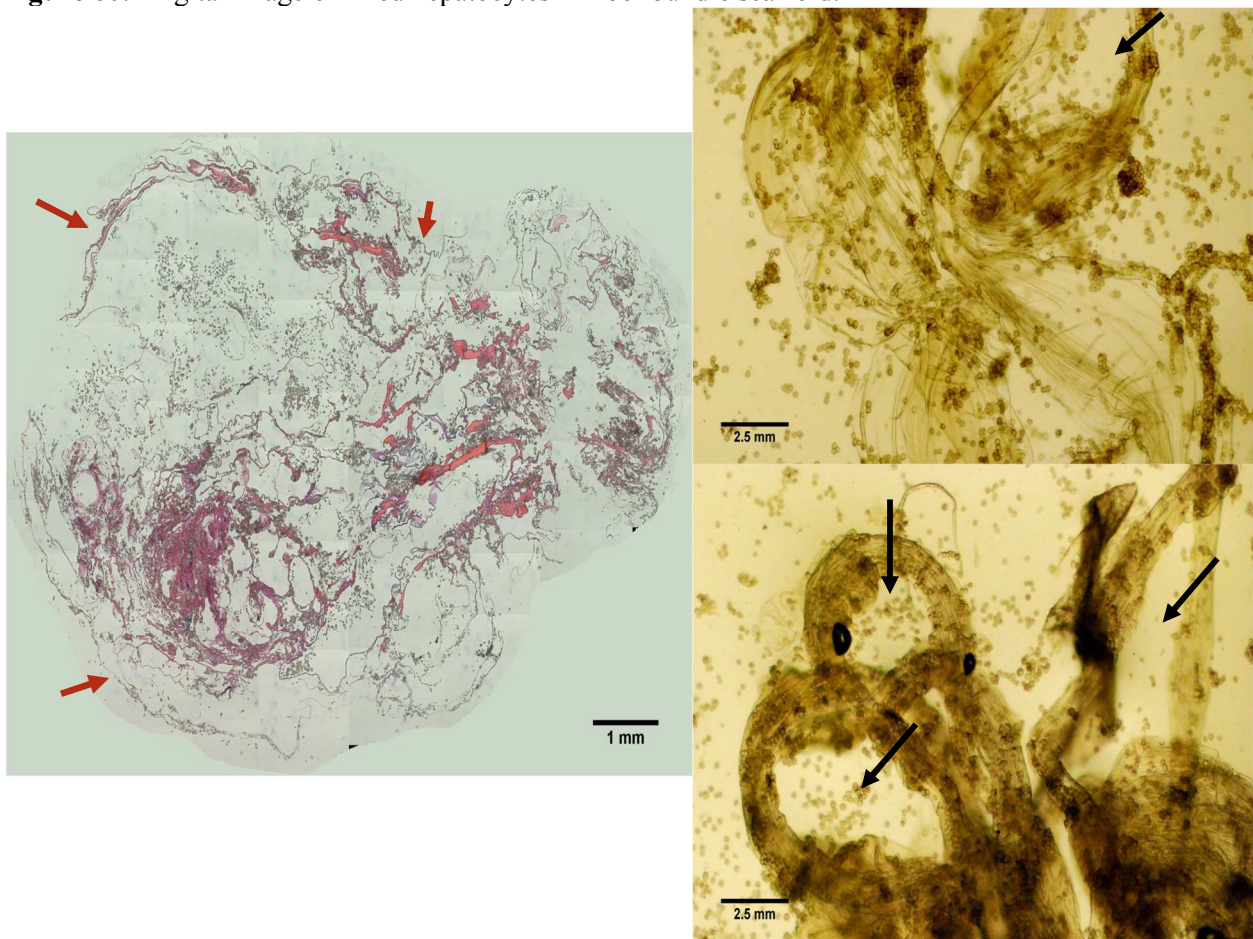


Figure 61: Cell distribution and fibers architecture in a wrapped bundle. (Left) H&E histology image of a whole cross sectional area for fixed hepatocytes in fiber bundle scaffold. (Right) phase contrast images of the fibers bundle.

7.4 Discussion

The hyaluronic acid based fibers makes a promising approach in the field of modular tissue engineering. They form thick membranes, easy to handle and elastic fibers which make them of a better choice among other GAGs; e.g. chondroitin sulfate A. The major challenge with the fiber system presented in this work was the ruptures of the fibers, where they lose their contents rapidly even in static culture. The depressed metabolic functions seen were due to the loss of the aggregates during media changes. Albumin was not detected because it is considered to be a relatively large protein (MW about 67,000 Da) that may have not diffused from the aggregates through the membranes walls and into the medium. V. Lin and H. Matthew, 2002 [121] calculated effective diffusivity for albumin to be the lowest among other materials that have lower molecular weights.

Fibers with diameters higher than 500 μm will generate aggregates of the same diameters and those are known to develop necrotic centers as they will experience mass transfer limitations of metabolites and oxygen in the core [91]. An automated system of pulling the fibers at a speed that was less or equal to the extruding rate was required to ensure the minimum diameter possible to reach; thinner fibers are preferred as there will be more material to carry a given volume load. Another important parameter was the architecture of fiber wrapping that will play significant role in overall strength of the loaded scaffold.

As the remaining GAG solution may stay inside the fibers (GAG molecules that are not incorporated to the walls by reacting with chitosan molecules); the water molecules will diffuse through the fibers membrane into the fibers interior causing them to swell and eventually rupture. Reducing the internal content of GAG by incorporating other particles to the interior will be a possible solution to the rupture problem. Currently, other students in our lab are

investigating these alternatives; e.g. adding chitosan microcarriers or collagen microcarriers to the microcapsules and fibers interiors.

7.5 Conclusions and Future Work

- Thinner fibers are better to use (should be $<300\mu\text{m}$); ensure no mass transfer limitations and more material to carry a given volume load.
- The architecture of fiber wrapping plays significant role in overall strength of the loaded scaffold.
- High porous scaffolds with high cell densities can be achieved using the fiber wrapping system. The fiber bundles can be also perfused in the bioreactor system once the fiber rupturing problem is addressed.
- Enforcing the fibers membranes with chitosan microfibers to enhance their mechanical strength might be a valid solution for the issues faced in this work.
- Further modifications to the interior of the capsules are needed in order to minimize the GAGs content and hence eliminate the rupture issue. Incorporating chitosan microcarriers or collagen microcarriers to the interior environment of the fibers will help decreasing the GAG content.

REFERENCES

- [1] J. W. Grisham, "Cell types in rat liver cultures: their identification and isolation," *Mol Cell Biochem*, vol. 53-54, pp. 23-33, 1983.
- [2] T. Koura, S. Kaneko, E. Matsushita, H. Ohno, K. Kaji, and K. Kobayashi, "Investigation of albumin-synthesizing ability in rat cirrhotic liver-derived hepatocytes using primary hepatocyte culture," *J Hepatol*, vol. 31, pp. 293-9, Aug 1999.
- [3] J. W. Allen and S. N. Bhatia, "Formation of steady-state oxygen gradients in vitro: application to liver zonation," *Biotechnol Bioeng*, vol. 82, pp. 253-62, May 5 2003.
- [4] A. v. d. Plaats, "The Groningen hypothermic liver perfusion system for improved preservation in organ transplantation," *Dissertation- University of Gorningen* 2005.
- [5] "Hepatic Acini Diagram," *Access online:* http://www.vivo.colostate.edu/hbooks/pathphys/digestion/liver/histo_acinus.html.
- [6] "Digital camera shot of human liver sinusoid through a microscope " *Access online:* <http://en.wikipedia.org/wiki/File:Sinusoid.JPG#metadata>.
- [7] "Sinusoid of a rat liver with fenestrated endothelial cells," *access online:* <http://en.wikipedia.org/wiki/File:Sinusoid.jpeg>.
- [8] *U.S. Organ Procurement and Transplantation Network*. Available: <http://optn.transplant.hrsa.gov>
- [9] T. S. Bentley, "2011 U.S. Organ and Tissue Transplant Cost Estimates and Discussion," 2011.
- [10] C. Chan, F. Berthiaume, B. D. Nath, A. W. Tilles, M. Toner, and M. L. Yarmush, "Hepatic tissue engineering for adjunct and temporary liver support: Critical technologies," *Liver Transplantation*, vol. 10, pp. 1331-1342, 2004.

- [11] G. Catapano and J. Gerlach, "Bioreactors for liver tissue engineering," *Ashammakhi N, Reis R, Chiellini E (eds.) Topics in tissue engineering*, pp. 1-41, 2007.
- [12] M. Muraca, G. Gerunda, D. Neri, M. T. Vilei, A. Granato, P. Feltracco, *et al.*, "Hepatocyte transplantation as a treatment for glycogen storage disease type 1a," *Lancet*, vol. 359, pp. 317-8, Jan 26 2002.
- [13] S. Gupta, "Hepatocyte transplantation," *J Gastroenterol Hepatol*, vol. 17 Suppl 3, pp. S287-93, Dec 2002.
- [14] S. Gupta and J. R. Chowdhury, "Therapeutic potential of hepatocyte transplantation," *Semin Cell Dev Biol*, vol. 13, pp. 439-46, Dec 2002.
- [15] A. J. Strain and J. M. Neuberger, "A bioartificial liver--state of the art," *Science*, vol. 295, pp. 1005-9, Feb 8 2002.
- [16] S. M. Chia, K. W. Leong, J. Li, X. Xu, K. Zeng, P. N. Er, *et al.*, "Hepatocyte encapsulation for enhanced cellular functions," *Tissue Eng*, vol. 6, pp. 481-95, Oct 2000.
- [17] J. S. Lee, J. Shin, H. M. Park, Y. G. Kim, B. G. Kim, J. W. Oh, *et al.*, "Liver extracellular matrix providing dual functions of two-dimensional substrate coating and three-dimensional injectable hydrogel platform for liver tissue engineering," *Biomacromolecules*, vol. 15, pp. 206-18, Jan 13 2014.
- [18] Y. Liu, H. Li, S. Yan, J. Wei, and X. Li, "Hepatocyte cocultures with endothelial cells and fibroblasts on micropatterned fibrous mats to promote liver-specific functions and capillary formation capabilities," *Biomacromolecules*, vol. 15, pp. 1044-54, Mar 10 2014.
- [19] K. Lee, E. A. Silva, and D. J. Mooney, "Growth factor delivery-based tissue engineering: general approaches and a review of recent developments," *J R Soc Interface*, vol. 8, pp. 153-70, Feb 6 2011.

- [20] J.-k. Park and D.-h. Lee, "Bioartificial liver systems: current status and future perspective," *Journal of Bioscience and Bioengineering*, vol. 99, pp. 311-319, 4// 2005.
- [21] J. Li, L. Li, H. Yu, H. Cao, C. Gao, and Y. Gong, "Growth and Metabolism of Human Hepatocytes on Biomodified Collagen Poly(lactic-co-glycolic acid) Three-Dimensional Scaffold," *ASAIO Journal*, vol. 52, pp. 321-327 10.1097/01.mat.0000217794.35830.4a, 2006.
- [22] K. Gelse, E. Poschl, and T. Aigner, "Collagens--structure, function, and biosynthesis," *Adv Drug Deliv Rev*, vol. 55, pp. 1531-46, Nov 28 2003.
- [23] J. Kasuya and K. Tanishita, "Microporous membrane-based liver tissue engineering for the reconstruction of three-dimensional functional liver tissues in vitro," *Biomatter*, vol. 2, pp. 290-5, Oct-Dec 2012.
- [24] S. Giri, U. D. Braumann, P. Giri, A. Acikgoz, P. Scheibe, K. Nieber, *et al.*, "Nanostructured self-assembling peptides as a defined extracellular matrix for long-term functional maintenance of primary hepatocytes in a bioartificial liver modular device," *Int J Nanomedicine*, vol. 8, pp. 1525-39, 2013.
- [25] K. Choi, W. P. Pfund, M. E. Andersen, R. S. Thomas, H. J. Clewell, and E. L. LeCluyse, "Development of 3D dynamic flow model of human liver and its application to prediction of metabolic clearance of 7-ethoxycoumarin," *Tissue Eng Part C Methods*, vol. 20, pp. 641-51, Aug 2014.
- [26] J. Li, J. Pan, L. Zhang, X. Guo, and Y. Yu, "Culture of primary rat hepatocytes within porous chitosan scaffolds," *Journal of Biomedical Materials Research Part A*, vol. 67A, pp. 938-943, 2003.

- [27] X.-H. Chu, X.-L. Shi, Z.-Q. Feng, Z.-Z. Gu, and Y.-T. Ding, "Chitosan nanofiber scaffold enhances hepatocyte adhesion and function," *Biotechnology Letters*, vol. 31, pp. 347-352, 2009.
- [28] J. C. Y. Dunn, R. G. Tompkins, and M. L. Yarmush, "Long-term in vitro function of adult hepatocytes in a collagen sandwich configuration," *Biotechnology Progress*, vol. 7, pp. 237-245, 1991/05/01 1991.
- [29] N. Nieto and M. P. Lutolf, "Extracellular matrix bioengineering and systems biology approaches in liver disease," *Syst Synth Biol*, vol. 5, pp. 11-20, Jun 2011.
- [30] S. V. Madihally and H. W. T. Matthew, "Porous chitosan scaffolds for tissue engineering," *Biomaterials*, vol. 20, pp. 1133-1142, 6// 1999.
- [31] T. Kean and M. Thanou, "Biodegradation, biodistribution and toxicity of chitosan," *Adv Drug Deliv Rev*, vol. 62, pp. 3-11, Jan 31 2010.
- [32] H. Onishi and Y. Machida, "Biodegradation and distribution of water-soluble chitosan in mice," *Biomaterials*, vol. 20, pp. 175-82, Jan 1999.
- [33] E. Khor and L. Y. Lim, "Implantable applications of chitin and chitosan," *Biomaterials*, vol. 24, pp. 2339-49, Jun 2003.
- [34] H. Jiankang, L. Dichen, L. Yaxiong, Y. Bo, Z. Hanxiang, L. Qin, *et al.*, "Preparation of chitosan-gelatin hybrid scaffolds with well-organized microstructures for hepatic tissue engineering," *Acta Biomater*, vol. 5, pp. 453-61, Jan 2009.
- [35] T. Bou-Akl, "Design and evaluation of an angiogenic scaffold for hepatocyte transplantation," Ph.D. 3225810, Wayne State University, United States -- Michigan, 2006.

- [36] M. Warda and R. J. Linhardt, "Dromedary glycosaminoglycans: molecular characterization of camel lung and liver heparan sulfate," *Comp Biochem Physiol B Biochem Mol Biol*, vol. 143, pp. 37-43, Jan 2006.
- [37] B. E. Saygili, "Mesenchymal stem cells on polysaccharide based materials: Growth, differentiation and potential in neuronal regeneration," Ph.D. 3211001, Wayne State University, United States -- Michigan, 2006.
- [38] M. Fujita, D. C. Spray, H. Choi, J. C. Saez, T. Watanabe, L. C. Rosenberg, *et al.*, "Glycosaminoglycans and proteoglycans induce gap junction expression and restore transcription of tissue-specific mRNAs in primary liver cultures," *Hepatology*, vol. 7, pp. 1S-9S, 1987.
- [39] G. T. Hermanson, *Bioconjugate techniques*: Academic press, 1996.
- [40] D.-K. Kweon, S.-B. Song, and Y.-Y. Park, "Preparation of water-soluble chitosan/heparin complex and its application as wound healing accelerator," *Biomaterials*, vol. 24, pp. 1595-1601, 4// 2003.
- [41] J. You, D. S. Shin, D. Patel, Y. Gao, and A. Revzin, "Multilayered heparin hydrogel microwells for cultivation of primary hepatocytes," *Adv Healthc Mater*, vol. 3, pp. 126-32, Jan 2014.
- [42] M. M. Zegers and D. Hoekstra, "Mechanisms and functional features of polarized membrane traffic in epithelial and hepatic cells," *The Biochemical journal*, vol. 336 (Pt 2), pp. 257-269, 12/ 1998.
- [43] F. Goulet, C. Normand, and O. Morin, "Cellular interactions promote tissue-specific function, biomatrix deposition and junctional communication of primary cultured hepatocytes," *Hepatology*, vol. 8, pp. 1010-1018, 1988.

- [44] P. V. Moghe, F. Berthiaume, R. M. Ezzell, M. Toner, R. G. Tompkins, and M. L. Yarmush, "Culture matrix configuration and composition in the maintenance of hepatocyte polarity and function," *Biomaterials*, vol. 17, pp. 373-385, // 1996.
- [45] B. N. G. Giepmans and S. C. D. van Ijzendoorn, "Epithelial cell-cell junctions and plasma membrane domains," *Biochimica et Biophysica Acta (BBA) - Biomembranes*, vol. 1788, pp. 820-831, 4// 2009.
- [46] F. Berthiaume, P. V. Moghe, M. Toner, and M. L. Yarmush, "Effect of extracellular matrix topology on cell structure, function, and physiological responsiveness: hepatocytes cultured in a sandwich configuration," *The FASEB Journal*, vol. 10, pp. 1471-84, November 1, 1996 1996.
- [47] S. N. Bhatia, U. J. Balis, M. L. Yarmush, and M. Toner, "Effect of cell-cell interactions in preservation of cellular phenotype: cocultivation of hepatocytes and nonparenchymal cells," *The FASEB Journal*, vol. 13, pp. 1883-1900, November 1, 1999 1999.
- [48] J. W. Grisham, "Cell types in rat liver cultures: their identification and isolation," *Molecular and Cellular Biochemistry*, vol. 53-54, pp. 23-33, 1983.
- [49] Y. Nahmias, R. E. Schwartz, W. S. Hu, C. M. Verfaillie, and D. J. Odde, "Endothelium-mediated hepatocyte recruitment in the establishment of liver-like tissue in vitro," *Tissue Eng*, vol. 12, pp. 1627-38, Jun 2006.
- [50] K. Kim, K. Ohashi, R. Utoh, K. Kano, and T. Okano, "Preserved liver-specific functions of hepatocytes in 3D co-culture with endothelial cell sheets," *Biomaterials*, vol. 33, pp. 1406-1413, 2// 2012.

- [51] R. Sudo, S. Chung, I. K. Zervantonakis, V. Vickerman, Y. Toshimitsu, L. G. Griffith, *et al.*, "Transport-mediated angiogenesis in 3D epithelial coculture," *The FASEB Journal*, vol. 23, pp. 2155-2164, July 1, 2009.
- [52] A. Soto-Gutierrez, N. Navarro-Alvarez, H. Yagi, Y. Nahmias, M. L. Yarmush, and N. Kobayashi, "Engineering of an hepatic organoid to develop liver assist devices," *Cell Transplant*, vol. 19, pp. 815-22, 2010.
- [53] A. Martinez-Hernandez and P. S. Amenta, "The hepatic extracellular matrix. I. Components and distribution in normal liver," *Virchows Arch A Pathol Anat Histopathol*, vol. 423, pp. 1-11, 1993.
- [54] A. Martinez-Hernandez and P. S. Amenta, "The hepatic extracellular matrix. II. Ontogenesis, regeneration and cirrhosis," *Virchows Arch A Pathol Anat Histopathol*, vol. 423, pp. 77-84, 1995.
- [55] H.-F. Lu, K.-N. Chua, P.-C. Zhang, W.-S. Lim, S. Ramakrishna, K. W. Leong, *et al.*, "Three-dimensional co-culture of rat hepatocyte spheroids and NIH/3T3 fibroblasts enhances hepatocyte functional maintenance," *Acta Biomaterialia*, vol. 1, pp. 399-410, 7// 2005.
- [56] S. Abu-Absi, L. Hansen, and W.-S. Hu, "Three-dimensional co-culture of hepatocytes and stellate cells," *Cytotechnology*, vol. 45, pp. 125-140, 2004.
- [57] A. Bader, E. Knop, A. Kern, K. Böker, N. Frühauf, O. Crome, *et al.*, "3-D Coculture of Hepatic Sinusoidal Cells with Primary Hepatocytes—Design of an Organotypical Model," *Experimental Cell Research*, vol. 226, pp. 223-233, 7/10/ 1996.

- [58] K. Yamada, M. Kamihira, and S. Iijima, "Enhanced cell aggregation and liver functions using polymers modified with a cell-specific ligand in primary hepatocyte cultures," *Journal of Bioscience and Bioengineering*, vol. 88, pp. 557-562, // 1999.
- [59] A. Gomez-Aristizabal, A. Keating, and J. E. Davies, "Mesenchymal stromal cells as supportive cells for hepatocytes," *Mol Ther*, vol. 17, pp. 1504-8, Sep 2009.
- [60] V. Volarevic, J. Nurkovic, N. Arsenijevic, and M. Stojkovic, "Concise review: Therapeutic potential of mesenchymal stem cells for the treatment of acute liver failure and cirrhosis," *Stem Cells*, Aug 22 2014.
- [61] P. Stock, S. Bruckner, S. Winkler, M. M. Dollinger, and B. Christ, "Human Bone Marrow Mesenchymal Stem Cell-Derived Hepatocytes Improve the Mouse Liver after Acute Acetaminophen Intoxication by Preventing Progress of Injury," *International Journal of Molecular Sciences*, vol. 15, pp. 7004-7028, Apr 2014.
- [62] T. A. Brieva and P. V. Moghe, "Functional engineering of hepatocytes via heterocellular presentation of a homoadhesive molecule, E-cadherin," *Biotechnology and Bioengineering*, vol. 76, pp. 295-302, Nov 2001.
- [63] H. He, X. Liu, L. Peng, Z. Gao, Y. Ye, Y. Su, *et al.*, "Promotion of hepatic differentiation of bone marrow mesenchymal stem cells on decellularized cell-deposited extracellular matrix," *Biomed Res Int*, vol. 2013, p. 406871, 2013.
- [64] H. Wang, G. M. Riha, S. Yan, M. Li, H. Chai, H. Yang, *et al.*, "Shear stress induces endothelial differentiation from a murine embryonic mesenchymal progenitor cell line," *Arterioscler Thromb Vasc Biol*, vol. 25, pp. 1817-23, Sep 2005.

- [65] M. Y. Chen, P. C. Lie, Z. L. Li, and X. Wei, "Endothelial differentiation of Wharton's jelly-derived mesenchymal stem cells in comparison with bone marrow-derived mesenchymal stem cells," *Exp Hematol*, vol. 37, pp. 629-40, May 2009.
- [66] D. Pankajakshan, V. Kansal, and D. K. Agrawal, "In vitro differentiation of bone marrow derived porcine mesenchymal stem cells to endothelial cells," *J Tissue Eng Regen Med*, vol. 7, pp. 911-20, Nov 2013.
- [67] J. Chen, H. C. Park, F. Addabbo, J. Ni, E. Pelger, H. Li, *et al.*, "Kidney-derived mesenchymal stem cells contribute to vasculogenesis, angiogenesis and endothelial repair," *Kidney Int*, vol. 74, pp. 879-89, Oct 2008.
- [68] J. W. Liu, S. Dunoyer-Geindre, V. Serre-Beinier, G. Mai, J. F. Lambert, R. J. Fish, *et al.*, "Characterization of endothelial-like cells derived from human mesenchymal stem cells," *J Thromb Haemost*, vol. 5, pp. 826-34, Apr 2007.
- [69] Y. Cao, Z. Sun, L. Liao, Y. Meng, Q. Han, and R. C. Zhao, "Human adipose tissue-derived stem cells differentiate into endothelial cells in vitro and improve postnatal neovascularization in vivo," *Biochem Biophys Res Commun*, vol. 332, pp. 370-9, Jul 1 2005.
- [70] J. Kasuya, R. Sudo, T. Mitaka, M. Ikeda, and K. Tanishita, "Hepatic stellate cell-mediated three-dimensional hepatocyte and endothelial cell triculture model," *Tissue Eng Part A*, vol. 17, pp. 361-70, Feb 2011.
- [71] J. P. Chen and C. T. Lin, "Dynamic seeding and perfusion culture of hepatocytes with galactosylated vegetable sponge in packed-bed bioreactor," *Journal of Bioscience and Bioengineering*, vol. 102, pp. 41-45, Jul 2006.

- [72] S. S. Bale, L. Verneti, N. Senutovitch, R. Jindal, M. Hegde, A. Gough, *et al.*, "In vitro platforms for evaluating liver toxicity," *Exp Biol Med (Maywood)*, vol. 239, pp. 1180-91, Sep 2014.
- [73] A. Nussler, S. Konig, M. Ott, E. Sokal, B. Christ, W. Thasler, *et al.*, "Present status and perspectives of cell-based therapies for liver diseases," *J Hepatol*, vol. 45, pp. 144-59, Jul 2006.
- [74] F. Timm and B. Vollmar, "Heterogeneity of the intrahepatic portal venous blood flow: impact on hepatocyte transplantation," *Microvasc Res*, vol. 86, pp. 34-41, Mar 2013.
- [75] T. Takebe, K. Sekine, M. Enomura, H. Koike, M. Kimura, T. Ogaeri, *et al.*, "Vascularized and functional human liver from an iPSC-derived organ bud transplant," *Nature*, vol. 499, pp. 481-4, Jul 25 2013.
- [76] K. Asonuma, J. C. Gilbert, J. E. Stein, T. Takeda, and J. P. Vacanti, "Quantitation of transplanted hepatic mass necessary to cure the Gunn rat model of hyperbilirubinemia," *Journal of Pediatric Surgery*, vol. 27, pp. 298-301, 3// 1992.
- [77] N. Rajan, J. Habermehl, M.-F. Cote, C. J. Doillon, and D. Mantovani, "Preparation of ready-to-use, storable and reconstituted type I collagen from rat tail tendon for tissue engineering applications," *Nat. Protocols*, vol. 1, pp. 2753-2758, 01//print 2007.
- [78] T. Elsdale and J. Bard, "COLLAGEN SUBSTRATA FOR STUDIES ON CELL BEHAVIOR," *The Journal of Cell Biology*, vol. 54, pp. 626-637, 03/06/received 04/24/revised 1972.
- [79] P. O. Seglen, "Preparation of isolated rat liver cells," *Methods Cell Biol* vol. 13, pp. 29-83, 1976.

- [80] H. W. T. Matthew, J. Sternberg, P. Stefanovich, J. R. Morgan, M. Toner, R. G. Tompkins, *et al.*, "Effects of plasma exposure on cultured hepatocytes: Implications for bioartificial liver support," *Biotechnology and Bioengineering*, vol. 51, pp. 100-111, 1996.
- [81] J. Yang, A. Ichikawa, and T. Tsuchiya, "A novel function of connexin 32: marked enhancement of liver function in a hepatoma cell line," *Biochem Biophys Res Commun*, vol. 307, pp. 80-5, Jul 18 2003.
- [82] J. M. Anderson, B. R. Stevenson, L. A. Jesaitis, D. A. Goodenough, and M. S. Mooseker, "Characterization of ZO-1, a protein component of the tight junction from mouse liver and Madin-Darby canine kidney cells," *J Cell Biol*, vol. 106, pp. 1141-9, Apr 1988.
- [83] M. Hegde, R. Jindal, A. Bhushan, S. S. Bale, W. J. McCarty, I. Golberg, *et al.*, "Dynamic interplay of flow and collagen stabilizes primary hepatocytes culture in a microfluidic platform," *Lab Chip*, vol. 14, pp. 2033-9, Jun 21 2014.
- [84] E. Rozet, V. Wascotte, *et al.* , "Improvement of the decision efficiency of the accuracy profile by means of a desirability function for analytical methods validation. Application to a diacetyl-monoxime colorimetric assay used for the determination of urea in transdermal iontophoretic extracts," *Anal Chim Acta* vol. 591, pp. 239-247, 2007.
- [85] Y. M. Tanaka Y., Okano T., Kitamori T. and Sato K., "Evaluation of effects of shear stress on hepatocytes by a microchip-based system," *MEASUREMENT SCIENCE AND TECHNOLOGY*, vol. 17, pp. 3167–3170, 26 October 2006 2006.
- [86] A. Rotem, M. Toner, R. G. Tompkins, and M. L. Yarmush, "Oxygen uptake rates in cultured rat hepatocytes," *Biotechnol Bioeng*, vol. 40, pp. 1286-91, Dec 5 1992.

- [87] B. D. Foy, A. Rotem, M. Toner, R. G. Tompkins, and M. L. Yarmush, "A device to measure the oxygen uptake rate of attached cells: importance in bioartificial organ design," *Cell Transplant*, vol. 3, pp. 515-27, Nov-Dec 1994.
- [88] M. Miyazawa, T. Torii, Y. Toshimitsu, K. Okada, and I. Koyama, "Hepatocyte dynamics in a three-dimensional rotating bioreactor," *J Gastroenterol Hepatol*, vol. 22, pp. 1959-64, Nov 2007.
- [89] M. J. Powers, K. Domansky, M. R. Kaazempur-Mofrad, A. Kalezi, A. Capitano, A. Upadhyaya, *et al.*, "A microfabricated array bioreactor for perfused 3D liver culture," *Biotechnol Bioeng*, vol. 78, pp. 257-69, May 5 2002.
- [90] C. M. Brophy, J. L. Luebke-Wheeler, B. P. Amiot, H. Khan, R. P. Remmel, P. Rinaldo, *et al.*, "Rat hepatocyte spheroids formed by rocked technique maintain differentiated hepatocyte gene expression and function," *Hepatology*, vol. 49, pp. 578-86, Feb 2009.
- [91] E. Curcio, S. Salerno, G. Barbieri, L. De Bartolo, E. Drioli, and A. Bader, "Mass transfer and metabolic reactions in hepatocyte spheroids cultured in rotating wall gas-permeable membrane system," *Biomaterials*, vol. 28, pp. 5487-97, Dec 2007.
- [92] A. Acikgöz, S. Giri, M.-G. Cho, and A. Bader, "Morphological and Functional Analysis of Hepatocyte Spheroids Generated on Poly-HEMA-Treated Surfaces under the Influence of Fetal Calf Serum and Nonparenchymal Cells," *Biomolecules*, vol. 3, pp. 242-269, 03/07

12/21/received

02/07/revised

02/11/accepted 2013.

- [93] E. Torok, C. Vogel, M. Lutgehetmann, P. X. Ma, M. Dandri, J. Petersen, *et al.*, "Morphological and functional analysis of rat hepatocyte spheroids generated on poly(L-lactic acid) polymer in a pulsatile flow bioreactor," *Tissue Eng*, vol. 12, pp. 1881-90, Jul 2006.
- [94] S. SURAPANENI, T. PRYOR, M. D. KLEIN, and H. W. T. MATTHEW, "Rapid Hepatocyte Spheroid Formation: Optimization and Long Term Function in Perfused Microcapsules," *ASAIO Journal*, vol. 43, p. M854, 1997.
- [95] L. D. A. Assay, *MAK066 SIGMA:*
<http://www.sigmaaldrich.com/catalog/product/sigma/mak066?lang=en®ion=US>.
- [96] AlamarBlue, *Life Technologies:*
<http://www.lifetechnologies.com/us/en/home/brands/molecular-probes/key-molecular-probes-products/alamarblue-rapid-and-accurate-cell-health-indicator.html>.
- [97] A. J. Hwa, R. C. Fry, A. Sivaraman, P. T. So, L. D. Samson, D. B. Stolz, *et al.*, "Rat liver sinusoidal endothelial cells survive without exogenous VEGF in 3D perfused co-cultures with hepatocytes," *FASEB J*, vol. 21, pp. 2564-79, Aug 2007.
- [98] T. Tokairin, Y. Nishikawa, Y. Doi, H. Watanabe, T. Yoshioka, M. Su, *et al.*, "A highly specific isolation of rat sinusoidal endothelial cells by the immunomagnetic bead method using SE-1 monoclonal antibody," *J Hepatol*, vol. 36, pp. 725-33, Jun 2002.
- [99] F. Manconi, R. Markham, and I. S. Fraser, "Culturing endothelial cells of microvascular origin," *Methods Cell Sci*, vol. 22, pp. 89-99, 2000.
- [100] C. Frye and C. Patrick, "Isolation and culture of rat microvascular endothelial cells," *In Vitro Cellular & Developmental Biology - Animal*, vol. 38, pp. 208-212, 2002.

- [101] J. Oswald, S. Boxberger, B. Jorgensen, S. Feldmann, G. Ehninger, M. Bornhauser, *et al.*, "Mesenchymal stem cells can be differentiated into endothelial cells in vitro," *Stem Cells*, vol. 22, pp. 377-384, 2004.
- [102] K. H. Wu, B. Zhou, S. H. Lu, B. Feng, S. G. Yang, W. T. Du, *et al.*, "In vitro and in vivo differentiation of human umbilical cord derived stem cells into endothelial cells," *J Cell Biochem*, vol. 100, pp. 608-16, Feb 15 2007.
- [103] A. Piryaei, M. R. Valojerdi, M. Shahsavani, and H. Baharvand, "Differentiation of bone marrow-derived mesenchymal stem cells into hepatocyte-like cells on nanofibers and their transplantation into a carbon tetrachloride-induced liver fibrosis model," *Stem Cell Rev*, vol. 7, pp. 103-18, Mar 2011.
- [104] N. Lin, J. Lin, L. Bo, P. Weidong, S. Chen, and R. Xu, "Differentiation of bone marrow-derived mesenchymal stem cells into hepatocyte-like cells in an alginate scaffold," *Cell Prolif*, vol. 43, pp. 427-34, Oct 2010.
- [105] S. Snykers, J. De Kock, V. Tamara, and V. Rogiers, "Hepatic differentiation of mesenchymal stem cells: in vitro strategies," *Methods Mol Biol*, vol. 698, pp. 305-14, 2011.
- [106] S. Snykers, T. Vanhaecke, P. Papeleu, A. Luttun, Y. Jiang, Y. Vander Heyden, *et al.*, "Sequential exposure to cytokines reflecting embryogenesis: the key for in vitro differentiation of adult bone marrow stem cells into functional hepatocyte-like cells," *Toxicol Sci*, vol. 94, pp. 330-41; discussion 235-9, Dec 2006.
- [107] I. R. Murray, C. C. West, W. R. Hardy, A. W. James, T. S. Park, A. Nguyen, *et al.*, "Natural history of mesenchymal stem cells, from vessel walls to culture vessels," *Cell Mol Life Sci*, vol. 71, pp. 1353-74, Apr 2014.

- [108] E. Karaoz, A. Aksoy, S. Ayhan, A. E. Sariboyaci, F. Kaymaz, and M. Kasap, "Characterization of mesenchymal stem cells from rat bone marrow: ultrastructural properties, differentiation potential and immunophenotypic markers," *Histochem Cell Biol*, vol. 132, pp. 533-46, Nov 2009.
- [109] J. Gu, X. Shi, Y. Zhang, and Y. Ding, "Heterotypic interactions in the preservation of morphology and functionality of porcine hepatocytes by bone marrow mesenchymal stem cells in vitro," *J Cell Physiol*, vol. 219, pp. 100-8, Apr 2009.
- [110] R. Glicklis, J. C. Merchuk, and S. Cohen, "Modeling mass transfer in hepatocyte spheroids via cell viability, spheroid size, and hepatocellular functions," *Biotechnol Bioeng*, vol. 86, pp. 672-80, Jun 20 2004.
- [111] T. Kashiwagura, D. F. Wilson, and M. Erecinska, "Oxygen dependence of cellular metabolism: the effect of O₂ tension on gluconeogenesis and urea synthesis in isolated rat hepatocytes," *J Cell Physiol*, vol. 120, pp. 13-8, Jul 1984.
- [112] W. M. Saltzman, "Engineering Principles for the Design of Replacement Organs and Tissues," *Oxford University Press*, p. Appendix B, 2004.
- [113] K. Isoda, M. Kojima, M. Takeda, S. Higashiyama, M. Kawase, and K. Yagi, "Maintenance of hepatocyte functions by coculture with bone marrow stromal cells," *J Biosci Bioeng*, vol. 97, pp. 343-6, 2004.
- [114] T. Yuki, Y. Masayuki, O. Teruo, K. Takehiko, and S. Kiichi, "Evaluation of effects of shear stress on hepatocytes by a microchip-based system," *Measurement Science and Technology*, vol. 17, p. 3167, 2006.

- [115] M. M. Salek, P. Sattari, and R. J. Martinuzzi, "Analysis of fluid flow and wall shear stress patterns inside partially filled agitated culture well plates," *Ann Biomed Eng*, vol. 40, pp. 707-28, Mar 2012.
- [116] A. W. Tilles, H. Baskaran, P. Roy, M. L. Yarmush, and M. Toner, "Effects of oxygenation and flow on the viability and function of rat hepatocytes cocultured in a microchannel flat-plate bioreactor," *Biotechnol Bioeng*, vol. 73, pp. 379-89, Jun 5 2001.
- [117] R. N. Palchesko, J. M. Szymanski, A. Sahu, and A. W. Feinberg, "Shrink Wrapping Cells in a Defined Extracellular Matrix to Modulate the Chemo-Mechanical Microenvironment," *Cell Mol Bioeng*, vol. 7, pp. 355-368, Sep 2014.
- [118] H. W. Matthew, S. O. Salley, W. D. Peterson, and M. D. Klein, "Complex coacervate microcapsules for mammalian cell culture and artificial organ development," *Biotechnol Prog*, vol. 9, pp. 510-9, Sep-Oct 1993.
- [119] E. T. Papoutsakis, "Media additives for protecting freely suspended animal cells against agitation and aeration damage," *Trends Biotechnol*, vol. 9, pp. 316-24, Sep 1991.
- [120] R. Tiruvannamalai-Annamalai, D. R. Armant, and H. W. Matthew, "A glycosaminoglycan based, modular tissue scaffold system for rapid assembly of perfusable, high cell density, engineered tissues," *PLoS One*, vol. 9, p. e84287, 2014.
- [121] V. S. Lin and H. W. T. Matthew, "Microencapsulation Methods: Glycosaminoglycans and Chitosan," *Methods of Tissue Engineering*, vol. Chapter 72, pp. 815-823, 2002.
- [122] H. W. Matthew, S. Basu, W. D. Peterson, S. O. Salley, and M. D. Klein, "Performance of plasma-perfused, microencapsulated hepatocytes: prospects for extracorporeal liver support," *J Pediatr Surg*, vol. 28, pp. 1423-7; discussion 1427-8, Nov 1993.

ABSTRACT**DEVELOPMENT OF SCAFFOLD ARCHITECTURES AND HETEROTYPIC CELL SYSTEMS FOR HEPATOCYTE TRANSPLANTATION**

by

DALIA ABDELRAHIM ALZEBDEH**May 2015****Advisor:** Dr. Howard W. T. Matthew**Major:** Biomedical Engineering**Degree:** Doctor of Philosophy

In vitro assembly of functional liver tissue is needed to enable the transplantation of tissue-engineered livers. In addition, there is an increasing demand for *in vitro* models that replicate complex events occurring in the liver. However, tissue engineering of sizable implantable liver systems is currently limited by the difficulty of assembling three dimensional hepatocyte cultures of a useful size, while maintaining full cell viability, an issue which is closely related to the high metabolic rate of hepatocytes. In this study, we first compared two designs of highly porous chitosan-heparin scaffolds seeded with hepatocytes in dynamic perfusion bioreactor systems. The aim was to promote cell seeding efficiency by effectively entrapping 100 million hepatocytes at high density. We found that scaffolds with radially tapering pore architecture had highly efficient cell entrapment that maximized donor hepatocyte utilization, compared to alternate pore structures. Hepatocytes showed higher seeding efficiency

and metabolic function when seeded as single cell suspensions as opposed to pre-formed, 100 μ m aggregates. Seeding efficiency was found to increase with flow rate, with single cell and aggregate suspension exhibiting different optimal flow rates. However, metabolic performance results indicated significant shear damage to cells at high efficiency flow rates. To better maintain hepatocyte basement membrane and cell polarity, spheroid co-cultures with mesenchymal stem cells (MSC) were investigated. Hepatocytes and MSCs were seeded in three different architectures in an effort to optimize the spatial arrangement of the two cell types. MSC co-culture greatly enhanced hepatocyte metabolic function in agitated cultures. Interestingly, the effects of diffusion limitations in spheroid culture, coupled with shear damage and subsequent removal of outer hepatocyte layers produced a defined oscillation of urea production rates in certain co-culture arrangements. A mathematical model of urea synthesis in shear-exposed, co-culture spheroids reproduced the metabolic oscillations observed. This result together with culture observations suggests that MSCs can provide both physiological support and some direct shear protection to hepatocytes in perfused or shear-exposed culture environments. Finally, in order to reduce hepatocyte exposure to excessive shear forces in perfused scaffolds, a modular scaffold design based on polyelectrolyte fiber encapsulation was explored. Scaffolds with uniformly distributed, shear protected cells were achieved.

AUTOBIOGRAPHICAL STATEMENT

EDUCATION

Master of Science: Biomedical Engineering with focus on Materials Science and Tissue Engineering. Wayne State University/ Detroit, MI. MAY 2010- DEC 2011. GPA: 4.0/4.0

Bachelor of Science: Biomedical Engineering. Jordan University of Science and Technology/ Jordan. AUG 1998- JUNE 2003 80.4% (* Very good).

PAPERS IN REFEREED JOURNALS AWAITING REVIEW:

Dalia Alzebdeh and Howard W.T. Matthew; Seeding Architecture Effects on Primary Rat Hepatocyte When Cultured with Rat Bone Marrow Mesenchymal Stem Cells in Chitosan-Heparin Porous Scaffolds. Paper is in process to be submitted to Journal of Tissue Engineering and Regenerative Medicine.

Therese Bou-Akl, Dalia Alzebdeh, Basak E. Uygun and Howard W.T. Matthew; Self-Assembly and Function of Primary Hepatocytes Cultured on Glycosaminoglycan-Chitosan Membranes. Paper is ready to be submitted to Journal of Tissue Engineering and Journal of Biomedical Materials Research Part A.

CONFERENCE PRESENTATIONS

Alzebdeh, D.A. and Matthew H.W.; Poster presentation accepted title: “Analysis of Perfusion-Enhanced Diffusion, Shear Damage and Metabolic Function in Spheroid-Seeded and Suspension Seeded Hepatocyte Scaffolds”. Biomedical Engineering Society (BMES) Annual Meeting. San Antonio, TX. OCT 2014.

Alzebdeh, D.A. and Matthew H.W.; Poster presentation title: “Dynamic Perfusion System for Hepatic Tissue Engineering: The Effects of Seeding Method on Cell-Loading Efficiency, Hepatocyte Viability and Specific Functions”. Wayne State University Graduate Exhibition, 2014. Detroit, MI. MAR 2014.

Alzebdeh, D.A. and Matthew H.W.; Poster presentation title: “Porous Scaffold Designs for Perfusion Culture and Liver Tissue Engineering: Evaluation of Cell-Loading Efficiency and Seeding Time”. Biomedical Engineering Society (BMES) Annual Meeting. Seattle, WA. SEP 2013.